Genetic dissection of peripheral pathways in the visual system of *Drosophila*

Dissertation zur Erlangung des
naturwissenschaftlichen Doktorgrades
der Bayerischen Julius-Maximilians-Universität Würzburg

vorgelegt von

Jens Rister
aus Ansbach

Würzburg, 2007

Eingereicht am: .....

Mitglieder der Promotionskommission:

Vorsitzender: .....

Gutachter: Prof. Dr. Martin Heisenberg

Gutachter: Prof. Dr. Wolfgang Rössler

Tag des Promotionskolloquiums: .....

Doktorurkunde ausgehändigt am: .....

Erklärung gemäß § 4 Absatz 3 der Promotionsordnung der Fakultät für Biologie der Bayerischen Julius-Maximilians-Universität zu Würzburg vom 15. März 1999:

Hiermit erkläre ich die vorgelegte Dissertation selbständig angefertigt zu haben und keine anderen als die von mir angegebenen Quellen und Hilfsmittel verwendet zu haben. Die mit meinen Publikationen (siehe list of publications) wortgleichen oder nahezu wortgleichen Textpassagen habe ich selbst verfasst. Alle aus der Literatur genommenen Stellen sind als solche kenntlich gemacht.

Des Weiteren erkläre ich, dass die vorliegende Arbeit weder in gleicher noch in ähnlicher Form bereits in einem anderen Prüfungsverfahren vorgelegen hat. Zuvor habe ich keine akademischen Grade erworben oder zu erwerben versucht.

Würzburg, den

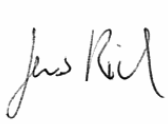

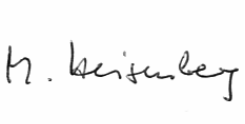

Jens Rister Prof. Martin Heisenberg

Table of contents

1. Introduction

1.1. Neuroanatomy of the peripheral visual system of *Drosophila*

Vision in *Drosophila melanogaster* is mediated by the two compound eyes, three dorsal ocelli and extraretinal photoreceptors. Each compound eye (Fig. 1A) is composed of a regular hexagonal array of about 750 units, the ommatidia. An ommatidium contains eight photoreceptors (R1-R8; Fig. 1B) with specialized structures, the rhabdomeres (Fig. 1B, upper panel) that absorb photons.

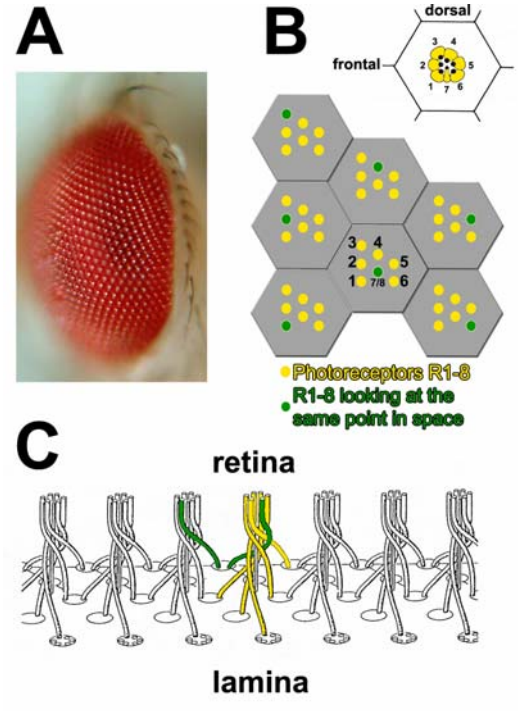

Figure 1: **The two photoreceptor subsystems of the *Drosophila* retina.**
(A) The *Drosophila* eye is composed of about 750 single unit eyes called ommatidia.
(B) Each hexagonal ommatidium (grey) contains eight photoreceptors (R1-8, yellow) that carry light-sensitive structures, the rhabdomeres (black, upper panel). The photoreceptors can be grouped in two subsystems, the "inner" tandem R7/8 and the surrounding "outer" R1-6. Of the latter, six different ones in six neighboring ommatidia (green) are directed towards the same point in space.
(C) Neuronal superposition of the axon terminals of photoreceptors R1-6 in the lamina that are facing the same point in space (modified from Franceschini et al., 1989). The photoreceptor axon fibers of one ommatidium (yellow) project into six lamina cartridges and group with those of neighboring ommatidia facing the same point in space (two highlighted in green).

1.1.1. Two functionally specialized photoreceptor subsystems in the *Drosophila* retina

According to the position of the rhabdomeres in the ommatidium, *Drosophila* photoreceptors (Fig. 1B) can be divided into six "outer" ones (R1-6) surrounding two "inner" ones (R7 and R8). The latter are located as a central tandem along the optical axis of the ommatidium, viewing the same point in space. The "outer" R1-6 have slightly divergent optical axes and therefore sample different points in space.

Photoreceptor subsystem R1-6 has been shown to be necessary and sufficient for motion-driven behavior (Heisenberg and Buchner, 1977; Yamaguchi et al., in preparation), whereas R7 and R8 mediate color vision (Menne and Spatz, 1977) and

contribute to phototaxis and tropotaxis (review: Heisenberg and Wolf, 1984). The fact that insects have separate sets of photoreceptors for processing motion and color (Kaiser, 1975; Heisenberg and Buchner, 1977; Bausenwein et al., 1992) is reminiscent of the vertebrate retina that also separates visual modalities such as color and motion (reviewed in Livingstone and Hubel, 1988).

1.1.2. Fundamental building principles of the peripheral visual system

The optic lobe of adult *Drosophila* is subdivided into four neuropils, the lamina, the medulla, the lobula and the lobula plate. In these neuropils, a retinotopic map (i.e. preserving the spatial input arrangement from the retina) is established by columnar neurons (Fischbach and Dittrich, 1989) such that neighboring image points detected by the lattice of units sampling visual space (visual sampling units, VSUs; Franceschini, 1975) are represented in an orderly array of neighboring columns.

VSUs are groups of eight photoreceptors that are distributed in seven neighboring ommatidia (Fig. 1C) and are directed towards the same point in space. These divide into six photoreceptors R1-6 from six adjacent ommatidia that project together through the outer optic chiasm to the same region in the first synaptic neuropil of the optic lobe, the lamina, forming a cartridge (or neuro-ommatidium, Fig. 1C and 2A; Braitenberg, 1967; Strausfeld, 1971). As photoreceptors with parallel optical axes sampling the same point in space converge in a single lamina cartridge, the latter (not the ommatidium) represents the functional lattice element of the peripheral visual system (Hengstenberg and Götz, 1967). R7 and R8 bypass their home cartridge and terminate instead in the corresponding column of the second, more proximal neuropil, the medulla.

This wiring principle between retina and lamina is called neuronal superposition (Braitenberg, 1967; Kirschfeld, 1967). It requires that the angular separation of the optical axes of neighboring rhabdomeres is the same as the divergence angle $\Delta\varphi$ between neighboring ommatidia (Kirschfeld, 1967). Pooling equivalent information from R1-6 results in an improvement in signal to noise ratio by a factor of $\sqrt{6}$ (Scholes, 1969) due to increased photon catch without deterioration of visual acuity or resolution (Land, 1997).

1.1.3. Structure and cell types of the lamina cartridge

The organization of the lamina cartridge has been studied in detail on the light microscopical and ultrastructural level (Fig. 2A). It contains 15 cell types (Braitenberg,

1971; Boschek, 1971; Shaw, 1984; Strausfeld and Campos-Ortega, 1977; Fischbach and Dittrich, 1989; Meinertzhagen and O'Neil, 1991; Meinertzhagen and Sorra, 2001) that can be subdivided in several classes: first, 3 types of photoreceptor (R1-6, R7, R8); second, five types of monopolar cell (L1-L5); third, three types of medulla cell (C2, C3, T1) and fourth, the wide field tangential (LamTan) and amacrine cells (amc). Most, if not all of their anatomical connections are believed to be known in *Drosophila* (Meinertzhagen and O'Neil, 1991).

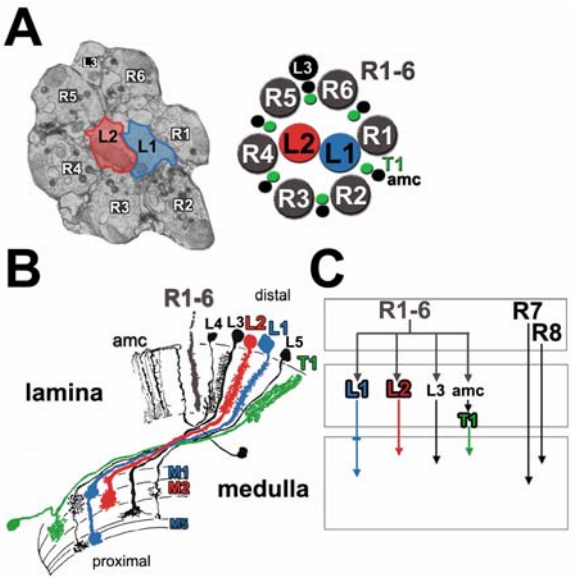

Figure 2: Anatomy of the lamina cartridge and peripheral interneurons that constitute parallel pathways.

(A) Electron microscopical (left, modified from Heisenberg and Wolf, 1984) and schematic cross-section through the lamina cartridge (right) formed by photoreceptors R1-6 (grey) sharing the same optical axis and making synaptic contacts with monopolar cells L1, L2, L3 and amacrine processes (amc). L1 (blue) and L2 (red) are located in the center of the cartridge. L4, L5 and T1 represent second-order interneurons with T1 being postsynaptic to amc.
(B) Neurons of the lamina cartridge (modified from Fischbach and Dittrich, 1989). For visibility, only one R1-6 terminal is shown (grey). Interneurons genetically addressed in this thesis (L1, L2, and T1) are shown in color.
(C) In the lamina cartridge, photoreceptors R1-6 provide input to the L1, L2, L3 and amc pathways. R7 and R8 bypass this arrangement.

Four cartridge interneurons receive common input from R1-6: L1, L2, L3 and the amc (Fig. 2B; Meinertzhagen and O'Neil, 1991). The two large monopolar cells L1 and L2 are located in the center of the cartridge and have radially oriented dendritic spines throughout its depth (Fig. 1B; Fischbach and Dittrich, 1989; Meinertzhagen and O'Neil, 1991). Their position, as well as the impressive size and number of their dendrites suggest a key role in peripheral processing that can be visualized by ^{3}H-deoxyglucose activity labelling (Buchner et al., 1984; Bausenwein et al., 1992).

The monopolar neuron L3 has asymmetric dendrites that are arranged to one side like bristles on a toothbrush (Fischbach and Dittrich, 1989). It receives only one fourth to one fifth of the synaptic input compared to L1 and L2 (Meinertzhagen and Sorra, 2001). Finally, the amc is also postsynaptic to R1-6 (Meinertzhagen and O'Neil, 1991). It provides the only lamina input to the second-order interneuron T1 that is characterized by six fibers in the lamina that form a "basket" (Fig. 2B).

1.1.4. What is the functional role of the lamina pathways?

Neuronal superposition of the axon terminals of photoreceptors in the lamina not only enhances the signal to noise ratio (see above), but also reduces the number of visual pathways from eight to three (R1-6, R7 and R8; Heisenberg and Wolf, 1984). Moreover, transmitting redundant information from R1-6 to four types of afferent cells (L1-3 and amc) in one cartridge can be interpreted as the early splitting into four retinotopically organized, parallel pathways (Fig. 2C; Fischbach and Dittrich, 1989; Bausenwein et al., 1992).

Anatomical differences between L1-L3 suggest functional specializations. First, they have their terminal arborizations in separate layers of the medulla (Fischbach and Dittrich, 1989; Fig. 1B). Second, only L2 has feedback synapses onto R1-6 (Meinertzhagen and O'Neil, 1991) that might play a role in neuronal adaptation and could exert a modulatory influence on the photoreceptor output. Third, L2 innervates, and reciprocally receives input (and therefore feedback) from a second-order interneuron, L4, of its own cartridge, as well as from adjacent cartridges. This constitutes a horizontal network of lateral connections, as each L4 neuron has two backward oriented collaterals connecting its own cartridge to two neighboring cartridges along the x- and y-axes of the neuroommatidial array (Fig. 3F; Braitenberg, 1970; Braitenberg and Debbage, 1974; Strausfeld and Braitenberg, 1970; Meinertzhagen and O'Neil, 1991). It has been speculated that this conspicuous extension of the L4 collaterals might have its functional correlate in the prevalence of front-to-back motion in the visual flow field of fast moving flies (Braitenberg and Debbage, 1974).

As L3 receives significantly less input than L1 and L2 in the lamina (Meinertzhagen and Sorra, 2001), it is thought to have a higher response threshold for light intensity, possibly constituting a third color pathway (in addition to R7 and R8; Strausfeld, 1984; Anderson and Laughlin, 2000). It has also been considered as a candidate for processing e-vector orientation (Wolf et al., 1980). Finally, amcs invade several cartridges where they are postsynaptic to R1-6 and relay this information to T1. The amc/T1 pathway could therefore be involved in phenomena like wide-field adaptation to ambient light levels or lateral inhibition (Järvilehto and Zettler, 1973).

Single unit recordings of lamina monopolar cells L1 and L2 can be routinely performed in large flies. However, the results were mostly reported without

distinguishing between the two interneurons that were assumed to have very similar response profiles (e.g. Laughlin, 1981a). Rarely, electrophysiological recordings were combined with intracellular dye fills for the identification of the recorded cell types. Gilbert et al. (1991) found no differences in the responses of L1 and L2 to motion and flicker at equivalent contrast frequencies. Two other reports detected subtle differences between L1-L3 in the response plateau and the off-transient (Hardie and Weckström 1990; Laughlin and Osorio, 1989). However, the functional relevance of this finding is not known.

1.2. Motion detection in insects

For most animals, motion vision is a prerequisite for navigating through the environment. A visually elicited, innate behavioral response to motion stimuli is the optomotor response that serves the stabilization of gaze in walking and flight. In the classical assay, a striped drum pattern is rotated around the animal that responds with compensatory turning maneuvers (Fig. 3A). It is usually tethered in order to fix the eyes in space and to prevent it from interfering by its own behavior with the visual input ("open loop conditions"; Hassenstein and Reichardt, 1956; Götz, 1964; Heisenberg and Wolf, 1993).

This paradigm was used in pioneering studies performed by Hassenstein and Reichardt (1956) who proposed a first mathematical model of motion detection (see chapter 1.2.1.) that was based on the quantitative analysis of the optomotor response of the beetle *Chlorophanus*. Later, flies became an attractive model system and their optomotor response was measured in walking (Götz and Wenking, 1973; Buchner, 1976) and flight (Götz, 1964; Heisenberg and Wolf, 1984). This allowed studying the parameters that determine fundamental transfer properties of the compound eye (Hassenstein and Reichardt, 1956; Götz, 1964, 1965) and lead to first insights into the cellular mechanisms underlying motion detection (Götz, 1968; Buchner, 1976; Heisenberg and Buchner, 1977; review: Heisenberg and Wolf, 1984; Borst and Egelhaaf, 1993).

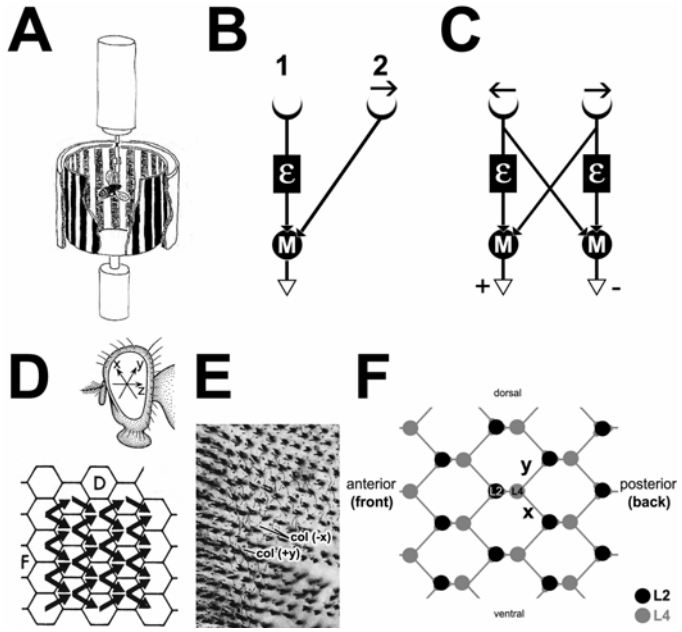

Figure 3: Optomotor response and elementary motion detection.
(A) Schematic drawing of the setup used to measure optomotor responses in tethered flight (modified from Wolf and Heisenberg, 1997). Yaw turning responses are recorded in response to clockwise and counterclockwise horizontal rotation of the striped drum. (B) Unidirectional elementary motion detector (EMD; Borst and Egelhaaf, 1989). It consists of two input channels (1 and 2, from neighboring visual elements) that are successively activated when a stimulus moves (arrow) from 1 to 2 across their receptive fields. The signal of channel 1 is delayed (ε) in order to coincide with the signal of channel 2 at the multiplication stage M, leading to a directionally selective output signal. (C) The combination of two unidirectional EMDs (shown in B) with opposite preferred directions gives a bidirectional detector. (D) Motion-detection network composed of the two dominant EMDs mediating optomotor responses in tethered walking *Drosophila* (from Heisenberg and Buchner, 1977). Upper panel: Orientation of the coordinates x, y and z with respect to the fly's eye and head (from Braitenberg, 1970). (E) The L4 network in the lamina of *Musca*. The collaterals (col) of this second-order interneuron are arranged along the –x and +y coordinates (compare to D) of the neuroommatidial lattice (from Braitenberg and Debbage, 1974). (F) In *Drosophila*, the two collaterals (grey lines) of each L4 neuron (grey circle) connect the L2 neurons of the home cartridge (adjacent black circle) to the neighboring dorso-posterior and ventro-posterior one.

1.2.1. The elementary motion detector (EMD)

A first model for the computation of directional motion was developed by Hassenstein and Reichardt (1956) that was based on the quantitative analysis of the optomotor response of the beetle *Chlorophanus*. Its key element is the elementary motion detector (EMD; Buchner, 1976) which is the minimal functional unit capable of detecting directional motion. It detects motion stimuli in the visual input by measuring the temporal coincidence between the light flux in adjacent VSUs. As the EMD (Fig. 3B) performs a correlation between the two input signals, it is therefore also called "correlation-type" motion detector. Arrays of EMDs with different directional sensitivities allow the animal to analyze optic flow fields in its entire visual field (Götz 1964, 1968; Buchner, 1976).

In its simplest form, the EMD has three main processing features (Figs. 3B, C; Hassenstein and Reichardt, 1956; Borst and Egelhaaf, 1989): two input channels with a defined sampling base, a delay or filtering unit and a cross-correlation unit. First, two input channels are required in order to distinguish motion from flicker. Their sampling

distance, the divergence angle Δφ between neighboring ommatidia, is the fundamental spatial input parameter. In *Drosophila*, Δφ of neighboring VSUs was found to be about 4.6° (Götz, 1965; Götz and Hengstenberg, 1967; Buchner, 1976; Heisenberg and Buchner, 1977).

Investigations in frontolateral *Drosophila* eye regions have revealed that motion perception in the optomotor course control mainly involves nearest-neighbor-interactions of VSUs (Fig. 3D; Buchner, 1976). Note that this resembles the conspicuous orientation of the collaterals of L4 neurons (Figs. 3E, F). However, under low ambient illumination conditions or after dark adaptation, spatial pooling and recruitment of widely separated EMD inputs was shown to occur in several fly species in behavioral (*Drosophila*: Heisenberg and Buchner, 1977; *Musca*: Pick and Buchner, 1979) and electrophysiological experiments (*Lucilia*: Srinivasan and Dvorak, 1980; *Calliphora*: Schuling et al., 1989). During daylight conditions, ommatidia separated up to eight times Δφ were found to contribute to the response of H1, a lobula plate tangential cell (Schuling et al., 1989).

Second, the two inputs have to be differentially processed by filtering operations (e.g. by introducing a delay, Fig. 3B), in order to determine which channel was excited first. This step is essential for directional selectivity. Third, a nonlinear interaction between the two input signals is required which can be achieved by a multiplication of both signals (Hassenstein and Reichardt, 1956; Borst and Egelhaaf, 1989), by sign (corresponding to the direction of movement) and amount (magnitude of stimulus change). This is crucial, as simply averaging the input signals would cause a loss of directional selectivity. The calculation is performed twice in a mirror-symmetrical fashion (Fig. 3C), providing two unidirectional EMDs with opposite preferred direction.

However, even such an arrangement does not exclusively respond to motion, but also to global changes in illumination (flicker). A subsequent subtraction of the outputs of the two antidirectional EMDs (Borst and Egelhaaf, 1990) removes direction-independent response components and gives a fully direction-selective signal. Brightness changes detected by both subunits thereby cancel out. Depending on the direction of motion, the EMD output is either positive or negative.

The existence of unidirectional EMDs, as suggested by the Hassenstein/Reichardt model, was supported by the analysis of mutants in *Drosophila*. *No-on-transient* A^{H2} mutants were found to have a severely reduced response to front-to-back motion (Heisenberg, 1972), but an only little impaired sensitivity to the

opposite direction of motion. In contrast, in *optomotor blind*^{H31} mutants the response to back-to-front motion was much more impaired than the response to front-to-back motion (Bausenwein et al., 1986; review: Pflugfelder and Heisenberg, 1995).

1.2.2. The search for neuronal correlates of the elementary motion detector

The neuronal network underlying the EMD remains to be discovered. However, several hypotheses about the functional relevance of the divergence of the motion channel into four parallel pathways (L1, L2, L3 and amc) have been suggested (reviews: Laughlin, 1981a; Heisenberg and Wolf, 1984; Shaw, 1984; Borst and Haag, 2002; Douglass and Strausfeld, 2003). For instance, it has been speculated that L1 and L2 could represent the two inputs of the EMD (Braitenberg and Hauser-Holschuh, 1972; Fig. 3B), or that one of the two is specialized for the detection of front-to-back, and the other for back-to-front motion. In this respect, the L2/L4 pathway due to its conspicuous connections in the lamina (Fig. 3E, F) was a candidate for front-to-back motion processing (Braitenberg and Debbage, 1974). In contrast, Coombe et al. (1989) have claimed that L1 and L2 should be dispensable for the detection of directional motion. These suggestions and controversies can now be addressed in *Drosophila melanogaster*.

1.3. *Drosophila melanogaster* as a model organism for structure-function correlations in the visual system

The fly *Drosophila melanogaster* is one of the most popular model organisms in neuroscience. It has a rich behavioral repertoire and offers a unique collection of genetic tools ranging from the classical study of single gene mutants (Benzer, 1967) to novel molecular genetic approaches for neuronal circuit analysis (reviews: White et al., 2001; Roman, 2004).

1.3.1. Classical approaches for correlating structure and function in the visual system

As mentioned above, the visual system of *Drosophila* has been investigated in considerable detail on the light microscopical and in the lamina also on the ultrastructural level. However, a functional understanding of the underlying circuitry has not yet emerged. As a start into dissecting the visual network, single gene mutants were isolated in forward genetic screens for defects in phototaxis and the optomotor

response (Benzer 1967; Heisenberg, 1972; Heisenberg and Götz, 1975; review: Heisenberg, 1997). This lead to insights into the genetic basis of cellular processes underlying visual behavior (e.g. phototransduction, review: Hardie and Raghu, 2001), served as a method for dissecting complex behaviors (e.g. motion and color vision; Heisenberg and Buchner, 1977) and was a first step into identifying neuronal correlates of optomotor behavior and genetic factors that are required for their development (Heisenberg et al., 1978; Fischbach, 1983; Coombe and Heisenberg, 1986). However, even single gene mutations can affect several developmental processes and many different cell types due to the pleiotropic nature of genes (Pflugfelder, 1998). Moreover, the expressivity of structural defects can be variable and depends on genetic background (de Belle and Heisenberg, 1996).

Novel transgenic techniques like the binary UAS/GAL4 system allow spatially and temporally controlled genetic intervention in neuronal subsystems. This recent progress may eventually lead to an understanding how the diverse cells of the visual system extract and process behaviorally relevant information.

1.3.2. The UAS/GAL4 system as a genetic tool for dissecting neuronal networks

The UAS/GAL4 system (Fig. 4) is currently the most widely used technique for targeted transgene expression in *Drosophila* (reviews: Phelps and Brand, 1998; Duffy, 2002). It allows the expression of an effector transgene ("what") that is temporally ("when") and spatially ("where") restricted by a GAL4 driver line (Fig. 4).

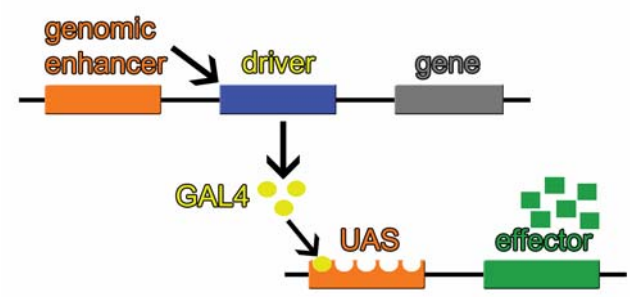

Figure 4: The UAS/GAL4 system for targeted transgene expression.
The transcription factor GAL4 (yellow circles) is expressed in a spatially ("where") and temporally ("when") restricted pattern that is determined by the genomic enhancer of a *Drosophila* gene. The GAL4 protein binds to its recognition site, the upstream activation sequence (UAS) and thereby drives expression of a transgene ("what") that encodes for the desired effector (green squares).

GAL4 driver lines

The driver line is a transgenic fly stock that carries the gene of the yeast transcriptional activator GAL4 in a P-element cassette in its genome. The GAL4 line is generated by germ-line transformation of this construct, resulting in a preferential

insertion of the construct in the 5' upstream, non-protein coding region of a gene (Spradling et al., 1995). The P-element then functions as an "enhancer trap" or "enhancer detector" (review: Bellen, 1999), as it reflects the activity of an endogenous promoter/enhancer. As an alternative, GAL4 can also be cloned downstream of the promoter/enhancer of a previously identified gene. Both methods will be used in this thesis.

The transcription factor GAL4 has no known targets in *Drosophila* and can drive expression of any desired transgene, if the latter is placed downstream of a tandem array of a GAL4 binding site, the Upstream Activation Sequence (UAS). A fly stock carrying a UAS-linked transgene is called effector strain which is eventually crossed to the GAL4 line. When GAL4 and UAS are combined in the genome of the F1 progeny, this leads to the expression of the effector transgene ("what") that is temporally ("when") and spatially ("where") restricted by the enhancer/GAL4 activity pattern (Fig. 4).

Effectors for structure-function correlations: Tools for labelling cells and blocking synaptic transmission

An effector line can, for instance, be used to identify the cell types that are labelled by GAL4 in the driver line. A very popular tool is the cytoplasmatic reporter UAS-Green Fluorescent Protein (GFP) or its membrane-targeted variant mCD8-GFP (Lee and Luo, 2001).

After selecting driver lines for the cells of interest, one can use the GAL4 transcription factor to express e.g. a toxin gene in them to unravel their function in the neuronal network. Two potent tools (Fig. 5) have been described that allow targeted suppression of synaptic activity in *Drosophila* (Sweeney et al., 1995; Kitamoto, 2001). The clostridial Tetanus neurotoxin (TNT) selectively cleaves the synaptic vesicle protein neuronal Synaptobrevin (Sweeney et al., 1995), reducing spontaneous presynaptic vesicle release and blocking action-potential evoked exocytosis (Fig. 5; Deitcher et al., 1998). The toxic effect of TNT was localized to its light chain (Schiavo et al., 1992). The corresponding DNA was introduced into the *Drosophila* genome as an UAS-linked transgene and successfully used to interfere with neurotransmission in larvae and adult flies (review: Martin et al., 2002).

A second effector for blocking chemical synapses in *Drosophila* is the temperature sensitive, dominant-negative allele of the *shibire* gene (shi^{ts1}; Kitamoto, 2001). *Shibire* encodes the GTPase Dynamin that is essential for endocytosis and

synaptic vesicle recycling (Fig. 5; Kosaka and Ikeda, 1983; Koenig and Ikeda, 1989). In neurons expressing the mutant allele *shi*^{ts1}, a shift to the restrictive temperature causes a reversible depletion of the synaptic vesicle pool (Delgado et al., 2000; Kawasaki et al., 2000). In contrast to the TNT effector, Shi^{ts1} activity can therefore be induced at the desired developmental stage by raising the temperature above 30°C (restrictive temperature) and reverted by shifting the flies back to the lower (permissive) temperature. Shi^{ts1} has been successfully used to dissect the neuronal circuitry of complex behaviors like courtship (Kitamoto, 2002; Stockinger et al., 2005) and olfactory learning (e.g. McGuire et al., 2001).

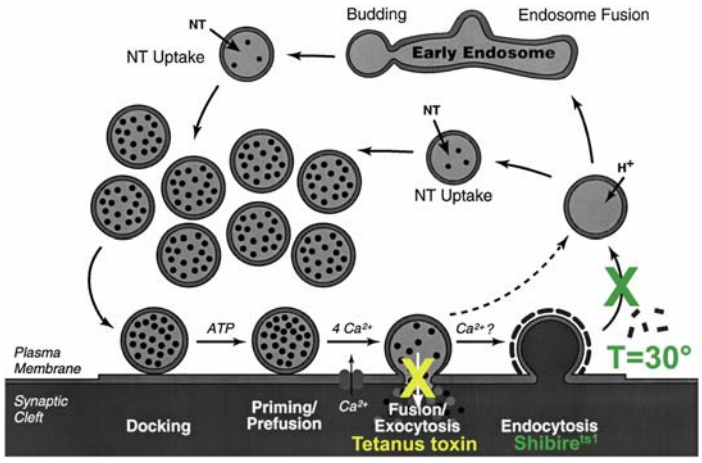

Figure 5: Two effectors that affect synaptic transmission.
Tetanus toxin selectively cleaves the synaptic vesicle protein neuronal Synaptobrevin, causing a block (indicated by yellow "X") of evoked exocytosis at the presynapse.
The *shibire* gene encodes the GTPase Dynamin that plays a vital role in endocytosis and synaptic vesicle recycling. The mutant variant, Shibire^{ts1}, is temperature-sensitive and acts in a dominant-negative manner. At temperatures of T=30°, it reversibly blocks synaptic output (indicated by green "X"; modified from Fernandez-Chacon and Südhof, 1999).

Occasionally, an attenuated version of the bacterial Diphtheria Toxin (DTI; Bellen et al., 1992; Han et al., 2000) and the human inwardly rectifying potassium channel KIR$^{2.1}$ (Baines et al., 2001) were used for genetic intervention in this thesis. The former causes cell death by inhibiting protein synthesis through ADP-ribosylation of elongation factor 2 (review: Pappenheimer, 1977) and by acting as an endonuclease (Chang et al. 1989), whereas KIR$^{2.1}$ inhibits the generation of action potentials (Johns et al. 1999).

Limitations of the UAS/GAL4 system

There are several limitations of the UAS/GAL4 system. First, GAL4 lines often label many cells in addition to the neurons of interest. Second, transcription of the UAS-target gene is not always absent without driver and appears to be insertion-dependent (Keller et al., 2002; Ito et al., 2003). This "leakiness" can be avoided by remobilizing

the construct or testing different insertions in different genomic regions. Third, effector activity depends on the expression level of GAL4. Fourth, in the original version of the binary system, it is not possible to influence the temporal expression of GAL4, for instance by restricting its expression to the adult stage. This is a major problem, as developmental expression of toxins often leads to lethality in early stages or might cause developmental defects which could be misinterpreted as consequences of effector expression at the adult stage (see Results).

Methods for adding temporal control to the UAS/GAL4 system

Several approaches have been undertaken in order to add temporal control to the UAS/GAL4 system. This ranges from the employment of the yeast FLP/FRT recombination system (Keller et al., 2002), to tetracycline-responsive transcription factors (Stebbins et al., 2001) and hormone inducible GAL4 chimeras (reviews: White et al., 2001; Duffy, 2002; McGuire et al., 2004; Roman, 2004).

An elegant solution is the TARGET system (for temporal and regional gene expression targeting; Fig. 6). It employs a temperature sensitive variant of GAL80 ($GAL80^{ts}$), the silencer of GAL4, that was fused downstream of the *tubulin* (*tub*) promoter, driving ubiquitous expression of $GAL80^{ts}$ (McGuire et al., 2003). At 18°C, the latter is active in all cells and prevents GAL4 from binding to the UAS (Fig. 6A). When the temperature is raised above 30°C, $GAL80^{ts}$ is inactivated and transgene expression commences (Fig. 6B). To make use of the existing collection of UAS-linked effectors, they have to be combined with *tub*-$GAL80^{ts}$. This has been done with several effector lines (Thum et al., 2006). By this means, toxic effectors can be switched on specifically in the adult animal, circumventing developmental defects or even lethality. Possible disadvantages are that elevated temperatures can cause mutant phenotypes (but this can be addressed by performing appropriate control experiments) and that the stability, i.e. the turnover rate of the effector protein is often unknown.

Combining the UAS/GAL4 method with behavioral analysis should allow a targeted genetic dissection of the visual system and offer strategies for distinguishing if an identified cell type is necessary and/or sufficient for a given type of visual behavior. This thesis is a first step into analyzing the role of peripheral channels of the visual system of *Drosophila*, using these techniques.

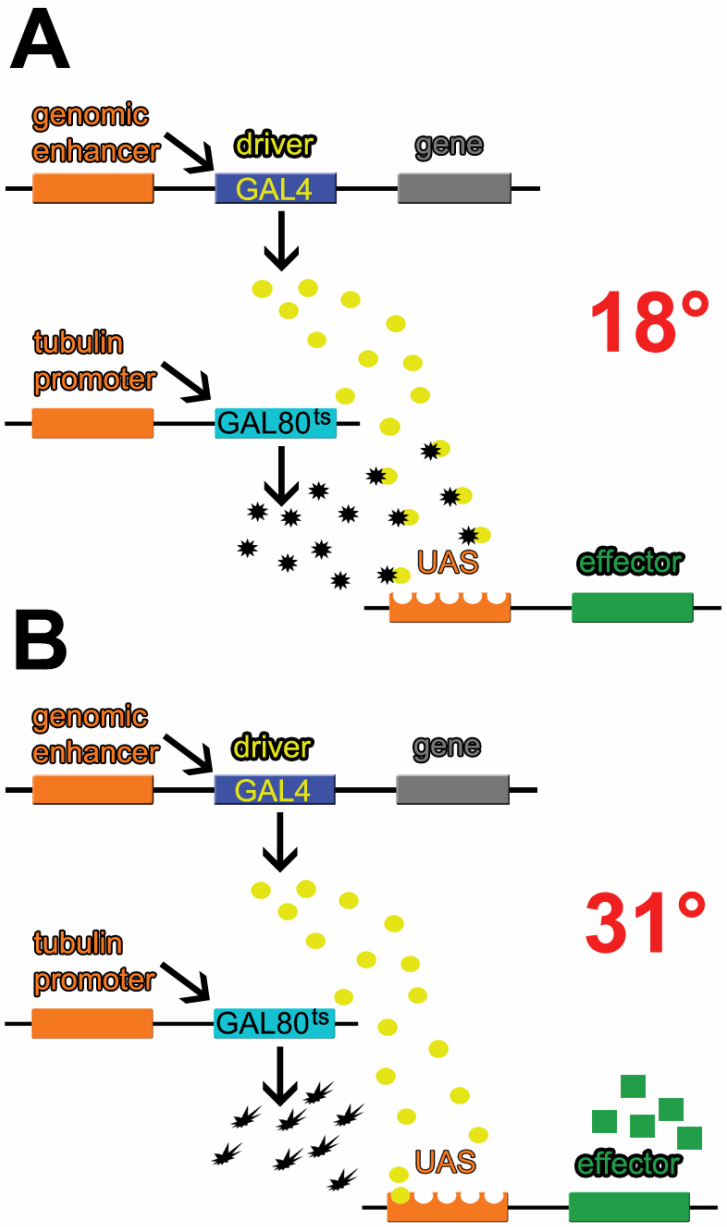

Figure 6: The TARGET (**t**emporal **a**nd **r**egional **g**ene **e**xpression **t**argeting) **system adds temporal control to the UAS/GAL4 system.** It consists of a P-element construct containing the *tubulin* promoter fused to a temperature sensitive allele of the GAL4 inhibitor GAL80 ($GAL80^{ts}$).
(A) At 18°C, $GAL80^{ts}$ (black asterisks) is expressed in all cells and prevents GAL4 (yellow circles) from binding to the UAS sequence. The effector gene is therefore not expressed under these conditions.
(B) After a temperature shift to 31°C, $GAL80^{ts}$ is inactivated (misshaped black asterisks). GAL4 can drive effector expression (green squares).

2. Results

2.1. Genetic intervention in photoreceptors

As a prelude into genetically dissecting the peripheral visual system, Tetanus neurotoxin (TNT) was expressed in photoreceptors, as described by Keller et al. (2002). These authors reported that expression of TNT with the driver GMR-GAL4 (Freeman, 1996) throughout eye development in all photoreceptor cells (R1-R8) abolished the optomotor response of tethered walking flies (paradigm designed by Buchner, 1976). As expected, control flies expressing a mutationally inactivated TNT protein (IMPTNT; Sweeney et al., 1995), behaved like wild type. These results were reproduced (Fig. 7A).

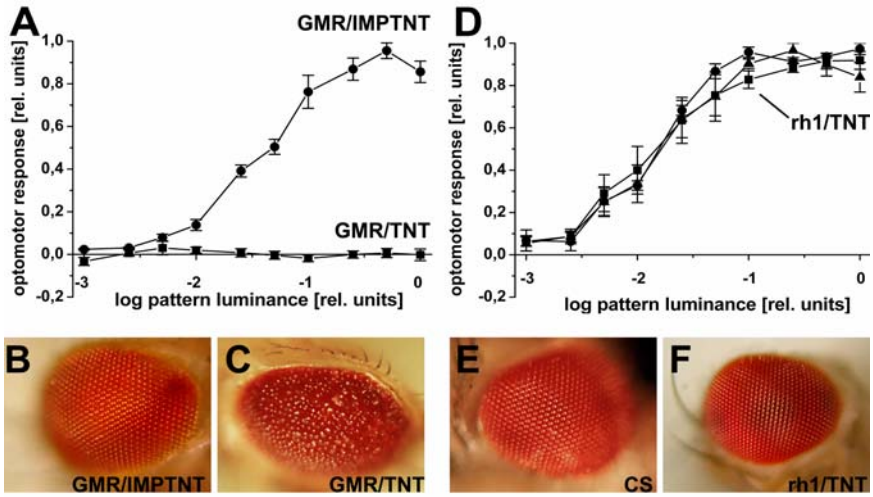

Figure 7: Effect of Tetanus toxin (TNT) expression in *Drosophila* photoreceptors.
(A) Optomotor response (ω/λ=1Hz; λ=45°) as a function of pattern luminance, of tethered walking flies expressing active (GMR-GAL4/UAS-TNT, squares; N=5) or inactive TNT (GMR-GAL4/UAS-IMPTNT, circles; N=4) in all photoreceptors throughout development.
(B, C) Adult eye structure of flies belonging to the genotypes measured in (A). The retina of GMR-GAL4/UAS-IMPTNT flies (B) is wild-type (compare to E), whereas in GMR-GAL4/UAS-TNT flies (C) it is severely impaired.
(D) Optomotor response [same conditions as in (A)] of the genotypes *rh1*-GAL4/UAS-TNT (N=6; squares), in comparison to the effector UAS-TNT/+ (N=3; circles) and driver *rh1*-GAL4/+ (N=3; triangles) control. Note that no significant difference is found between the three genotypes ($p>>0.05$ in all cases; ANOVA test), even near the low intensity threshold ($p>0.7$).
(E) Adult eye structure of wild type Canton S (CS) controls and flies expressing TNT in photoreceptor subset R1-R6 driven by *rh1*-GAL4 starting in late pupal development (F).

Next, for selectively interfering with peripheral motion processing, the aim was to block synaptic output from photoreceptor subset R1-6 that is known to be necessary and sufficient for mediating the optomotor response (Heisenberg and Buchner, 1977). Surprisingly, these flies showed wild-type optomotor behavior in the same paradigm as described above (Fig. 7D), although the driver *rh1*-GAL4 (Fig. 8; Mollereau et al.,

2000) caused high expression levels of TNT in the R1-6 terminals (see Fig. 8B for TNT detection in optic lobe section obtained directly after the behavioral test).

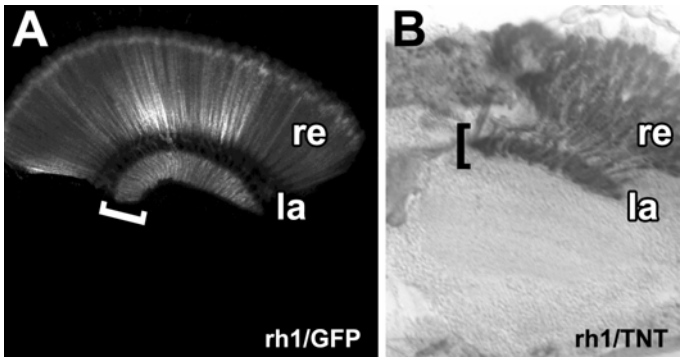

Figure 8: Comparison of the expression of two effector transgenes with the *rh1*-GAL4 driver.
(A) *rh1*-GAL4 drives cytoplasmatic GFP visualizing the R1-6 photoreceptors which terminate in the lamina (la, bracketed).
(B) Detection of *rh1* driven TNT expression with a monoclonal anti-TNT antibody. The cryosection was obtained immediately after the measurement of wild-type optomotor behavior in the optomotor assay (Fig. 7D). A strong immunopositive signal is detected in the retina (re) and the corresponding photoreceptor axon terminals in the lamina (la, bracketed).

A reason for this unexpected discrepancy could be the difference in developmental activity of the drivers: GMR-GAL4 activity begins already at the larval stage (e.g. Yang and Kunes, 2004), whereas the onset of *rh1* promotor activity is during late pupal development (Kumar and Ready, 1995). This hypothesis is supported by the severe eye defects of GMR-GAL4/UAS-TNT flies, which were not found in flies expressing the impotent TNT under GMR control (Figs. 7B, C). In contrast, eyes of *rh1*-GAL4/UAS-TNT flies were normal, implying that indeed the onset of driver activity was critical for the mutant phenotype (Figs. 7E, F).

In addition, GMR-GAL4/UAS-TNT flies exhibited a severe hypoplasia of the lamina neuropil (bracketed in Fig. 9A), as revealed by an antibody against the synaptic vesicle marker Cysteine String Protein (Zinsmaier et al., 1994). This defect was neither found in heterozygous effector control flies (Fig. 9B), nor in flies expressing the impotent TNT under GMR control (Fig. 9C), nor in *rh1*-GAL4/UAS-TNT flies (Fig. 9D).

Taken together, expression of active TNT throughout eye development by means of the driver GMR-GAL4 affected eye structure and the lamina neuropil. Late expression of the toxin during pupal development with the driver *rh1*-GAL4 did not cause this defect.

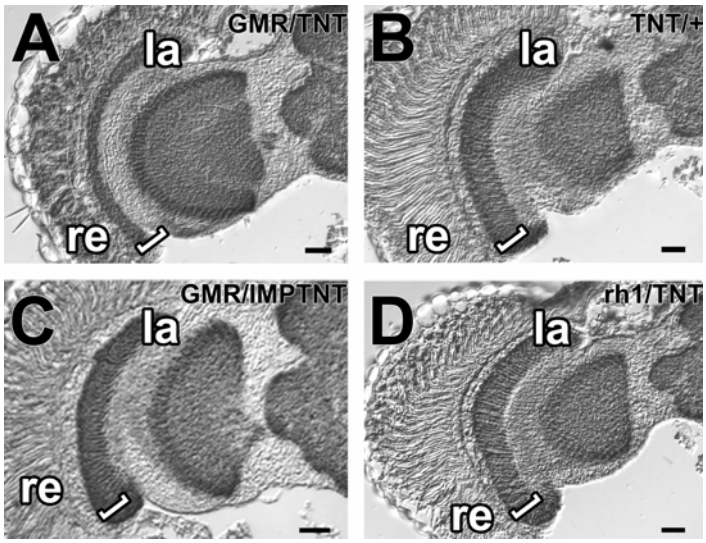

Figure 9: Frontal cryosections stained against the synaptic vesicle marker Cysteine String Protein.
(A) Flies expressing TNT throughout photoreceptor development (GMR-GAL4/UAS-TNT) are characterized by a severely impaired retina (re) and a hypoplasia of the lamina neuropil (la, bracketed; compare to B-D). These defects are not found in the control genotypes UAS-TNT/+ (B) and GMR-GAL4/UAS-IMPTNT (C). (D) *rh1*-GAL4/UAS-TNT flies that express TNT in photoreceptors starting with late pupal development have a wild-type retina and lamina anatomy. Scale bars: 20 μm.

2.1.1. Critical periods for the structural and functional defects found after Tetanus toxin expression in developing photoreceptors

As other differences except the onset of expression of the two photoreceptor drivers, *rh1*-GAL4 and GMR-GAL4, can not be fully excluded, a decisive experiment would be to induce the GMR-GAL4 driver at defined developmental stages that had caused motion blindness in combination with TNT (see above). This was achieved by using the TARGET system (McGuire et al., 2003; Thum et al., 2006) that allowed temporal control of GMR-GAL4 driven TNT expression. Developing flies were shifted to the restrictive temperature (T=31.5°C) at defined developmental stages (Bainbridge and Bownes, 1981), inducing TNT expression. After 24 hours they were shifted back to 18°C, in order to block further synthesis of TNT. Next, the functionality of the mature photoreceptor synapses was tested by measuring optomotor responses and recording the electroretinogram (ERG; Heisenberg, 1971). The ERG in response to an intense one second light pulse typically consists of the sustained negative photoreceptor potentials and phasic responses of downstream lamina neurons. These “on”- and “off”-transients indicate synaptic transmission from R1-6 onto lamina monopolar cells (Coombe, 1986; Hardie, 1989).

At 18°C, pupal development including a 24h induction phase at 31.5°C lasted about 8 days until time of eclosion. The respective developmental stages were timed by measuring the number of hours that had passed after puparium formation (corresponding to 0% pupal period), and were expressed as a % value after dividing by 191 h (x100). TNT induction in photoreceptors 24 hours before and ending with

puparium formation (day 0 in Fig. 10A) had no significant behavioral or anatomical consequences.

However, if TNT was induced in early pupae for one day between day 0 (0% PP) and the midpupal stage (50% PP), synaptic transmission was irreversibly blocked until adulthood, as revealed by the complete absence of optomotor behavior (Fig. 10A). Moreover, at days 0 (0% PP) and 1 (12.5% PP), the 24h TNT induction also caused abnormal retinae (N=21; Fig. 10B). This mutant phenotype was stronger when compared to flies expressing TNT throughout eye development at 25°C (compare Fig. 10B to Fig. 7C). As already the GMR/+ control flies had mildly roughened eyes (not shown) after being heat-shocked in the same time window (but without showing an optomotor deficit, Fig. 10A), the enhancement is most likely caused by an additional detrimental effect of the higher temperature (T=31.5°C) during induction. Most importantly, the temperature alone did not affect eye development, as UAS-TNT/+; *tub*-GAL80^{ts}/+ control animals appeared normal (not shown).

Flies induced at day 4 (50% PP) specifically showed the TNT-induced hypoplasia of the lamina, but had a wildtype eye morphology (Figs. 10C-E). The adult flies had no “on”/ “off”-transients in the ERG (N=4; data not shown) and did not show significant optomotor behavior. Control flies (GMR-GAL4/+ and UAS-TNT/+; *tub*-GAL80^{ts}/+) were kept in parallel and their responses were unaffected by this treatment at all investigated time points (Figs. 10A, D, H).

A transition phase for TNT induced defects was observed at day 5 (~63% PP), when pigmentation started spreading across the pupal eye (corresponding to stage P8 of Bainbridge and Bownes, 1981). Toxin expression from day 6 on (~75% PP; stage P9/10 of Bainbridge and Bownes, 1981), when the developing eyes had a bright orange pigmentation, neither affected the structure nor the function of the peripheral visual system, as shown by the wild-type ERG and optomotor behavior. These results are in line with the absence of behavioral, physiological or anatomical mutant phenotypes of *rh1*-GAL4/UAS-TNT flies. Immunohistochemistry against the target of TNT, neuronal Synaptobrevin, suggests that the toxin lost its potency at this stage (Figs. 10F, G).

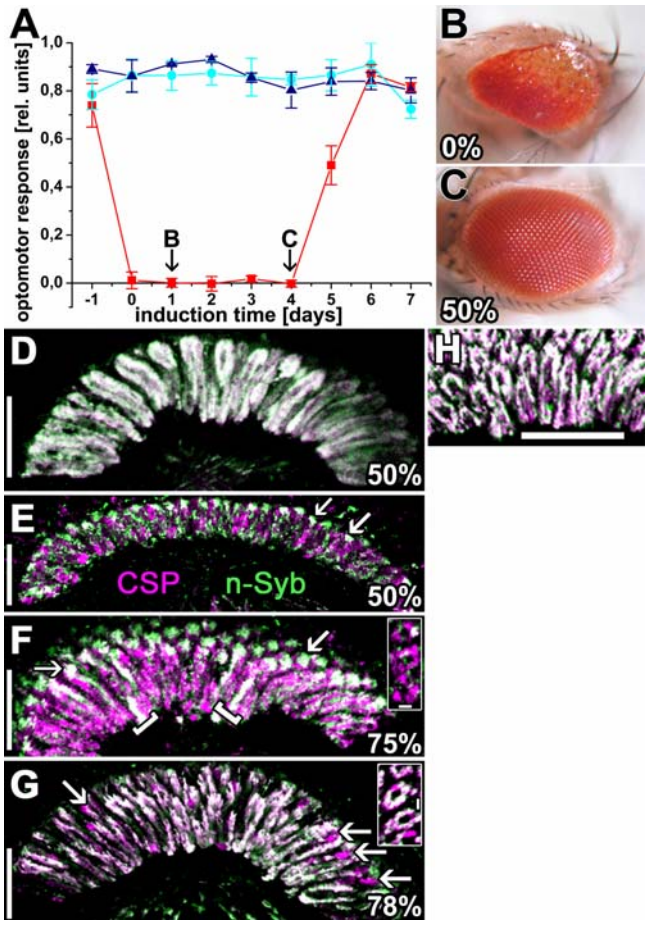

Figure 10: Differential effects of Tetanus toxin expression in photoreceptors at defined developmental stages.
(A) Effects on optomotor behavior. Data points indicate the averaged optomotor responses (ω/λ=1Hz; λ=45°; maximal light intensity) of up to 13 adult flies performing up to 30 trials after induction of TNT (at 31.5°C) for 24h starting at the given time point [days of pupal development]. Time zero corresponds to puparium formation; eclosion time is at the end of day 7. Squares: experimental flies (GMR-GAL4/UAS-TNT; *tub*-GAL80^{ts}/+); circles: driver control (GMR-GAL4/+), triangles: effector control (UAS-TNT/+; *tub*-GAL80^{ts}/+). The toxin caused blindness in adult flies when induced in the time window between the onset (day 0) and day 4 (corresponding to 50% PP) of pupal development. The arrows indicate the corresponding induction time points leading to the eyes shown in (B) and (C). (B), (C): Effects on adult eye morphology after TNT expression at two different time points. (B) When TNT was expressed for 24h beginning at day 1 (0% PP) of pupal development, fused facets were observed. (C) In contrast, when induction started at day 4 (50% PP), the adult flies had normal eyes consisting of precisely organized hexagonal ommatidia. (D-H): Comparison of laminae (D-H) double stained with antisera against the synaptic vesicle proteins CSP (purple) and n-Syb (green). Shown are 7-13 µm thick confocal image stacks of horizontal agarose sections. Insets in (F) and (G) show 0.8 µm cross-sections of lamina cartridges. Temporal is up, nasal down. Scale bars: 20 µm [insets in (F, G): 2 µm]. (D) Lamina of a control fly expressing impotent TNT under GMR-control that was shifted to the inductive temperature at the same time point as the experimental fly in (E). All cartridges show a significant overlap (white) between CSP and n-Syb. (E) Distribution of CSP (purple) and n-Syb (green) in the lamina after GMR-GAL4 driven TNT expression in all photoreceptors starting at 50% PP (see Methods). N-Syb immunoreactivity is dramatically reduced in comparison to the effector control [UAS-TNT; *tub*-GAL80^{ts}, (H)]. White dotted structures in the distal lamina are stained by both antibodies and presumably correspond to C2 terminals (arrowed). Note that the proximal-distal extent of the lamina is significantly reduced while eye structure (C) is unaffected. (F) Effect of TNT expression at 75% PP. The toxin causes a significant reduction of n-Syb staining in the axons of R1-6 defining the lamina cartridges (see also inset) which, in contrast, are strongly stained by the CSP antiserum. Few profiles of single photoreceptor terminals (bracketed) retain significant amounts of n-Syb (see also uppermost cartridge in the inset). C2 terminals can be easily identified [arrows, compare to (E)].
(G) Flies expressing TNT under control of *rh1*-GAL4 (with promoter activity starting at ~78% PP) exhibit a weak reduction of n-Syb in only few R1-R6 profiles (arrows). The *inset* shows cross-sections of lamina cartridges with n-Syb immunoreactivity lacking in only a minority of receptor terminals (purple). (H) Lamina of a control fly carrying the effector constructs UAS-TNT and *tub*-GAL80ts but no GAL4 driver. Both vesicle markers show a clear cut overlap (white) in all optic cartridges. Oblique section revealing also cross-sectioned cartridge profiles [compare to insets in (F, G)].

In summary, several conclusions for UAS-TNT as a tool for neurogenetic analysis can be drawn from these results. First, TNT clearly caused developmental defects in photoreceptor neurons. Therefore, its expression during development should be avoided and temporally restricted expression (e.g. by using the TARGET system) is vital for obtaining valid results. Moreover, developmental TNT expression can lead to misinterpretations of mutant phenotypes found in adult flies. For instance, if a driver would label photoreceptors only during early pupal development, mutant phenotypes observed in mature flies could be wrongly attributed to other cells labelled by the driver at this stage.

2.1.2. Signal transmission at the mature photoreceptor synapse is blocked by Shibire^{ts1}

The behavioral experiments with the *rh1*-GAL4 driver provided evidence that TNT does not suppress synaptic transmission if specifically expressed in mature photoreceptors. This view was confirmed by driving TNT with GMR-GAL4 exclusively in the adult fly. Temporal control was again achieved by combining the driver with the TARGET system. Shifting these flies to the restrictive temperature (T=31.5°C) for 24 hours during adulthood inactivated *tub*-GAL80^{ts} and induced TNT expression in photoreceptors, without affecting the structure of the retina or the lamina (Fig. 11A).

The amount of TNT in the lamina as judged by immunohistochemistry was lower than in *rh1*-GAL4/UAS-TNT flies (Fig. 8B) suggesting that this difference is a result of TNT accumulation in the latter flies due to the longer total expression time. In contrast, *tub*-GAL80^{ts} largely prevented toxin expression at 18°C (Fig. 11B). Under these conditions, experimental flies had normal eyes and laminae.

In line with the results obtained with the *rh1*-GAL4 driver, optomotor responses of induced experimental flies were not significantly different from those of uninduced control flies, neither under optimal stimulus conditions (Fig. 11C), nor at low signal strength in the vicinity of the low light intensity threshold (N=6; data not shown). The cause of optomotor blindness in GMR-GAL4/UAS-TNT flies, therefore, had to be a detrimental effect of the toxin during development.

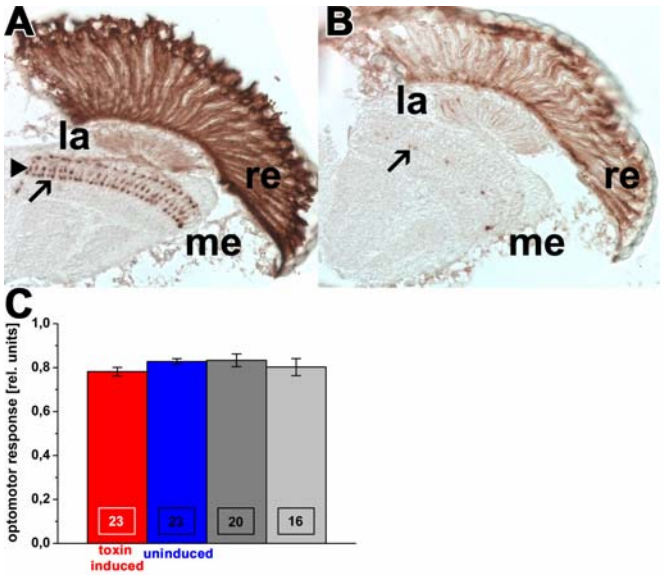

Figure 11: Expression of tetanus toxin specifically in adult photoreceptors has no effect on optomotor behavior.
(A, B) Targeted temporal induction of TNT in adult photoreceptors in GMR-GAL4/UAS-TNT; *tub*-GAL80^{ts}/+ flies visualized with a monoclonal anti-TNT antibody. (A) TNT expression was successfully induced in adult flies with a 24h temperature shift to 31.5°C. Strongly stained are the retina, columnar fibers in the lamina (corresponding to terminals of R1-6 and axons of R7 and R8) and terminals of R7 (arrow) and R8 (open arrowhead) in the distal medulla. In horizontal head sections of uninduced animals raised at 18°C (B), some leaky expression of TNT was detected in the retina (re), the anterior lamina (la; arrowheads) and in very few terminals of R7 in the distal medulla (arrows). Scale bars: 20 µm.
(C) Optomotor responses (contrast frequency ω/λ=1Hz; λ=45°) of walking GMR-GAL4/UAS-TNT; *tub*-GAL80ts/+ flies raised at 18° (N=4; blue bar) were neither different from flies of the same genotype with induced toxin expression (N=6; red bar), nor from the control genotypes UAS-TNT/+; *tub*-GAL80^{ts}/+ (N=5; dark grey bar) and GMR-GAL4/+ (N=4; light grey bar). Controls were treated like the experimental group, i.e. shifted for 24h to 31.5°C. All groups are not significantly different from each other (ANOVA test; p>0.44). Numbers on the bars denote performed trials.

These data provide evidence that the synapses of R1-6 were not blocked in *rh1*-GAL4/UAS-TNT flies despite the high expression level (Fig. 8B). To demonstrate this more directly, the ERG was recorded. The "on"- and "off"-transients (arrowed in Fig. 12C) that represent synaptic transmission from R1-6 to lamina interneurons, were wildtype in all experimental flies tested (N=6; Figs. 12A-C). This further implies that when no mutant phenotype is detected after TNT expression, it is not possible to exclude a functional role of the investigated cell type in a given task, unless it is shown by electrophysiological recordings that the respective synapse was fully blocked.

Finally, it needs to be ruled out that other properties of the *rh1*-GAL4 driver, e.g. incomplete labelling of R1-6 (but see Figs. 8A, B), were responsible for the lack of effect on signal transmission. To this end, *rh1*-GAL4 was combined with UAS-*shi*^{ts1}. This transgene is known to cause a reversible, temperature-dependent block of vesicle endocytosis (Kitamoto, 2002). At the permissive temperature (T=25°C) these animals had a normal ERG (Fig. 12D, left panel) but after 8 min at the restrictive temperature (T=31.5°C), a complete loss of the transients was observed (Fig. 12D, arrows in right panel). Moreover, yaw torque responses in flight (Fig. 13A; Pauls, 2006) as well as head yaw or roll optomotor responses (contrast frequency: 1.5 Hz; λ=60°), were

abolished after effector induction (data not shown). The optomotor response in walking could also be suppressed by Shi^{ts1} induction in the same experimental setup that was used in the TNT experiment (Fig. 13B).

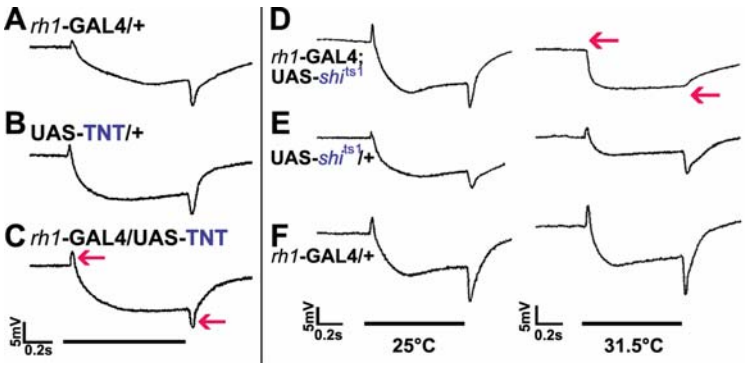

Figure 12: Electrophysiological analysis of the consequences of Tetanus toxin and Shibire^{ts1} expression in mature photoreceptors on synaptic transmission.
Electroretinograms (ERGs) of driver (A) and effector (B) controls in comparison to flies expressing *rh1*-GAL4 driven TNT in photoreceptor subsystem R1-R6 (C). Note that expression of the toxin had no effect on synaptic transmission as reflected by the persistence of the two transient peaks at lights on and lights off in the ERG (arrowed). (D-F) ERGs of flies expressing the dominant negative *shibire* allele (*shi*^{ts1}) by *rh1*-GAL4 (D) in comparison to the effector (E) and driver (F) controls. At the permissive temperature (25°C, left panel), all genotypes show the typical transient peaks at lights on and lights off. At the restrictive temperature (31.5°C, right panel) signal transmission stops only in the experimental group (D) as indicated by the absence of the transients (arrows). Horizontal bars indicate the duration of the light pulse.

Taken together, the suppression of the lamina transients in the ERG and of the optomotor response demonstrated that with the appropriate effector gene, *shi*^{ts1}, the synapses of photoreceptors R1-6 could be blocked. This tool also had turned out to be the most potent in another recent publication in which several effectors were compared (Thum et al., 2006). For this reason, all further blocking experiments of this thesis were performed with UAS-*shi*^{ts1}.

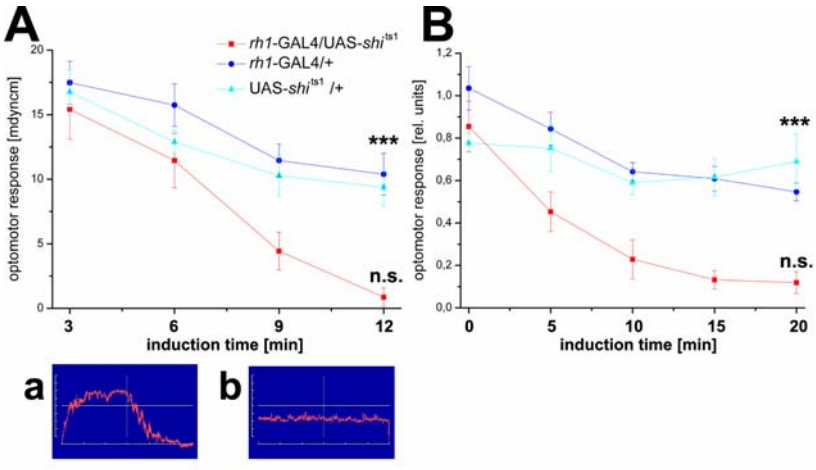

Figure 13: The consequences of *shi*^{ts1} expression in photoreceptor subsystem R1-6 on optomotor responses in tethered flying (A) and walking (B) *Drosophila*.
(A) After 12 minutes at T=31-33°C, optomotor yaw responses in flight were abolished in experimental flies (red), but not in driver (dark

blue) or effector (light blue) control animals ($p<0.001$; ANOVA test).
(a, b) Yaw torque traces of an experimental fly at the beginning of the temperature shift (a). Vertical dotted line indicates the change of pattern rotation from clockwise to counterclockwise. The same fly after 12 minutes at the restrictive temperature (b). Note that the animal still shows yaw torque activity, but does not significantly respond to the moving pattern.
(B) *Shi*^{ts1} also blocked optomotor responses in tethered walking flies after 20 minutes at the restrictive temperature ($p<0.001$; ANOVA test). Genotypes are the same as in (A).

2.2. Genetic intervention in peripheral pathways of the visual system

Several strategies were pursued to obtain GAL4 lines labelling lamina interneurons as a tool for the genetic dissection of the peripheral visual system. First, as these cells receive histaminergic input from R1-6 (Hardie, 1989; Pollack and Hofbauer, 1989; Melzig et al., 1998), enhancer-GAL4 lines for two genes encoding histamine receptor subunits were generated by A. Thum (Würzburg), in cooperation with T. Roeder (Kiel). Second, a GAL4 enhancer trap image database (Hayashi et al., 2002; cooperation with K. Ito, Tokyo) containing about 4000 driver lines was screened. Third, two GAL4 lines that had been described earlier (GH146 and 21D, Heimbeck et al., 2001; Keller, 2002) were used for anatomical and behavioral analysis.

2.2.1. Histamine receptor-GAL4 lines

Recently, three groups reported the cloning of two *Drosophila* genes that encode histamine-gated chloride channel subunits, *ort* (*hisclA*) *and hisclB* (Gisselmann et al., 2002; Witte et al., 2002; Zheng et al., 2002). As the first-order interneurons of the lamina are known to receive histaminergic input from R1-6 (Hardie, 1989; Pollack and Hofbauer, 1991; Melzig et al., 1998), the enhancer regions of these genes could be used to specifically drive GAL4 in lamina interneurons.

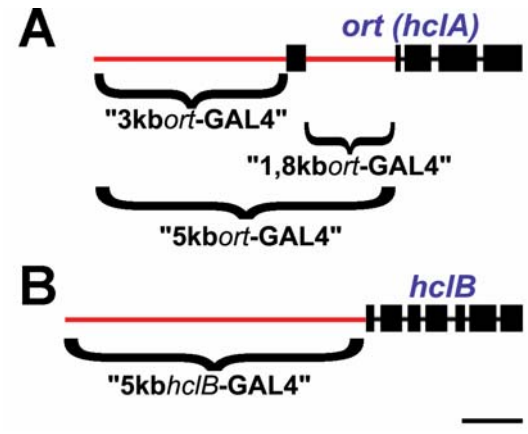

Figure 14: Schematic structure of two genes, *hclA* (A) and *hclB* (B) that encode histamine receptor subunits.
Red lines indicate putative enhancer regions that were cloned and used to drive GAL4. Brackets indicate the position and length of the respective DNA fragments.
Scale bar: 1kb.

2.2.1.1. *Ort* (*hisclA*)-GAL4 lines

All known *ort* mutants are characterized by the lack of "on" and "off" transients in the electroretinogram (Pak, 1975; Buchner, 1991; Burg et al., 1993), indicating a defect in signal transmission from histaminergic photoreceptors to postsynaptic lamina interneurons (Coombe, 1986; Hardie, 1989). Gengs et al. (2002) were able to restore these ERG transients by P-element mediated germ-line rescue with ort^{+} cDNA. This is strong evidence that *ort* encodes a histamine receptor subunit that is located in the first-order lamina interneurons and is further supported by the *ort* positive *in situ* hybridization signals in cell bodies of the lamina cortex (Witte et al., 2002).

Expression patterns of *ort* enhancer-GAL4 lines

An *ort* enhancer-GAL4 line should therefore label the first-order interneurons, but not the other lamina cell types. For this reason, several *ort* enhancer-GAL4 constructs were generated and provided by A. Thum (Würzburg), in cooperation with T. Roeder (Kiel). First, an upstream 3kb fragment was analyzed (Fig. 14A). As expected, GFP expression was detected in lamina monopolar cells. Their large cell bodies in the lamina cell body layer were immunopositive, as well as radially oriented dendrites in the lamina neuropil. In the medulla, terminals of L1 and L2 were stained (Fig. 15A), but the ones of L3 were only weakly labelled (indicated by arrowhead in inset of Fig. 15A). However, the overall staining pattern was patchy (indicated by arrows in Fig. 15A) and its intensity was variable in neurons of the same cell type (inset in Fig. 15A). This was found independently of the insertion of the GAL4 construct (three were investigated) and the immunohistochemical method. It showed in agarose sections as well as in whole mounts stained against the reporter GFP, as well as in cryosections stained against the effector TNT (data not shown). A L1L2-driver (NP 6298, see below) stained in parallel did not exhibit this phenomenon. As the combination of a second- and a third-chromosomal insertion resulted in an enhanced labelling of the monopolar cells (Fig. 15B), especially concerning the L3 terminals (filled arrowhead), this implies that the variable concentration or variable binding efficiency of GAL4 was responsible for the mosaic pattern.

The medulla rind exhibited staining of cell bodies (cb in Figs. 15A, B) of transmedullary cells. Their columnar axons and distal stratifications (indicated by open arrowhead in Figs. 15A, B) were labelled in the medulla, as well as their terminals in the lobula (Fig. 15C). The staining of these cells, which are most likely the targets of R7

and R8 in the medulla, was more homogeneous. A lobula output neuron (arrowed in Fig. 15C) was also GFP positive.

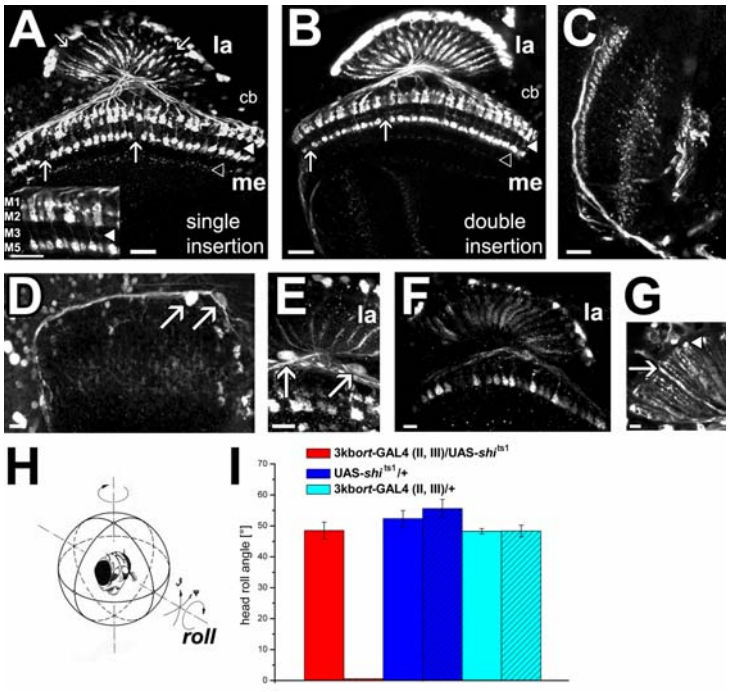

Figure 15: *Ort* enhancer-GAL4 lines.
(A) A single insertion of 3kb*ort*-GAL4 drives GFP in lamina (la) monopolar cells and medulla (me) cells (indicated by open arrowhead; cb: cell bodies). Note that the expression pattern is patchy (arrows). The arrowhead indicates the level of L3 terminals. Inset: 40x magnification of the distal medulla. Layers M1, M2 and M5 are strongly stained, corresponding to the specializations of L1 and L2. The L3 layer (M3, arrowhead) exhibits only weak staining. (B) Double insertion of 3kb*ort*-GAL4 driving GFP. Note that the staining in the distal medulla is less patchy (compare to A) and that the L3 staining is much more pronounced (filled arrowhead). However, cells of the same type still exhibit different effector expression levels (arrowed). (C) Several layers of the lobula are also GFP positive. Scale bars in (A-C), 20 µm. (D, E) At the level of the outer optic chiasm, two to three large cell bodies (arrowed) were stained that closely resemble those of optic lobe pioneer neurons (for details, see text). Scale bar: 10µm. (F) The small 1,8kb *ort* intron fragment drove GFP in L2 lamina monopolar cells. Staining intensity varied between individual cells. Scale bar: 8µm. (G) A 5kb*ort*-GAL4 line labelled looped fibers in the lamina (arrowed) and small nodular structures (arrowhead) that may correspond to amacrine cells. Scale bar: 4µm.
(H, I) Head roll optomotor responses (ω/λ = 3Hz; λ = 24°) around the body axis of the fly were wildtype (I) when *shi*^{ts1} was driven by the double insertion of 3kb*ort*-GAL4 under permissive conditions (red bar), but abolished after the temperature shift (second red bar). This was not observed in effector (dark blue bars) and driver (light blue bars) control animals that were unaffected by the elevated temperature.

In very patchy expression patterns of two independent insertions (II6 and III7-2) of 3kb*ort*-GAL4, a small number of unusually large cell bodies (arrowed in Figs. 15D, E) was noted at the level of the outer optic chiasm, sending their long axons tangentially to the outer rim of the medulla (Figs. 15D, E). These resembled the optic lobe pioneer cells (Fischbach and Dittrich, 1989; Tix et al. 1989) that are thought to have a pioneering function in optic lobe development. Their function in the adult brain is not known.

The first 1.8kb intronic DNA fragment of *ort* (Fig. 14A) drove GFP expression in a more restricted pattern (Fig. 15F). Patchy labelling of L2 was found, whereas the

other monopolar cells were not immunopositive. In addition, weak cell body labelling and specializations in the medulla of a columnar glia cell were detected.

When a 5kb DNA fragment covering the 3kb upstream region as well as the basal promoter and the first intron of the *ort* gene (Fig. 14A) was used to express GFP, patchy expression of lamina monopolar cells was still observed (not shown). Interestingly, looped fibers (arrowed in Fig. 15G) were immunopositive that could correspond to lamina amacrine processes. Distally, small nodular structures (arrowhead) were labelled that are a part of the tangential arborizations of amacrine cells in large flies (Douglass and Strausfeld, 2005).

In summary, the *ort* enhancer fragments tested expectedly labelled first-order lamina interneurons. Enhancer information was found in the 5' upstream region as well as in the first intron. Staining intensity of neurons of the same cell type was variable and could be enhanced by increasing the copy number of the GAL4 driver.

Behavioral consequences of blocking lamina interneurons labelled by *ort*-GAL4

Only the double insertion strain carrying two copies of 3kb*ort*-GAL4 was investigated in behavioral experiments. Head optomotor responses were measured that serve for gaze stabilization in walking and flight (Land, 1973; Hengstenberg, 1993; Kern et al., 2006). In the head roll paradigm (Fig. 15H), flies expressing shi^{ts1} in the first-order lamina interneurons at the restrictive temperature did not respond to the large-field motion stimulus (λ=12°; w/λ=3Hz) that rotated around the body axis of the fly (Fig. 15I). However, spontaneous head roll movements not consistent with the direction of motion were observed. At the permissive temperature, experimental and control genotypes were not significantly different from each other.

Using the same genotypes and induction protocol, but a lower spatial frequency (λ=60°) and a lower contrast frequency (w/λ=1.5Hz), Pauls (2006) found dramatically reduced, but significant turning responses (in average about 5°; N=16). Given the fact that seven experimental flies were motion blind and the others were strongly impaired, the most likely explanation for the failure of completely abolishing the response is the patchy expression pattern of the driver (see above): It had been shown earlier that few functional VSUs are sufficient to mediate optomotor responses (Götz, 1983). In tethered flight, responses not significantly different from zero were found for a low spatial wavelength of λ=7.2° (w/λ=1.4Hz; N=8; Pauls, 2006).

An alternative to blocking the output of L1 and L2 would be to prevent input into these cells by RNA mediated interference (RNAi; Cerutti, 2003; Roman, 2004) targeted against the *ort* mRNA. The often observed lack of specificity of lamina interneuron driver lines (see below) would then be a minor problem, as the RNAi construct would affect only those which express this histamine receptor. Therefore, it was attempted to create such a construct in cooperation with T. Roeder (Kiel) and A. Thum (Würzburg) and several independent insertion lines were established. An additional RNAi construct (Dietzl et al., 2007) against *ort* was kindly provided by Barry Dickson (Vienna). However, none of those was able to phenocopy the *ort*$^{-}$ phenotype, not even with the ubiquitous drivers *Actin*-GAL4 and *tubulin*-GAL4. This was not improved by raising the experimental flies at 29°C in order to provide maximal GAL4 activity (Brand and Perrimon, 1993; Duffy, 2002) and therefore highest RNAi effectiveness.

2.2.1.2. *hisclB*-GAL4

A second gene (*hisclB*; Fig. 14B) that encodes another histamine receptor subunit was recently described (Gisselmann et al., 2002; Zheng et al., 2002). As *in situ* hybridization data were not available, an enhancer-GAL4 line for *hisclB* could provide first insights into its expression pattern.

The GFP staining driven by 5kb*hisclB*-GAL4 (Fig. 16A) specifically labelled lamina intrinsic cells surrounding the neuroommatidia (Fig. 16B; arrowed in Figs. 16C, D) that are formed by R1-6 axon bundles (not stained; indicated by arrowhead in Fig. 16B).

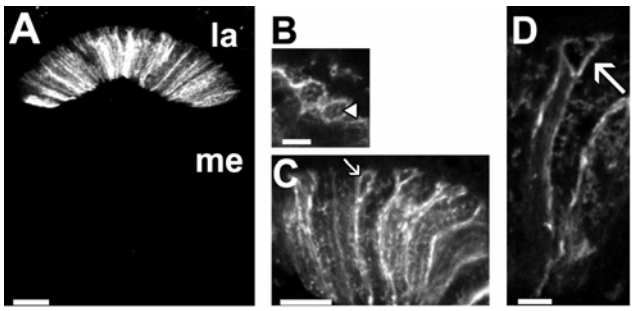

Figure 16: Projection views of the 5kb *hisclB* enhancer-GAL4 line driving expression of membrane targeted GFP. (A) Fibers in the lamina (la) were specifically labelled by this line. Note that no effector expression was detected in other regions of the optic lobe. Scale bar, 20 µm. Cartridge cross-sections reveal that the fibers surround the neuro-ommatidia (B). Note that the axon terminals of R1-6 were not stained (arrowhead). Scale bar: 5µm. (C, D) The fibers extend throughout the lamina and surround the cartridges (arrowed). Scale bars, 10 µm.

This expression pattern was found with three independent reporters (UAS-GFP, UAS-mCD8GFP, UAS-Cam$^{2.1}$) and resembled that of epithelial glia, similar to the ones revealed by an antibody against the Ebony protein that is specifically expressed in

lamina glia cells (see Figs. 3F, G in Richardt et al., 2002). Behavioral experiments were not performed with this driver line.

2.2.2. GAL4 line GH146 labels L1, L3 and L4

The enhancer trap GAL4 line GH146 had been described earlier by Heimbeck et al. (2001) and Keller (2002). These authors reported to have blocked evoked synaptic transmission "most likely" in L1 and L2 and other unidentified cell types in the medulla and lobula complex by constitutively driving expression of TNT. This resulted in a severe impairment of optomotor and orientation behavior.

First, the staining pattern of GH146-GAL4 (Figs. 17A-D) was reinvestigated using the homozygous driver line (obtained from T. Spall and A. Fiala, Würzburg) that was also homozygous for UAS-Cam$^{2.1}$ containing two GFP variants (Diegelmann et al., 2002). The specializations in the most proximal medulla layer (M10, Fig. 17B) closely resemble the dendrites of "bushy" T4 cells that project to the lobula plate. The immunopositive cells that have their arborizations in the most superficial lobula layer (Lo1, Fig. 17B) could be T5 cells that also have their synaptic output in the lobula plate (Fischbach and Dittrich, 1989; Strausfeld and Lee, 1991; Douglass and Strausfeld, 1995). Both cell types have their cell bodies in the cell body rind posterior to the lobula plate (arrowed in Fig. 17B; Fischbach and Dittrich, 1989) the fibers of which project through the inner optic chiasm (IOC in Fig. 17B).

In the distal medulla the specializations of L1 in M1 and M5 and the terminal arborizations of L3 (single terminal arrowed in Fig. 17C) were labelled. These are also indicated by the middle arrow in Fig. 26 of Keller (2002) that are more proximal than expected for L2's terminals that should be directly apposed to the distal arborization of L1 (see also below). Moreover, the terminals of the second-order interneuron L4 were stained (arrowed in Fig. 17D).

Heimbeck et al. (2001) and Keller (2002) found that after blocking the cells labelled by GH146-GAL4 with TNT, the flies did not respond to moving large-field stimuli, neither in walking, nor in a head roll optomotor paradigm. They also didn't show the visually elicited landing response, but were able to approach broad stationary landmarks of δ=60° width. This could be reproduced (Fig. 17E and data not shown). Consequently, the mutant phenotype would then have to be attributed to the block of L1, L3, L4 and/or the other stained cell types in the medulla and lobula complex.

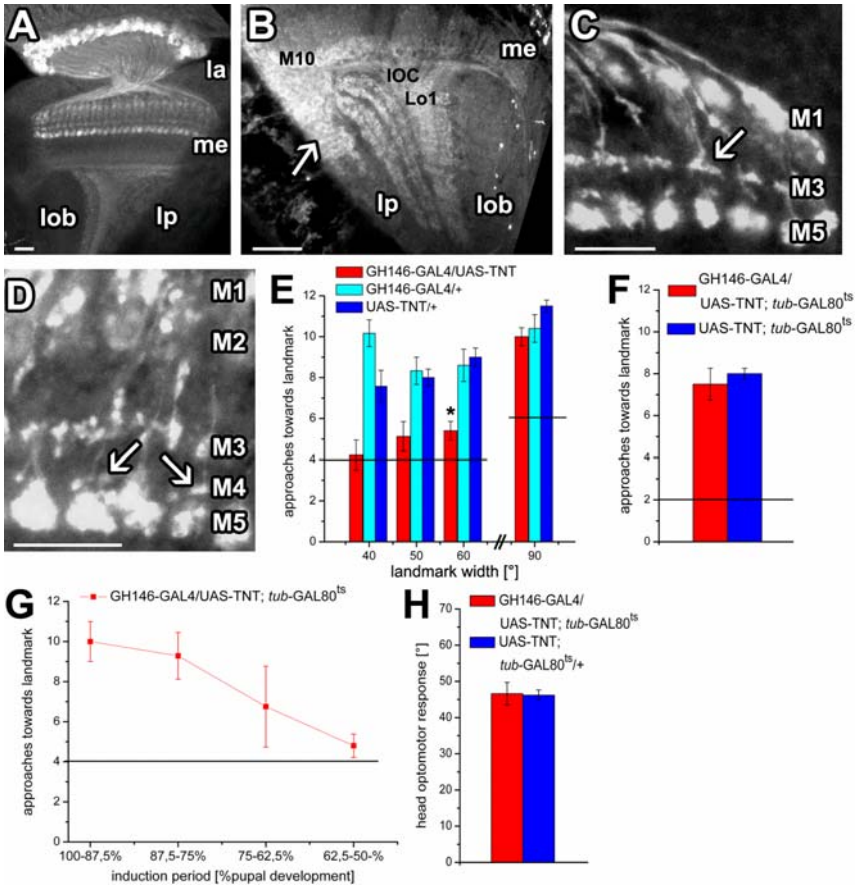

Figure 17: Expression pattern and behavioral analysis of enhancer trap GAL4 line GH146. (A) GH146 drives Cam$^{2.1}$ expression in all neuropils of the optic lobe. Scale bar, 20 µm. (B) Reporter expression is detected in the most proximal stratum of the medulla (M10), the inner optic chiasm (IOC), layers of the lobula plate (lp) and superficial layers of the lobula (lob). Cell bodies (arrowed) posterior to the lobula plate are also strongly stained. Scale bar, 10 µm. (C) In the distal medulla, GH146 labels the bistratified specializations of L1 (in M1 and M5), as well as the terminals of L3 (in M3). Scale bar, 10 µm. (D) The terminals of L4 interneurons in layer M4 were also immunopositive (arrowed). Scale bar, 10 µm. (E-F) Fixation experiments. Genotypes: experimental flies expressing Tetanus toxin under GH146 control (red), driver (light blue) and reporter (dark blue) controls. Horizontal lines indicate chance level. (E) Experimental flies expressing Tetanus toxin (red) throughout development did not fixate landmarks of less than 60° width. Fixation of the latter was significantly different from chance level ($p<0.05$; ANOVA test), but reduced in comparison to both control genotypes ($p<0.01$ and $p<0.001$; ANOVA test). In contrast, the fixation efficiency of 90° stripes was wildtype. (F) When the toxin was specifically expressed in adult flies, no mutant fixation behavior of 10° landmarks was observed. (G) Induction of the toxin at defined developmental stages revealed that the mutant phenotype had its origin at the midpupal stage (50-62.5% pupal development). (H) TNT induction at the adult stage also had no effect on head roll responses (ω/λ=3Hz; λ=24°).

In contrast to the mutant phenotypes after TNT expression, Keller (2002) noted that when UAS-*shi*^{ts1} was used as effector, head roll responses of GH146/UAS-*shi*^{ts1} flies were wildtype. The author explained this discrepancy by the assumption that the concentration of the mutant Shibire^{ts1} protein could have been insufficient. As TNT was constitutively expressed in this study, the findings of my thesis (see chapter 2.1.1.) hint at the possibility that TNT could have affected the development of cells labelled by GH146. Alternatively, one would therefore have to suggest that the mutant optomotor phenotype was not due to the block of the neurons labelled in the adult animal, but due to irreversible damage of developing cells required for this behavior. This hypothesis is

confirmed by the fact that adult-induced TNT expression by means of *tub*-GAL80^{ts} did not lead to any detectable mutant fixation phenotype (Fig. 17F). Even ten days of TNT induction did neither lead to abnormal fixation of 10° stripes nor mutant optomotor behavior (Figs. 17F, H). In contrast, targeted TNT expression in midpupae caused mutant orientation behavior (Fig. 17G). Head roll optomotor responses were unaffected when the toxin was induced for 24h specifically at the adult stage (Fig. 17H). All these data show that a developmental defect caused by TNT during pupal development was responsible for the mutant behavior. It was not further investigated which cell types were affected. Due to the rather unspecific expression pattern, the weak overall expression level and the lack of mutant phenotypes after adult *shi*^{ts1} and TNT induction, no further experiments were performed with this line. Apparently, the case of GH146-GAL4 is a second example demonstrating that it is crucial for circuit analysis to avoid toxin expression during development.

2.2.3. Studying the function of the L1, L2 and T1 pathways in motion detection

Despite the detailed knowledge of the anatomy of the lamina, the function of its pathways still remains to be understood. For instance, the role of the central pathways L1 and L2 is a controversial issue in the literature. Coombe and Heisenberg (1986) found that the *Drosophila* mutant *Vacuolar medulla*^{KS74} (*Vam*^{KS74}) exhibited degeneration of both, L1 and L2, and lacked optomotor responses. This result, however, was questioned by a subsequent study (Coombe et al., 1989) that claimed that in *Vam*^{KS74} degeneration of L1 and L2 did not significantly correlate with the absence of the optomotor response. As *Vam*^{KS74} showed also degeneration in the proximal and distal medulla, the loss of these unidentified cells could have been responsible for the mutant optomotor phenotype. It therefore needs to be clarified whether L1 and L2 are involved in motion detection. Second, Braitenberg and Hauser-Holschuh (1972) had speculated that L1 and L2 might represent the two inputs to the elementary motion detector (EMD; Fig. 4F). Both interneurons would then be required to detect directional motion. These suggestions can now be addressed by using neurogenetic techniques.

2.2.3.1. A screen for enhancer trap lines labelling lamina interneurons

To identify novel enhancer trap lines labelling monopolar cells a GAL4 driver/UAS-GFP image database (obtained from K. Ito, Tokyo) of about 4000 GAL4-

driver lines (GETDB, Hayashi et al., 2002) was screened. Next, these were characterized by expression and immunohistochemical detection of GFP in whole mounts of adult brains and horizontal agarose or plastic sections. Three GAL4 lines were identified that labelled the lamina monopolar cells L1 and L2 (NP 5214, NP 6298 and NP723; Fig. 18). These drivers also caused additional expression in the optic lobe and central brain. The corresponding enhancer trap constructs were associated with different genes (as annotated in GETDB; NP6298: *CG14760*, *pnut*; NP5214: *DptB*, *sano*; NP723: *CG30465*, *fus*).

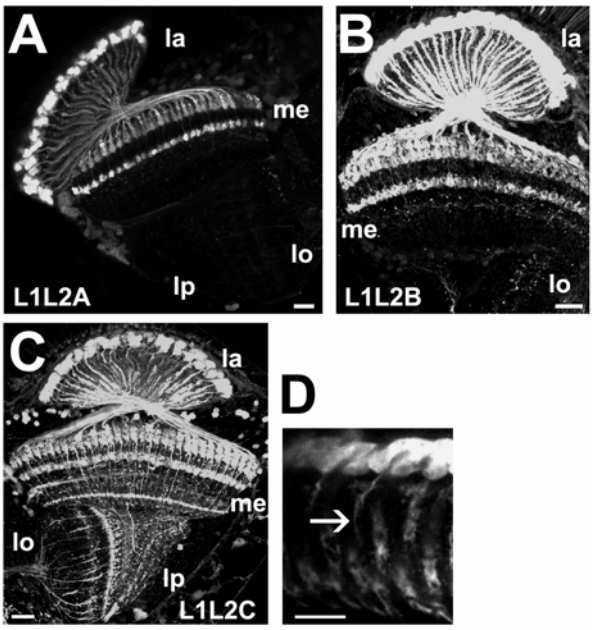

Figure 18: Expression patterns of three GAL4 lines labelling lamina monopolar cells L1 and L2.
(A-C) 10 µm confocal image stacks of a plastic section (A) and agarose sections (B, C) of three GAL4 lines, L1L2A, L1L2B and L1L2C, driving expression of GFP in L1 and L2. Reporter expression was detected in cell bodies and dendritic structures in the lamina (la). In the medulla (me), three rows of arborizations are labelled that correspond to L1 and L2. Note that all three lines also show expression in other cells of the optic lobe, for instance in the lobula (lo) and lobula plate (lp). Scale bars, 20µm.
(D) Line L1L2B drove GFP expression also in a columnar neuron (arrowed) with only few dendritic arborizations and smaller cell bodies in the lamina cortex, most likely corresponding to the L5 neuron. Scale bar, 10µm.

All three GAL4 lines drove GFP expression in the L1 and L2 monopolar cells (Fischbach and Dittrich, 1989). Their cell bodies in the lamina cortex, as well as their massive dendrites throughout the neuropil and axons projecting to the distal medulla were detected (Figs. 18A-C). L1 was identified by its bistratified terminal specializations in the first and the fifth layer of the medulla. As expected, L2's terminals were found in the second medulla layer, immediately beneath the outer swellings of the distal L1 arborizations. L1L2B (NP5214) additionally labelled L5 neurons characterized by a columnar fiber with much fewer distal dendritic swellings (Fig. 18D). Their terminals overlapped with those of L1 and L2 in the medulla (compare to Fig. 20A). Both lines, L1L2A (NP6298) and L1L2B showed additional, weaker and apparently non-overlapping expression in medulla and lobula complex neurons, as well as in the central brain. L1L2C (NP723) showed a similar, but weaker expression pattern than L1L2A and L1L2B in the lamina and other medulla and lobula complex cells (not

shown). When Cam$^{2.1}$ was used to enhance the signal, L1 and L2 were visible, as were cell bodies and projections of columnar transmedullary neurons that terminated in the lobula (Fig. 18C). Tangential arborizations in the medulla, as well as a lobula output neuron and layers of the lobula plate were also labelled.

Moreover, drivers were found that labelled only one of the two interneurons. An enhancer trap line (c202a; renamed here L1-GAL4) labelled L1 in the lamina and additional cells of the optic lobe (Fig. 19A). A GAL4 line for L2 (21D-GAL4; renamed here L2-GAL4), had been isolated in the Heisenberg lab and was described by Gorska-Andrzejak et al. (2005). The GFP staining revealed typical features of L2 neurons (Fig. 19B): big cell bodies in the lamina cortex, radially arranged dendrites in the lamina neuropil and axons that project via the outer optic chiasm to the medulla terminating in layer 2 (Fig. 19B, compare to Fig. 20A). In some flies, occasionally an unknown cell in the distal medulla, presumably a glia cell, was faintly labelled (not seen in Fig. 19B).

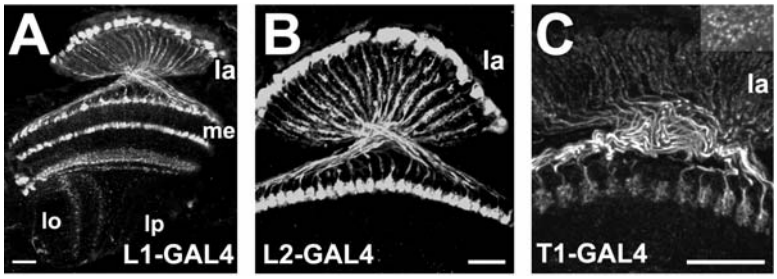

Figure 19: GAL4 drivers that label only one type of lamina interneuron.
(A) L1-GAL4 labels L1 neurons in the lamina that have their cell bodies in the lamina (la) cortex and arborize in two medulla (me) layers (compare to Fig. 2B). Note that there is additional expression in the proximal medulla (me), as well as in the lobula (lo). (B) and (C): 13-20 µm confocal image stacks of drivers expressing GFP in lamina interneurons L2 (L2-GAL4; B) and T1 (T1-GAL4; C). Inset in (C): horizontal section through optic cartridges reveals the ring of T1's basket processes that enclose R1-6 (compare to schematic in Fig. 2A). Note that both interneurons arborize in the same medulla layer (compare to Fig. 2B). Scale bars, 20µm.

The screen also yielded a driver for the T1 basket cell (T1-GAL4; NP1086). Its cell body is located in the medulla rind, giving rise to a cell body fiber that characteristically branches in a T-shape at the outer surface of the medulla (Fig. 19C). One branch ascends outwards to the lamina where it provides a basket-like bundle of processes that embraces the optic cartridge (Fig. 19C, inset). The other branch provides bush-like processes in the corresponding medullary column, at the level of the L2 ending (Fig. 19C, compare to Fig. 19B). T1 arborizes together with L2 in layer 2 of the medulla (Fig. 20A; Campos-Ortega and Strausfeld, 1973; Fischbach and Dittrich, 1989). In the same layer, L4 has distal arborizations. Together these elements are clearly separated from the bistratified specializations of L1 that are found at a more distal (layer M1) and a more proximal level (layer M5), and those of L3 that terminate in layer M3 (Fig. 20A).

2.2.3.2. L1 and/or L2 are necessary and sufficient for motion detection

The functional role of the L1 and L2 pathways (Figs. 20A, B) was studied by using two approaches. First, their requirement in visually guided behaviors was investigated by blocking their synaptic output by combining the driver lines described above with the effector UAS-*shi*^{ts1}. This demonstrates if a cell type is necessary for this behavior. Second, transgenic flies were generated that had all other afferent lamina-to-medulla channels impaired, but L1 and L2 functional. This strategy shows if a pathway is sufficient for a behavioral task.

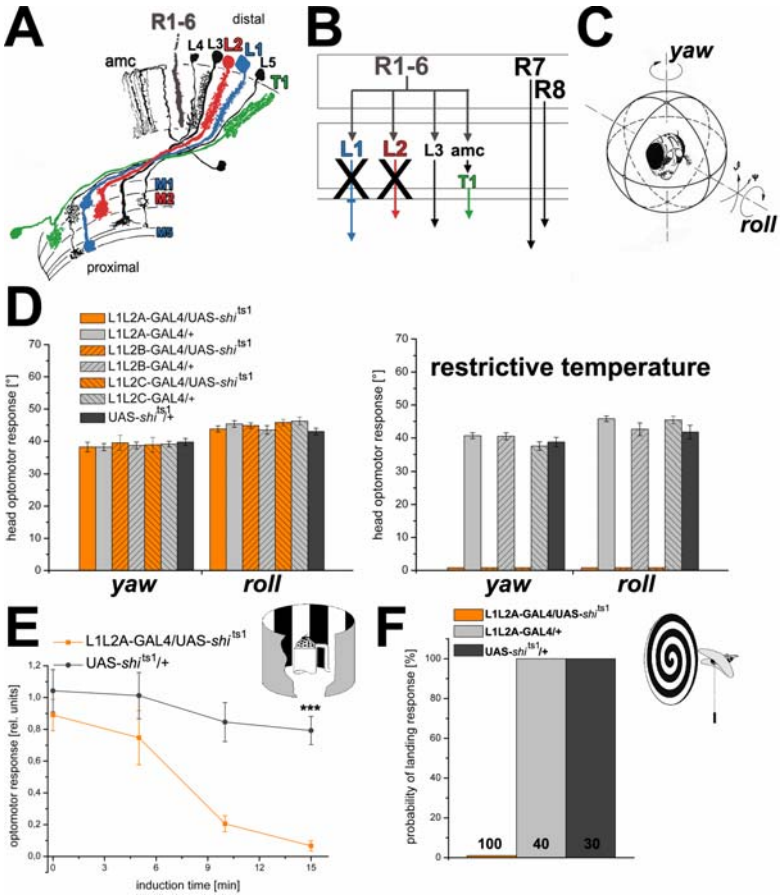

Figure 20: The functional role of L1 and L2 in motion detection.
(A) L1 (blue) and L2 (red) arborize in different layers of the medulla (M1/M5 and M2, respectively).
(B) Blocking the output of L1 and L2 blocks two peripheral channels of the lamina, whereas L3 and amc/T1, as well as photoreceptor subsystem R7/8 remain functional. (C) Schematic view of two degrees of freedom of head movements that serve the stabilization of gaze (modified from Heisenberg and Wolf, 1984). Head turning responses elicited by a large-field stimulus moving around the vertical axis are called yaw responses and around the animal's long body axis are called roll responses. (D) At the permissive temperature (left), head yaw and roll responses of all three experimental groups (L1L2A, B, C-GAL4/UAS-*shi*^{ts1}; orange bars) are indistinguishable from the respective driver (light grey bars) and effector (dark grey bar) controls. At the restrictive temperature (right), all experimental groups were invariably zero, whereas the controls were unaffected by the temperature shift. (E) Shi^{ts1} driven by driver line L1L2A also abolished optomotor responses of tethered walking experimental flies (N=4, orange curve) after 15 minutes at the restrictive temperature, in contrast to the effector control animals (grey, N=6; λ=45°; w/λ=1 Hz). P<0.001, t-test. The paradigm (modified from Keller, 2002) is shown to the upper right. (F) The visually induced landing response to an expanding stimulus (schematic kindly provided by R. Strauss, Mainz) was also absent (p>0.05; t-test) at restrictive conditions when Shi^{ts1} was driven by L1L2A (orange bar). Both control genotypes (light and dark gray bars) were unaffected by the elevated temperature. Numbers indicate performed trials.

If L1 and L2 were key players in motion detection, one would expect that their block (rescue) should abolish (restore) optomotor responses. To test this, head optomotor responses (Fig. 20C) of L1L2/*shi*^{ts1} flies were measured at stimulus conditions known to elicit maximal responses (pattern contrast m=100%; contrast frequency w/λ=3Hz). Before the temperature shift, no significant difference was found between experimental and control flies (Fig. 20D, left panel). Under restrictive conditions, i.e. with L1 and L2 blocked, neither significant yaw nor roll responses to a large-field striped-drum stimulus (λ=24°) were observed in all three experimental genotypes (Fig. 20D, right panel). Occasionally, spontaneous (random) yaw and roll movements not consistently in the direction of movement could be seen in these flies, indicating that the motor system was able to perform the respective movements after the shift to the restrictive temperature.

The driver L1L2A, which in terms of lamina expression is more specific than L1L2B (see above), was also used to block L1 and L2 in the paradigm measuring optomotor turning responses of tethered walking flies (Buchner, 1976; paradigm shown in Fig. 20E). Again, after 15 minutes of exposure to the restrictive temperature (see Material and Methods), the optomotor response was absent in the experimental group already at "optimal" stimulus conditions (λ=45°, w/λ=1Hz; Fig. 20E). As expected, the effector control flies were not significantly affected by the high temperature.

Unfortunately, all three experimental genotypes were reluctant to start flight in a striped drum after the temperature shift. Therefore, the optomotor response in tethered flight could not be measured. However, another visually guided behavior that can be elicited in tethered flight, the landing response (Fischbach, 1981), could be investigated in L1L2A/UAS-*shi*^{ts1} flies which showed brief flight episodes. In this paradigm, a rotating spiral pattern (Fig. 20F) simulates an expanding stimulus that triggers the landing response: the animals typically stretch their forelegs above the head and lower their middle and hind legs to attenuate a collision with the approaching object. After the temperature shift, this behavior could be elicited in control flies with 100% reliability, but not in L1L2A/*shi*^{ts1} flies (Fig. 20F) which kept flying without changing the position of their legs. Taken together, these data obtained with three independent GAL4 driver lines strongly suggest that the L1 and L2 pathways are <u>necessary</u> for optomotor responses and the perception of expanding stimuli.

These blocking experiments using UAS-*shi*^{ts1} do not allow judging whether L1 and L2 are also <u>sufficient</u> for motion detection. To address this question, a second

strategy was pursued that made use of the *ort* gene (see chapter 2.2.1.1.). Mutants of the histamine receptor gene *ort* (Koenig and Merriam, 1977; Gengs et al., 2002) are known to be defective in signal transmission from photoreceptors to postsynaptic lamina interneurons (Pak, 1975; Buchner, 1991; Burg et al., 1993; Gengs, 2002) in the electroretinogram (ERG). As vision in *Drosophila* is dependent on histamine signalling (Melzig et al., 1998) and therefore also on intact receptors for the amine, one can perform a "sufficiency" experiment by rescuing histamine receptor function by expressing wild-type ort^{+} cDNA in an otherwise *ort* mutant background with a GAL4 driver line labelling lamina interneurons.

Although all *ort* alleles described in the literature are known to abolish the transients in the ERG (Pak, 1975; Gengs et al., 2002), the mutant alleles used in this thesis (see Material and Methods) were not entirely (motion-) blind. Occasionally, very small responses were observed (see negative controls in Figs. 21A, B). Nevertheless, rescuing the *ort* receptor with ort^{+} cDNA in L1 and L2 (driver L1L2A) fully restored head yaw and roll optomotor responses to wild-type levels (orange bars in Fig. 21A, B). This demonstrates that the L1 and L2 pathways are sufficient for mediating head optomotor responses.

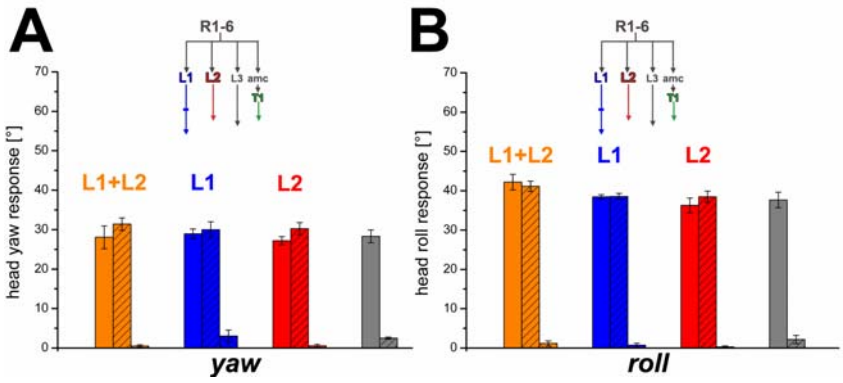

Figure 21: Studying the sufficiency of L1 and L2 in motion detection.
(A, B) Restoring both L1 and L2 (orange bar), or either L1 (blue bar) or L2 (red bar) in an *ort* mutant background (for details, see Results). Color coding: The first bar is always the rescue genotype, the second (hatched right up) is the positive (heterozygous) GAL4 control and the third (hatched left up) is the negative GAL4 control in the *ort* mutant background. Grey bar: positive (heterozygous) UAS-*ort* effector control; hatched bar: negative UAS-*ort* effector control in the mutant background. At 100% pattern contrast the rescue of both L1 and L2, as well as rescue of the single pathways is sufficient for mediating full-sized head optomotor yaw (A) and roll (B) responses. Panels above bars show the four lamina pathways. N=4-6 animals per genotype.

In summary, from the fact that with all three driver lines for L1 and L2, motion-driven behaviors were abolished after blocking synaptic output and that restoring these pathways was sufficient for mediating optomotor responses, it can be concluded that the L1 and L2 pathways are key players for the detection of large-field motion as well as of

expanding flow fields. These findings are in line with the original results of the mutant *Vam*^{KS74} that showed degeneration of L1 and L2 and did not respond to directional motion (Coombe and Heisenberg, 1986). The results would also be in line with the suggestion of Braitenberg and Hauser-Holschuh (1972; see Introduction) that L1 and L2 could be the respective inputs to the two branches of the EMD (Fig. 3B). The remaining lamina-to-medulla pathways L3, L5 and amc/T1 are neither necessary nor sufficient to mediate directional responses to motion.

2.2.3.3. L1 and L2 mediate motion detection independently of each other at high pattern contrast

The experiments reported above suggested an important role of L1 and/or L2 in motion processing. Yet, it could still be that only one of the two pathways was responsible for the absence/rescue of the ability to detect motion or that both channels are simply redundant, as suggested by Laughlin (1981a). Moreover, blocking or restoring one of the two channels would allow testing the suggestion of Braitenberg and Hauser-Holschuh (1972) that L1 and L2 could be the two input channels of the EMD (Fig. 3B). According to this model, restoring only one of the channels should not rescue the detection of directional motion, whereas its block should abolish optomotor responses.

Blocking or restoring specifically only the L1 or L2 pathway would resolve this issue. Therefore, *ort*$^{+}$ cDNA was expressed in the *ort* mutant either in L1 (blue bars, Figs. 21A, B) or L2 (red bars in Figs. 21A, B). The flies were then tested under the same experimental conditions used above. Both pathways were able to independently mediate wild-type optomotor responses (Figs. 21A, B). This result signifies that each of the two major lamina pathways alone can mediate optomotor responses. Under the experimental conditions used so far L1 and L2 are redundant. The hypothesis of Braitenberg and Hauser-Holschuh (1972) that they generally need to interact being specialized each for one of the branches of the EMD (see Introduction) must be refuted.

2.2.3.4. L1 and L2 interact at low, but not at intermediate pattern contrast

To investigate whether the L1 and L2 pathways were fully redundant, the experimental flies were tested under more challenging stimulus conditions. As in this case head roll and yaw measurements are compromised by the fly's head movements,

optomotor yaw torque responses in tethered flight were measured instead (paradigm shown in Fig. 22A). In this experiment the fly has its head glued to the thorax and is kept in the centre of a striped drum. Its yaw torque is recorded in real-time while it tries to turn with the rotating stripes (Götz, 1964; Heisenberg and Wolf, 1984).

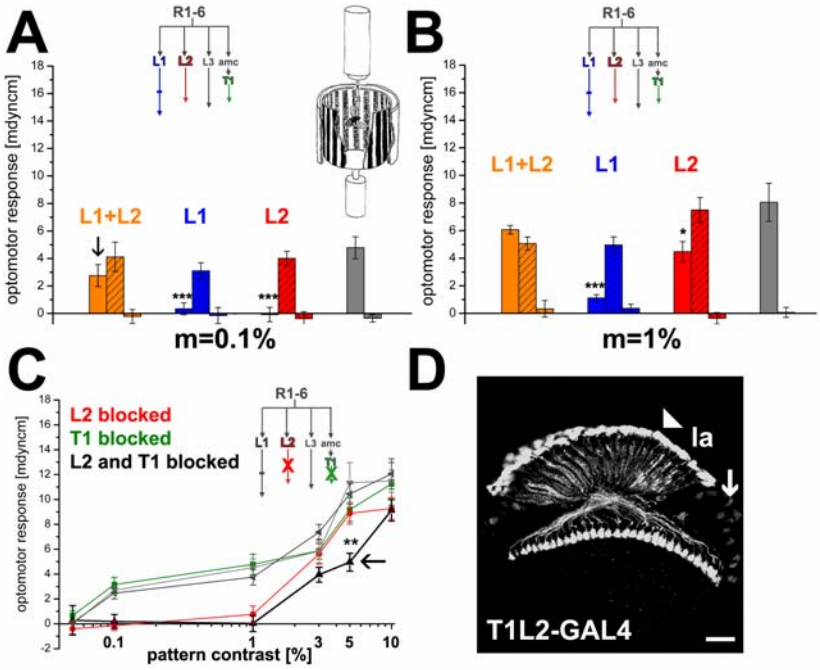

Figure 22: Differences between the L1, L2 and T1 lamina pathways at low pattern contrast.
Color coding and genotypes in (A) and (B) as in Fig. 21. (A) Upper right inset: Schematic drawing of the setup used to measure optomotor yaw torque responses in tethered flight (modified from Wolf and Heisenberg, 1997). Flies try to follow the motion of the striped drum by producing syndirectional yaw torque. At very low pattern contrast (m=0.1%) both the L1 and L2 pathways (orange bar, arrowed) have to be functional for motion vision. Rescue of either pathway alone is not sufficient (blue and red bar; $p<0.001$ in comparison to positive controls, ANOVA test). (B) At pattern contrast m=1%, again the rescue of both pathways leads to wildtype optomotor responses. The rescue of L1 is not sufficient ($p<0.001$ in comparison with the positive control and no significant difference in comparison with the negative control; ANOVA test). In contrast, restoring L2 leads to highly significant responses that are close to positive controls (hatched red bar; $p<0.05$; ANOVA test). This shows that the L2 pathway has a higher sensitivity under these conditions. N=5-11 per genotype. (C) Optomotor responses at different pattern contrasts of flies that had the output of L2 (red), T1 (green) and both interneurons (black; expression pattern shown in D) blocked. Pattern wavelength and contrast frequency were kept constant (λ=18°; w/λ=1 Hz). Light grey curve: heterozygous T1L2-GAL4/+ driver control, dark grey curve: heterozygous UAS-*shi*^{ts1} effector control. Blocking L2 prevented the response to contrasts of 1% and below. Note the significant reduction (**$p<0.01$ in comparison to both control genotypes; ANOVA test) after the block of T1 and L2 at 5% contrast (arrow). N=3-15 animals per data point. Error bars indicate SEM. (D) T1L2-GAL4 labels both interneurons. Note that only one medulla layer is labelled and that T1's cell bodies are located in the medulla rind (arrow), whereas those of L2 are found in the lamina cortex (arrowhead). Scale bar, 20µm.

At the lowest pattern contrast (m=0.1%), expressing *ort*$^{+}$-cDNA in L1 or L2 in an otherwise *ort* mutant background failed to rescue optomotor yaw responses (Fig. 22A). This shows that the L1 or L2 pathway alone was not sufficient. In the inverse approach, *shi*^{ts1} was expressed in L2 leaving only L1 of the L1/L2 pair functional. At the restrictive temperature optomotor yaw responses were entirely abolished at pattern contrast m=0.1% (Fig. 22C). This implies that both, L1 and L2 are required under these

stimulus conditions. As the L1 driver was not specific enough and additionally labelled other optic lobe cells, no experiments were performed with *shi*^{ts1}.

L2/*shi*^{ts1} flies also showed no significant optomotor yaw responses to pattern contrasts of m=1% (Fig. 22C). As L2 output is required under these conditions, this raises the question whether the L2 pathway alone would be sufficient to mediate turning responses under the same stimulus conditions. In *ort* mutant flies that expressed *ort*$^{+}$ cDNA in L2, the optomotor yaw torque response was only slightly smaller than in the positive controls ($p<0,05$; ANOVA test) already at 1% pattern contrast (Fig. 22B), indicating together with the blocking experiments above, that the L2 pathway is necessary and sufficient under these conditions. In the presence of L2 (and thus also its postsynaptic partner L4) L1 is dispensable at m=1% but required at m=0.1% pattern contrast. In accord with the L2 blocking and rescue experiments, optomotor responses of L1 rescue flies were not significant at 1% pattern contrast (Fig. 22B).

Remarkably, in flies expressing *shi*^{ts1} in L2, no significant difference to the control genotypes was detected at m=3% pattern contrast and above (Fig. 22C). This was also the case for flies that expressed *ort*$^{+}$ cDNA in L1 (data not shown). To summarize, the interaction between L1 and L2 that was found at low pattern contrast (m<1%) is not required at intermediate pattern contrast.

Qualitatively similar results were obtained in the head yaw paradigm (Figs. 23A, B), in which L2 was also required for the detection of a 1% contrast pattern. In contrast to the experiments in flight, a significant reduction was still found for m=3%, but at pattern contrasts of 5% and above, a synaptic block in L2 had no effect on the response. Flies with a restored L2 channel exhibited normal head yaw optomotor responses at m=5% (Fig. 23B). At m=1%, responses were slightly reduced compared to control flies. At 0.1% pattern contrast no reliable responses could be elicited in control flies in this paradigm.

Blocking L2 also abolished the head roll optomotor response to a vertically rotating drum at pattern contrast m=1% (Fig. 23C). A significant reduction of the response was also observed at 3% (not shown) and 5% pattern contrast. This demonstrates that the L2 pathway also plays a role in the detection of vertical flow fields at low pattern contrasts. For values equal to or bigger than 10%, no difference was detected between the experimental group and the controls. Note that in control flies, head roll responses, like body roll responses (Blondeau and Heisenberg, 1982) saturated at much higher pattern contrast than yaw torque responses. The latter are known to

reach their maximal output level at low stimulus strengths, suggesting a large open loop gain (Heisenberg and Wolf, 1984). Restoring L2 function led to head roll responses that were at the level of the positive controls at all pattern contrasts tested (Fig. 23D). Thus far, these results demonstrated that both, the L1 and L2 pathway can mediate motion detection independently from each other.

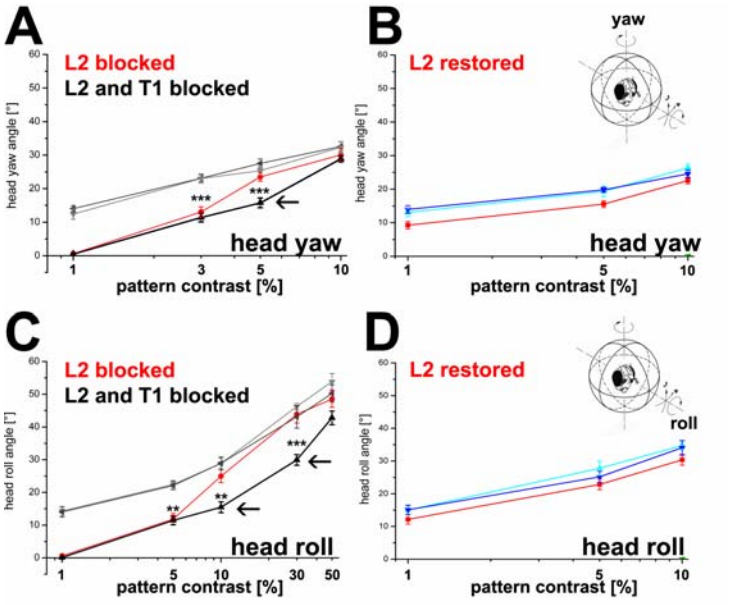

Figure 23: The involvement of lamina pathways T1 and L2 in head yaw (A, B) and roll responses (C, D) at low pattern contrasts.
(A) Head yaw optomotor responses (λ=24°, w/λ=3 Hz) were affected at 1-3% contrast when L2 was blocked (red curve). Blocking T1 and L2 (black curve) paralleled this effect, but additionally reduced the turning response level ($p<0.01$ and $p<0.001$; ANOVA) at intermediate contrast (5%, arrow). (B) Restoring the L2 pathway (red) rescued head yaw responses already at m=1%. Negative controls (green; $p<0.001$ in comparison to all other genotypes; ANOVA test) showed no significant responses ($p>0.05$; t-test) already at pattern contrast as high as m=10% and were therefore not measured at lower pattern contrasts (λ=24°; w/λ=3 Hz). (C) Head roll responses were affected at 1-5% contrast when L2 was blocked (red curve). At intermediate contrast (10-30%, arrows) the response was significantly reduced ($p<0.01$ and $p<0.001$; ANOVA test) after the block of T1 and L2 (black curve). Note that saturation of the head yaw response (A) was reached at much lower contrasts. N=4-18 animals per data point. (D) Restoring L2 (red curve) fully restored head roll responses at all pattern contrasts tested (λ=24°; w/λ=3 Hz). Negative controls (green; $p<0.001$ in comparison to all other genotypes; ANOVA test) showed no significant responses (t-test) at 10% pattern contrast and were therefore not measured at lower pattern contrasts.

It was also attempted to abolish electrical activity of L2 by expressing the human inwardly rectifying potassium channel $KIR^{2.1}$ (Baines et al., 2001). Keller (2002) had reported that L2-GAL4/UAS-KIR1 flies showed wild-type head roll responses at 100% pattern contrast (λ=60°; w/λ=1.2 Hz). This experiment could not be reproduced due to lethality of the L2-GAL4/UAS-KIR1 combination. When homozygous UAS-KIR1 virgins were crossed to L2-GAL4/TM3 males, only progeny carrying the TM3 balancer survived, indicating lethality of the 21D-GAL4/UAS-KIR1 constellation. This was also found with two other independent UAS-KIR strains, UAS-KIR1-EGFP (obtained from Richard Baines, Warwick) and UAS-KIR14-EGFP (obtained from Henrike Scholz, Würzburg). An explanation for this discrepancy is the fact that the eye pigmentation of the UAS-KIR1

stock used in this study was variable and that occasionally white eyed flies occurred, indicating the loss of the P-element.

2.2.3.5. The amc/T1 pathway exhibits a modulatory role at intermediate pattern contrast

As mentioned above (see chapter 2.2.3.1.), the screen for neurons labelling lamina interneurons also yielded a driver for the T1 cell (T1-GAL4; NP1086). Blocking synaptic output of T1 with *shi*^{ts1} had remarkably little effect on optomotor yaw torque as well as head yaw and roll responses at any of the pattern contrasts tested (Fig. 22C and data not shown). This was also true for flies that had the inwardly rectifying potassium channel (KIR$^{2.1}$; Baines et al., 2001) expressed in T1 for five days or the attenuated diphteria toxin (DTI; Bellen et al., 1992; Han et al., 2000) for seven days (data not shown), while four days were enough to block photoreceptors R1-6 using *rh1*-GAL4 as driver (Schnell, 2006). As T1 does not receive direct photoreceptor input (Shaw, 1984; Meinertzhagen and O'Neil, 1991), it was not possible to study its sufficiency by rescuing *ort* function.

Next, the drivers labelling T1 and L2 were combined to yield the stock T1L2-GAL4 that labelled both cell types (Fig. 22D), in order to test whether there are interactions between these two pathways. At low pattern contrasts (m<3%), blocking the combination of T1 and L2 paralleled the results of blocking only L2 at low contrasts in tethered flight (Fig. 22C). At 3% contrast, the effect of blocking T1 and L2 just failed to reach significance compared to control flies ($p=0.055$; Fig. 22C). At 5% contrast however, the block of both T1 and L2 led to a significant reduction of the optomotor response in comparison to the L2 block alone and the controls (arrow in Fig. 22C). This hints at an interaction of the T1 pathway with the L1-dependent motion circuitry that remains functional after the block of L2. At 10% contrast, however, the L1 motion circuitry was fully sufficient without T1.

This receives support from the measurement of head yaw responses. At intermediate (m=5%) pattern contrast, the block of both types of interneurons led to a significant reduction (arrowed in Fig. 23A) compared to all other genotypes. At 10% contrast, no reduction was found with a block of T1 and L2. When head roll responses of these experimental flies were measured, the reduction observed after blocking both interneurons was over a broader range of intermediate contrasts. For m=10-30%, a significant reduction of the response was observed in the T1L2/*shi*^{ts1} flies (arrow in Fig.

23C). Taken together, these data suggest that in the absence of L2, T1 contributes to the remaining afferent output (e.g. from L1) at an intermediate pattern contrast at which the response of that system reaches saturation.

2.2.3.6. At low pattern contrast, the L1 and L2 pathways mediate unidirectional optomotor responses

In the optomotor experiments performed thus far the rotatory large-field stimuli consisted of both, front-to-back motion on one eye and back-to-front motion on the other one. To test whether L1 or L2 specifically feed into one or the other of the antiparallel unidirectional motion detectors (Figs. 3B, C), these directional stimulus components were separated using a screen that restricted the motion stimulus to a Δ=45° window in the fronto-lateral visual field either on the right or the left side of the animal (see Material and Methods).

Under these conditions, positive control flies showed no reliable responses for pattern contrasts m<5%. At 5% pattern contrast, reliable responses were measured that did not differ between front-to-back and back-to-front motion in control genotypes (compare blue bars in Fig. 24A to Fig. 24B). Interestingly, in flies with restored L1 function (hatched red bars) in *ort* mutant background, the response to front-to-back motion was absent (Fig. 24A, right), while flies with a restored L2 pathway (red bars) were wild-type (Fig. 24A, left). In contrast, rescuing the L1 pathway allowed responses to back-to-front motion that were at the positive control level (Fig. 24B), whereas the L2 pathway alone reached significant responses only at 40% pattern contrast. Note that the response level of the L1-GAL4 driver control flies did not increase with increasing pattern contrast between 5 and 40%, suggesting a limiting effect of the P-element insertion on the motor output.

When L2 output was blocked, no significant responses were detected to front-to-back motion at m=5% (Fig. 25), confirming the findings reported above. However, at 10% contrast no asymmetry was found (Fig. 25). The reason for this discrepancy is not known. To summarize, at low pattern contrast the L1 and L2 pathways appear to independently mediate responses to back-to-front and front-to-back motion, respectively.

Figure 24: Unidirectional optomotor responses at intermediate pattern contrast.
Color coding and genotypes as in Fig. 22B. Dark grey bar: positive (heterozygous UAS-*ort* effector control; light grey bar: negative UAS-*ort* effector control in *ort* mutant background. (A)

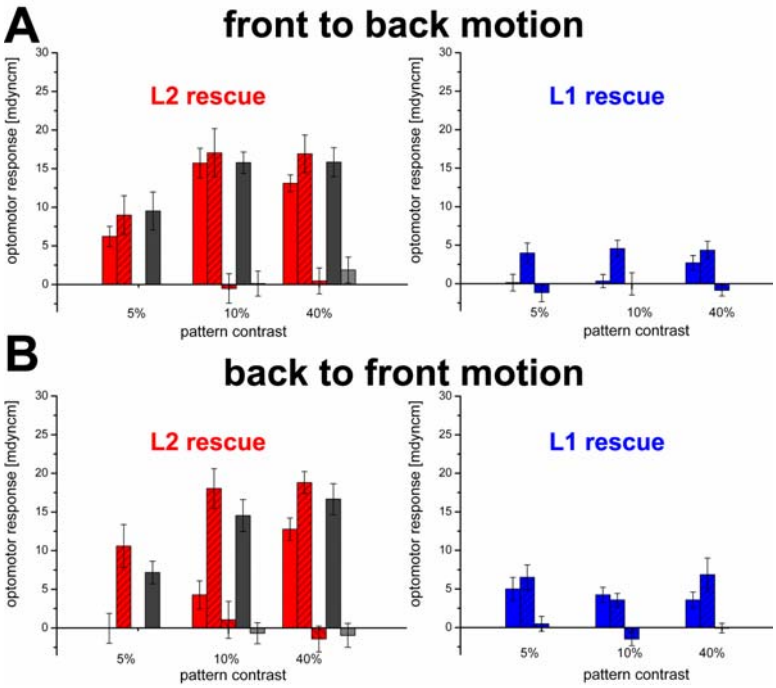

At low pattern contrast (m=5%), the L2 pathway mediates optomotor responses in tethered flight only to front-to-back motion ($p<0{,}001$; t-test). The back-to-front response is not different from zero. At 10% contrast, the back-to-front response deviated significantly from chance level ($p<0.05$; t-test), but was clearly reduced (**$p<0.01$; ANOVA test) in comparison to the positive control (driver control; light grey bars). At m=40%, no difference was detected between rescue and positive control flies. N=6-21 animals per genotype. Error bars indicate SEM. The L1 pathway mediates no responses to front-to-back motion at m=5% and m=10%. Responses to back-to-front motion are at the level of positive controls (compare right panel in A to right panel in B). Responses to front-to-back and back-to-front motion are not significantly different at m=40% pattern contrast.

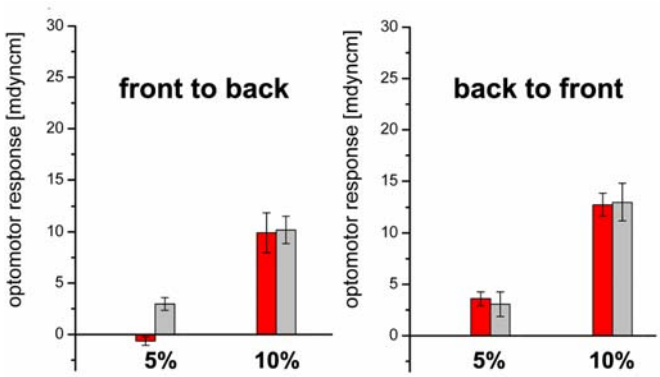

Figure 25: Blocking the output from L2 abolishes the response to front-to-back motion at 5% pattern contrast in tethered flight (red bar, left), but not to back-to-front motion. The response at 10% contrast was unaffected for both stimulus directions in comparison to the heterozygous UAS-*shi*^{ts1} effector controls (grey bar). Compare to L1 rescue data in Fig. 24. N=4-9 animals per genotype.

2.2.3.7. The L2 pathway is necessary and sufficient at low light intensity

The L2 pathway was necessary for the detection of low pattern contrasts (see chapter 2.2.3.4.). In order to determine if this also applied for low light intensities, tethered flying flies were tested in the same setup as above, with the pattern contrast (m=100%), wavelength (λ=18°) and contrast frequency (w/λ=1Hz) kept constant. The background light intensities were set to several orders of magnitude below usual room

illumination, close to the low intensity threshold of humans. Under these conditions, photon noise contaminates the photoreceptor responses and it is therefore difficult for the animal to detect pattern motion.

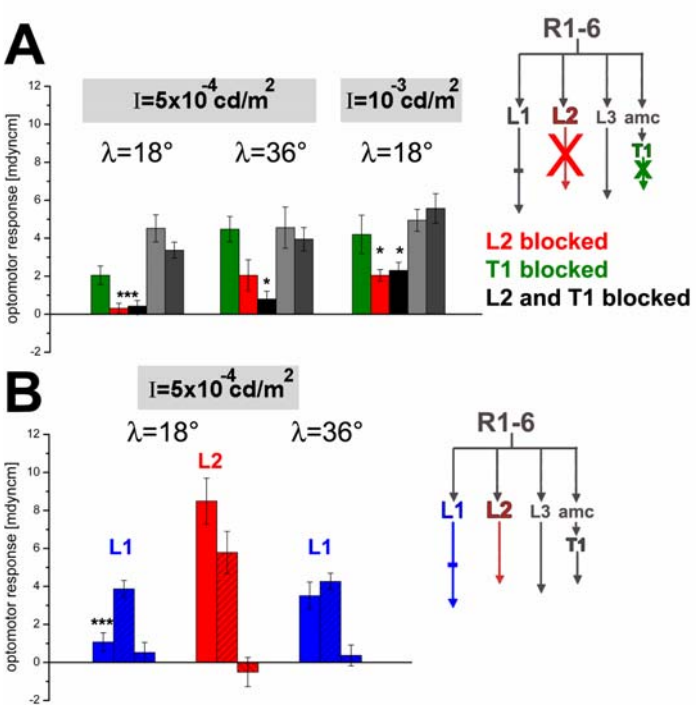

Figure 26: The role of the L1, L2 and T1 pathways at low light intensities.
(A) Blocking the L2 and T1 pathways at low light intensity reduces optomotor responses in tethered flight (w/λ=1Hz; pattern contrast m=100%). Color coding and genotypes as in Fig. 22C. L2 output was necessary for yaw turning responses at $I=5x10^{-4}cd/m^2$ and pattern wavelength of λ=18°. ***p<0.001 compared to both controls; ANOVA test. Doubling the pattern wavelength (λ=36°) to allow for spatial pooling led to significant responses without L2 output (red bar). A significant reduction (*p<0.05; ANOVA test) was found after blocking both interneurons L2 and T1 (black bar). N=9-18 flies per genotype. At a two times higher intensity, $I=10^{-3}cd/m^2$ (λ=18°; right panel), responses were significantly reduced (*p<0.05; ANOVA test) after blocking L2 (red bar), but well above zero (t-test). The additional block of T1 did not further decrease the score (black bar). Error bars indicate SEMs. (B) Studying the sufficiency of the L1 and L2 pathway at low light intensity. Color coding and genotypes as in Fig. 22C. The rescue of the L1 pathway alone was not sufficient to mediate significant responses at the lowest intensity (blue bar; p<0.001 in comparison to positive driver control; response was not significant in comparison to negative driver control; ANOVA test). N=7-17 animals per genotype. In contrast, restoring L2 function (red bar) led to a wild-type optomotor response at low light intensity ($I=5x10^{-4}cd/m^2$; λ=18°; w/λ=1 Hz). N=8-14 animals per genotype. At double pattern wavelength λ=36° flies with a restored L1 pathway showed wild-type responses (right). N=5-10 animals per genotype.

A reduction of the background illumination to $I=5x10^{-4}cd/m^2$ abolished the response of the L2/*shi*^{ts1} flies, whereas control flies still showed significant responses (Fig. 26A). Extensive dark adaptation of experimental flies before the test did not improve the score and, also, responses did not improve during the three minute recording time. This excludes that a putative effect on the dynamics of dark adaptation in the photoreceptors caused the mutant phenotype, for example due to the loss of feedback from L2 or L4. Flies without L2 output significantly responded at a background luminance of $I=10^{-3}cd/m^2$, but the response was reduced to about half of the average control level (Fig. 26A). Interfering with synaptic output from T1 at low

luminance had no significant effect and also the block of T1 and L2 did not enhance the deficit of L2/*shi*^{ts1} flies at low luminance (Fig. 26A).

The expression of the *ort*$^{+}$ cDNA in L2, but not in L1, fully restored the optomotor response at low light intensities ($I=5x10^{-4}cd/m^2$; Fig. 26B). The response was not significantly different from both positive controls. This demonstrates that flies with a restored L2 pathway are able to cope with low luminance levels in mediating optomotor responses, whereas L1 is not sufficient under these conditions. In summary, synaptic output from L2 is necessary and sufficient for motion vision not only at low pattern contrast, but also at light intensities in the vicinity of the low intensity threshold.

Synaptic output from L2 is dispensable for spatial pooling

Like humans, flies have been shown to have a special adaptation mechanism that enhances sensitivity at low light intensity conditions at the expense of visual acuity (*Drosophila*: Heisenberg and Buchner, 1977; *Musca*: Pick and Buchner, 1979). It improves motion sensitivity by pooling the visual input over many VSUs and acts at spatial wavelengths $\lambda>18°$. In order to determine whether the L2 pathway is also necessary for this pooling mechanism, L2/*shi*^{ts1} flies were again tested at the intensity of $I=5x10^{-4}cd/m^2$, but at the double spatial wavelength of $\lambda=36°$. If the response would still be abolished, then the L2 pathway would also be involved in the adaptation mechanism. Interestingly, under these conditions the experimental flies showed a significant optomotor response (Fig. 26A). Hence, L2 output seems to be dispensable for this mechanism trading sensitivity for acuity. This also implies that amongst the remaining pathways one or more must provide the necessary input for this special low intensity adaptation in the optomotor network. One candidate is the amc/T1 pathway that might again interact with the L1 pathway, since the block in L2 and T1 caused a significant reduction (Fig. 26A). However, the rescue of L1 function demonstrates that L1 alone is able to mediate spatial pooling, as the response was wild-type after doubling the spatial wavelength (Fig. 26B). The L1 pathway is therefore connected to an unknown neuronal substrate that mediates lateral interactions required for spatial pooling.

2.2.3.8. No evidence for an early separation in “on” or “off” pathways

Vertebrate retinae are characterized by an early segregation in “on” and “off” pathways. Separating the early visual system into cells that selectively respond to brightness increments (“on”) or decrements (“off”) is supposed to ensure efficient

information transfer (Kuffler, 1953; Clifford and Ibbotson, 2001). It had been suggested on the basis of electrophysiological experiments in large flies that these also have separate "on" and "off" channels (Franceschini et al., 1989; but see Egelhaaf and Borst, 1992). Franceschini et al. (1989) postulated the existence of an "on"-EMD and an "off"-EMD with both components being facilitated separately and independently. This would mean that the motion of black-to-white edges would be processed in one, the motion of white-to-black edges in the other channel. To ask whether L2 or amc/T1 feed into such an "on" or "off" channel, their output was blocked with *shi*^{ts1} and the head optomotor response to a gradient pattern containing moving edges of only one type was tested. No significant difference was detected between the response to edges of both polarities (Fig. 27, see Material and Methods for details).

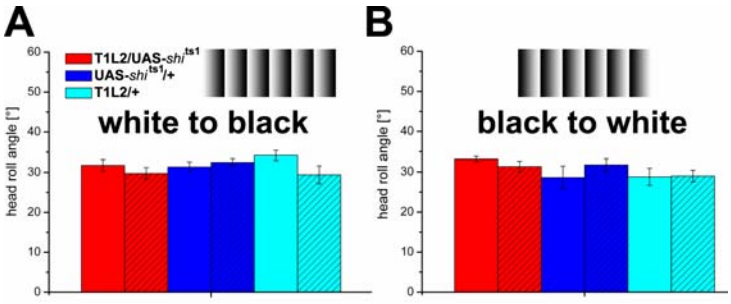

Figure 27: The response of flies with blocked T1 and L2 output (red bars) to moving white to black edges (left) and to moving black to white edges (right), respectively. No difference was found after the temperature shift (hatched bars) in comparison to effector (dark blue) and driver (light blue) control flies for both edge orientations. N=6 for each genotype.

2.2.3.9. No difference in the contrast frequency dependence between L2 and the other pathways

Next, it was asked if the contrast frequency tuning of elementary motion detectors of flies that have the L2 channel blocked would differ from those with a restored L2 channel, but all others impaired. Thus, both experimental genotypes were compared at various contrast frequencies ranging from w/λ =0.2 Hz to w/λ =40 Hz. The spatial wavelength (λ=18°) and pattern contrast (m=10%) were kept constant. Under

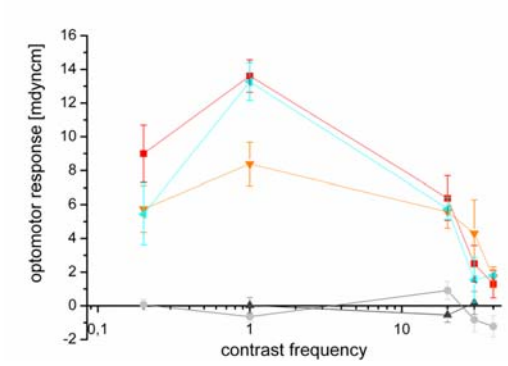

Figure 28: Flies that have the L2 channel blocked (orange triangles) do not differ from those with a restored L2 channel (red squares) in their contrast frequency optimum. Both experimental genotypes were compared at various contrast frequencies ranging from w/λ =0.2 Hz to w/λ =40 Hz. The spatial wavelength (λ=18°) and pattern contrast (m=10%) were kept constant. Light blue curve: *shi*^{ts1} effector control. Grey curves: negative controls (driver and effector in *ort*$^{-}$ background).

these conditions, no difference, neither in the contrast frequency optimum nor in the high or low frequency range, was detected between these two kinds of experimental animals (Fig. 28).

2.2.4. Studying the function of the L1, L2 and T1 pathways in orientation behavior

As had been shown above, flies lacking synaptic output from L1 and L2 failed in all motion driven behaviors tested (see chapter 2.2.3.2.). Yet, it remains to be studied what kind of other visually guided behaviors would be mediated by the remaining L3, amc and R7/8 pathways. Hence, orientation towards stationary landmarks (Heisenberg et al., 1978; Keller et al., 2002) was investigated in freely walking animals. In a pilot experiment, the entire motion channel, i.e. R1-6, was blocked using the driver *rh1*-GAL4 (Mollereau et al., 2000) to express *shi*^{ts1} (Rister and Heisenberg, 2006). These flies were not only motion blind (see above), but also did not fixate narrow landmarks of $\delta<30°$ (Fig. 29A; Schnell, 2006). This suggests that subsystems R7 and R8 are not sufficient to mediate fixation of narrow objects in this paradigm. However, from this experiment it cannot be deduced whether one or several of the four lamina pathways are necessary and sufficient for mediating fixation behavior.

L1 and L2 are not generally required for orientation towards stationary objects, but improve fixation efficiency

To investigate the role of the L1 and L2 pathways in landmark orientation behavior, all three L1L2/*shi*^{ts1} combinations were tested (Schnell, 2006). Their fixation efficiency of a 10° stripe was significantly reduced in comparison to control flies (Fig. 29A). The walking activity of the experimental genotypes was lower and walking trajectories were less straight. The fact that blocking L1 and L2 caused a similar reduction in all three experimental groups, suggests that motion detection might improve orientation behavior in freely walking flies. Moreover, if stripe width was diminished to $\delta=5°$, or if 10° stripes were presented at 75% pattern contrast, L1L2/*shi*^{ts1} flies no longer showed any preferred orientation, while orientation responses of control flies were only slightly smaller (Fig. 29B). These data provide further evidence that L1 and/or L2 do contribute to the orientation towards narrow stripes. As in both experimental situations the contrast transfer is reduced, the two pathways might also be involved in enhancing contrast edges.

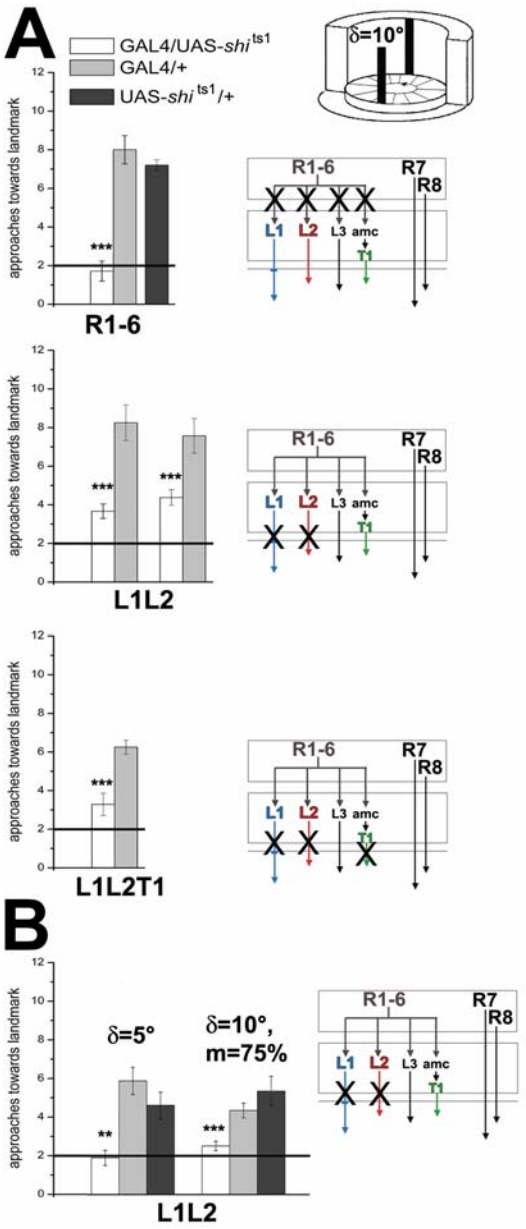

Figure 29: Role of lamina pathways in landmark orientation.
Single flies with clipped wings are released in the centre of an illuminated arena containing two vertical stripes (width δ =10°; schematic figure modified from Keller et al., 2002). Each fly performed 12 runs. As a measure of fixation efficiency, it was scored which of the 12 sectors the fly entered. After each run, the fly was caught and released again in the centre of the arena. Control flies (grey: heterozygous GAL4 driver controls, dark grey: UAS-*shi*^{ts1}effector control, pooled from all experiments in A) fixate these with high efficiency. Controls are compared to flies with blocked lamina interneurons (experimental group, white bar) that are listed below the x-axis. (A) Blocking the synaptic output of photoreceptors R1-6 (labelled by *rh1*-GAL4) abolished orientation responses of walking flies towards δ =10° wide objects. Blocking L1 and L2 (labelled in driver lines L1L2A and L1L2B) significantly reduced orientation (***p<0.001 for both drivers, ANOVA test) in comparison to the controls (grey and dark grey bars), but did not abolish it. The additional block of L5 (driver L1L2B) or T1 (driver L1L2T1-GAL4), did not further reduce the fixation efficiency towards δ =10° stripes. N=7-16 flies per genotype. Horizontal line: chance level. Error bars indicate SEM. (B) Output from L1 and L2 was required for the fixation of objects when the latter were narrow (δ=5°, left) or reduced in contrast (right: δ=10°, m=75%). In both cases, responses of experimental flies (white bars) were significantly different from control genotypes (**p<0.01 and ***p<0.001, respectively; ANOVA test) and not significantly different from chance level (indicated by horizontal line; p>0.05; t-test). N=6-16 flies per genotype.

As flies with L1 and L2 blocked were clearly able to fixate the 10° stripes, in contrast to flies which had R1-6 blocked (see above), this shows that it is not only motion detection that is contributed by the lamina to orientation behavior. Also position information is significantly improved (as R7 and R8 alone are not sufficient, see above) by one or several of the lamina pathways that remained functional. As in the driver line L1L2B also L5 was blocked in the *shi*^{ts1} experiment, this neuron can be excluded. To address the role of T1, L1L2A (labelling L1 and L2) was combined with the driver line labelling T1 (T1-GAL4, see above) to generate flies expressing *shi*^{ts1} in the three cell populations; L1, L2 and T1. In these animals, fixation of the 10° stripes was not further

reduced in comparison to the block of L1 and L2, suggesting that when L1, L2 and T1 are blocked, the remaining L3 pathway contributes to orientation towards narrow landmarks.

3. Discussion

3.1. Comparison of effector tools for genetic intervention in the visual system of *Drosophila*

Martin et al. (2002) described Tetanus neurotoxin (TNT) as a suitable effector for neuronal circuit analysis. However, as TNT caused developmental defects in case of three driver lines (GH146-GAL4 and GMR-GAL4) and also failed to block mature synapses, it cannot be generally recommended for genetic intervention anymore. When TNT is used as an effector, it is crucial to induce its expression specifically at the desired stage. Otherwise, the mutant phenotype can not be unambiguously attributed to the cells labelled at the stage of interest. If no behavioral consequences are caused by TNT expression, this does not allow concluding that the expressing cells are not required for the behavioral task, as they might be resistant to TNT, as are the photoreceptors R1-6. Interestingly, the adult mushroom bodies are a further case in which *shi*^{ts1}, but not TNT, is able to cause a behavioral defect (Thum et al., 2006). These data suggest that Shi^{ts1} is the more reliable effector.

Disadvantages of using Shi^{ts1} are that the temperature shift itself can influence the behavioral performance and that there is so far no way to detect Shi^{ts1} in the GAL4 expressing cells, as a GFP tagged version does not yet exist. Moreover, electrical synapses or other ways of signal transmission might not be affected by Shi^{ts1}, as its activity is thought to be restricted to chemical synapses. However, the effects of Shi^{ts1} do not appear to be synapse-specific: Expressing *shi*^{ts1} at the restrictive temperature has recently been found to perturb the organization of microtubules in the expressing cells (Sun and Meinertzhagen, personal communication). As Dynamin has also been shown to act on the processing of other membrane vesicles (Di et al., 2003) and to be involved in hormone secretion at the Golgi apparatus (Yang et al., 2001), Shi^{ts1} might even prevent the secretion of neuropeptides.

The rescue strategy employing the *ort* mutation and UAS linked *ort*$^{+}$ cDNA is a suitable method for studying the function of isolated lamina pathways. Combining this analysis with the findings from the experiments using Shi^{ts1} as an effector gave first insights into the functional organization of the peripheral visual network. Crucially, the experiments with UAS-*shi*^{ts1} and UAS-*ort* could be performed in exactly the same experimental context, allowing a direct comparison of the results which were complementary with only one minor exception (see chapter 2.2.3.6.).

A potential disadvantage of the rescue strategy could be that restoring a single pathway might lead to a compensation of the loss of the others, e.g. by increased formation of synapses from R1-6 onto the rescued interneuron and in consequence to a change of synaptic weights in the lamina. Several arguments speak against this hypothesis. First, the rescue experiments confirmed the findings that were obtained from experiments with *shi*^{ts1}, for instance the higher sensitivity of the L2 pathway at low signal to noise ratios. Second, the rescue of L1 and L2 alone lead to fundamentally different results, demonstrating the difference between these two pathways at low pattern contrasts and intensities. Third, it has recently been shown that synapse formation from R1-6 to lamina interneurons is a "hard-wired" process that leads to constant synapse numbers even in the absence of synaptic activity (Hiesinger et al., 2006). As the *ort* mutation is not a complete null (see Results), this should allow at least a low level of neurotransmission onto the other lamina interneurons that should be sufficient for the formation of the lamina network.

3.2. Interpretation of the expression patterns of the histamine receptor enhancer-GAL4 lines

As expected, the *ort*-enhancer-GAL4 lines labelled lamina interneurons that are known to receive histaminergic input from photoreceptors R1-6 (Hardie, 1989; Melzig et al., 1998; Gengs et al., 2002). An unexpected finding was the patchy expression pattern that was observed independent of technique, P-element insertion and antibodies used. In this respect, a major problem is that the precise localization and extent of regulatory sequences determining *ort* expression are not known. Often, widely separated enhancer fragments exert a regulatory influence, thereby determining the spatial pattern of gene expression. Essential information for the regulation of transcription can be found tens of kilobasepairs from the initation site, as enhancers can act over large distances (review: Arnosti, 2003). It is therefore possible that the DNA fragments cloned upstream of GAL4 did not contain the complete information necessary for achieving the same GAL4 level in all lamina interneurons. Interestingly, the intronic DNA segment contained enhancer information that drove reporter expression in only one type of interneuron (L2) and not the others, suggesting that these can be separately encoded.

The putative 5kb enhancer fragment of the second histamine receptor gene, *hclB*, caused a very different expression pattern when compared to the *ort* enhancer

constructs. It was surprisingly specific in the lamina and resembled stainings against the Ebony protein which is a marker for the epithelial glia cells (Richardt et al., 2002) that surround each cartridge (Meinertzhagen and O'Neil, 1991). These are known to be closely associated with the sites of histamine release and might be involved in removing histamine from the synaptic cleft after its release from photoreceptor terminals (Borycz et al., 2002). Interestingly, synapses from photoreceptors onto lamina glia have been described in large flies (Burkhardt and Braitenberg, 1976). This might require another type of ionotropic histamine receptor that could be involved in the fast histamine recycling processes in the lamina (True et al., 2005) and could be a special adaptation of dipteran insects, as these also lack the G protein coupled histamine receptors that are found in vertebrates (Nässel, 1999; Roeder, 2003).

Hong et al. (2006) recently presented whole mounts stained with an antibody directed against the HisclB protein. It was detected in the medulla, the pars intercerebralis, the suboesophagial ganglia, the lateral protocerebrum, the central brain and the thoracic ganglia. HisclB obviously only rarely colocalized with the Ort protein. This is in line with the assumption that both histamine receptor types have different functional roles and that Ort might be the main subunit for visual processing. The authors suggested that HisclB has no function in the visual system, but unfortunately did not show the laminae in their immunostained images. It would be interesting if HisclB is found in the lamina glia, as suggested by the enhancer-GAL4 line. This experiment can now be done by double staining the 5kb *hisclB*-GAL4/UAS-GFP flies with the HisclB antibody.

3.3. Genetic dissection of peripheral pathways in the visual system

This thesis is a first step into the genetic dissection of the neuronal circuitry mediating motion and position detection in the visual system of the fly. Despite the limited availability and specificity of driver lines and the limited knowledge about expression levels of transgenes, a few basic features emerged.

3.3.1. The L1 and L2 pathways are key players in motion processing

As R1-6 have been shown to be necessary and sufficient for motion detection (Heisenberg and Buchner, 1977; see also Results), the lamina cartridge formed by these receptors and the postsynaptic first order lamina-to-medulla interneurons therefore are

themselves components of the motion detection circuitry. The central position in the cartridge and the impressive size of L1 and L2 lead to speculations that these neurons could be a crucial part of the elementary motion detector (EMD; Braitenberg and Hauser-Holschuh, 1972). However, the experimental evidence so far had remained inconclusive (Coombe and Heisenberg, 1986; Coombe et al., 1989).

The results obtained with three driver lines labelling L1 and L2 suggest that these two central pathways indeed play the principal role in motion detection (summarized in Fig. 30). Flies with both L1 and L2 blocked are motion blind using motion-driven head optomotor responses and landing response as criteria. They can both process directional motion independently of each other and are remarkably redundant under a broad range of visual conditions. This is in line with the original findings of Coombe and Heisenberg (1986) on the mutant *Vam*^{KS74} that showed degeneration in L1 and L2 and also showed no responses to directional motion. The subsequent study of Coombe et al. (1989) had questioned the role of the two large monopolar cells in motion processing. As it is difficult, if not impossible, to monitor the absence of L1 and L2 in all cartridges stimulated during the experiment, incomplete degeneration of L1 and/or L2 in the *Vam*^{KS74} mutant appears to be the most likely explanation. As both L1 and L2 were able to independently mediate optomotor response at very low stimulus strengths, it would not be surprising if few remaining large monopolar cells were sufficient to mediate the response, like when there are few residual ommatidia in *sine oculis* mutant flies (Götz, 1983).

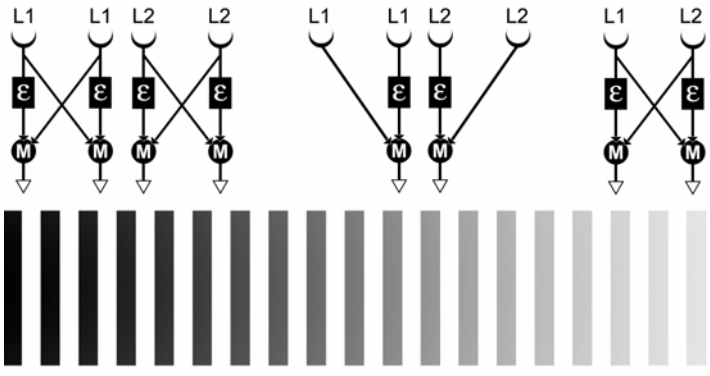

Figure 30: The L1 and L2 pathways both mediate motion responses. The two pathways are redundant at high pattern contrast, they are specialized for front-to-back (L2) and back-to-front (L1) motion in the intermediate contrast range and they cooperate at low contrast. (Note that at low pattern contrast motion detection might alternatively be unidirectional.)

Since as single neurons L1 and L2 can not exhibit directional selectivity (Mimura, 1974; Gilbert et al., 1991), it must be the pathways constituted by them that process directional motion, not the two neurons themselves. The latter also do not have the specific filter properties required for the EMD, but may rather provide input to these filters (see below). The necessary interactions for motion detection, prefiltering and

cross-correlation (see chapter 1.2.1.), obviously occur in neurons located downstream of L1 and L2.

L1 and L2 can mediate optomotor responses independent from each other at intermediate pattern contrasts

With exception of the lowest pattern contrast (m=0.1%) tested, the L1 and L2 pathway were able to mediate optomotor responses independently from each other. Notably, already at 1% pattern contrast, the L2 pathway in an *ort* mutant background was able to mediate optomotor responses. The filter properties of the delayed and non-delayed input channels to the EMD (Figs. 3B, C) obviously are not located in the L2 neurons, as these can serve for either channel. At pattern contrast m=3% or higher, even L1 alone can serve either input channel of the EMD, again arguing that L1, like L2 has no specialized filter properties for motion detection.

The superior contrast and intensity sensitivity of the L2 over the L1 pathway might be attributed to the feedback synapses of L2 (that were also blocked by shi^{ts1}) onto photoreceptors R1-6 thus providing some kind of gain control (Zheng et al., 2006). Alternatively it might be due to interactions with the L4 network. As L2 has synaptic input to L4 (Meinertzhagen and O'Neil, 1991), blocking or restoring the L2 pathway also affects the secondary L4 neurons that interconnect all cartridges and feed back onto L2. As long as no physiological data exist of L4 in *Drosophila*, it is not possible to tell whether the L4 network provides lateral inhibition, lateral pooling or the second input pathway for an array of front-to-back EMDs.

L1 and L2 mediate unidirectional optomotor responses at intermediate pattern contrast

L1 and L2 had been speculated to constitute separate input pathways to the two antidirectional EMDs mediating, respectively, the responses to front-to-back and back-to-front movement (Braitenberg and Hauser-Holschuh, 1972). Separate arrays of EMDs for these two stimulus directions had been suggested by the different strengths of optomotor responses described for large flies by Reichardt (1970) and for *Drosophila* mutants with reduced responses for only one of the two directions (Heisenberg, 1972; Bausenwein et al., 1986). At intermediate pattern contrasts that prevail in natural habitats of insects (Laughlin, 1981b), the L2/L4 pathway mediates responses to front-to-back movement, whereas L1 mediates back-to-front responses (Fig. 30). This suggests

that they indeed feed into unidirectional EMDs under these conditions. The neuronal substrates for this directional bias are not known. One candidate is the L4 network that might provide contrast enhancement for front-to-back motion.

At low pattern contrast, the unidirectional EMDs of opposite polarity that receive input from L1 and L2 are combined for improving the signal to noise ratio (Fig. 30). Already the original model of Hassenstein and Reichardt (1956) utilized a subtraction of the outputs of the two antidirectional EMDs in order to eliminate their dependency upon light intensity (see also Borst and Egelhaaf, 1990). Alternatively, the two pathways could also change their properties under these conditions to serve the delayed and non delayed branch of the EMD, respectively.

The L2 pathway and the other pathways do not differ in their contrast frequency optima

The existence of pathways with different EMD optima would allow the detection of the actual image velocity as was shown for honeybees (review: Srinivasan et al., 1999). These authors suggested that a minimal amount of two detectors with two different optimum spatio-temporal frequencies would be required to allow a system become tuned to image speed. However, the experimental comparison of the two systems “L2 blocked” and “L2 restored” does not support this hypothesis in *Drosophila* (see chapter 2.2.3.9.), as the contrast frequency optimum of the system without L2 was not different from the situation when L2 was rescued. This makes sense, as differing EMD optima would be detrimental when their outputs are subtracted (see above).

3.3.2. The amc/T1 pathway plays a role in gain control at intermediate pattern contrast

The amc/T1 pathway seems to have a purely modulatory role in motion detection. Optomotor responses were consistently reduced in several paradigms at the restrictive temperature at intermediate pattern contrast, if L2 was blocked as well. The amc/T1 pathway appears to support the L1 pathway at intermediate pattern contrast, at which its dose response curve reaches saturation. Under these conditions disturbance of T1 reduces the gain of the system and shifts the saturation range to higher contrast levels. This could involve the numerous feedback synaptic sites from amacrine cells to R1-6 (Meinertzhagen and Sorra, 2001) which represent an ideal substrate for gain

control and may be related to the adaptation mechanisms that were found at contrasts m> 4% by Buchner (1976) and McCann and MacGinitie (1965).

The finding that saturation is eventually reached, could be explained by the assumption that neurons like L5 with a presumed higher response threshold, might be added to the system at higher pattern contrast. In line with this hypothesis is the finding that the on-off units recorded by Arnett (1972) in the outer chiasm of large flies, that might correspond to L5 (Shaw, 1984), did not respond to contrasts smaller than 10% in electrophysiological recordings (Jansonius and van Hateren, 1991).

No evidence was obtained that the amc/T1 pathway would be essential for motion detection. The L2/L4 pathways alone without amc/T1, or any other parallel pathway, can obviously support motion detection under a wide range of stimulus conditions. Moreover, blocking the amc/T1 pathway alone has no detectable effect on optomotor responses. Even blocking T1 and L2 does not abolish the optomotor response.

Takemura and Meinertzhagen (personal communication) made the observation that the T1 neuron appears to have no conventional chemical synaptic output sites in the medulla as judged by its ultrastructure. Hence, it remains open whether and how *shi*^{ts1} expression in T1 might block a presumed non-synaptic output from T1. However, expressing *shi*^{ts1} at the restrictive temperature has, on the other hand, been found to perturb other cellular processes as well (see above). Moreover, expression of DTI and Kir$^{2.1}$ in T1 neurons also did not cause a substantial effect on optomotor behavior. Rather, T1 might have a more complex functional role that was not fully revealed in the experiments performed in this thesis that possibly did not sufficiently challenge the system to reveal T1's complete functional role.

3.3.3. Separating subsystems for motion and position processing

Evidence is accumulating, that orientation towards landmarks does not necessarily require the detection of motion. In *Drosophila*, torque responses towards stationary dark objects (δ=5°) have been documented by Bausenwein et al. (1986). In *Musca*, position-sensitive torque responses could be elicited by sinusoidally modulating the luminance of a stationary vertical stripe (Pick, 1974).

Motion vision and position vision can be genetically separated in *Drosophila*. Motion-blind animals are still able to approach landmarks, corroborating the notion that motion vision is not essential for the detection and fixation of a stationary object. In flies having the R1-6 channel blocked, already the color channel (R7/R8) alone provides

basic position information if the landmarks are at least 30° wide (Schnell, 2006). With only L1 and L2 blocked, flies are still completely motion blind in all paradigms tested, but their orientation behavior is distinctly superior to that of flies with photoreceptor subsystem R1-6 blocked. Remarkably, the motion detection pathway improves the fixation of landmarks, especially when these are narrow or have a reduced contrast.

Apparently, elements amongst the remaining lamina pathways improve landmark orientation as mediated by R7 and R8. Given that L5 was blocked in one of the lines without an additional impairment of orientation behavior, this implies that L5 did not substantially contribute to orientation behavior. T1 and L2 alone also were not generally necessary for fixation of landmarks. The L3 pathway, possibly interacting with the R7 and R8 pathways in color vision, may mediate orientation behavior, since flies without functional L1, L2/L4 and amc/T1 still show better orientation behavior than flies with the R1-6 channel blocked. The residual orientation behavior in flies without functional L1 and L2/L4 is very sensitive to a reduction in object contrast. This suggests that the underlying phototactic or tropotactic orientation mechanism might integrate the visual input over large parts of the visual field reducing the apparent pattern contrast of small targets. This spatial integration might occur at any level in the system.

In summary, position detection might be even more robust and redundant than motion vision. It seems to be processed in several redundant channels, involving both receptor subsystems. Detecting the position of an object in space may be a less sophisticated mechanism than motion detection requiring a nonlinear comparison of signals from neighboring visual sampling units.

4. Material and Methods

Fly Stocks

Fly strains were reared on standard *Drosophila* medium at 25°C (or 18°C for induction experiments) and a 14/10 hours light/dark cycle at 60% relative humidity. Only 2-4 days old female flies were investigated.

GAL4 drivers. GMR-GAL4 was obtained from Bloomington Stock Center (Indiana University), and a second chromosomal insertion of *rh1*-GAL4 was provided by Satoko Yamaguchi and C. Desplan (New York). GAL4 drivers from the NP collection (Hayashi et al., 2002) were received from Kei Ito (Tokyo). 21D-GAL4 was from the Würzburg stock collection and GH146, UAS-Cam$^{2.1}$ was obtained from Thomas Spall and André Fiala (Würzburg).

UAS effector strains. If not stated otherwise (see Results), a cantonized UAS-TNTE effector stock (Keller et al., 2002) was used for targeted TNT expression. Additional independent TNT insertions (TNT-C, TNT-G, TNT-H) were obtained from C. O'Kane, Cambridge. To allow targeted temporal induction of TNT, UAS-TNTE was combined with *tub*-GAL80^{ts} (Thum et al., 2006) of the TARGET system (obtained from Bloomington Stock Center; McGuire et al., 2003).

A strain with insertions of UAS-*shi*^{ts1} on the X- and 3rd chromosomes was used (Kitamoto, 2002). Heterozygous control genotypes were obtained by crossing the GAL4-driver and UAS-effector strains to wild-type Canton S.

UAS-KIR1 was obtained from the Würzburg stock collection, UAS-KIR1-EGFP from R. Baines (Warwick) and UAS-KIR14-EGFP from H. Scholz (Würzburg).

A third chromosomal insertion of UAS-GFP and a second chromosomal insertion of UAS-mCD8GFP were obtained from Arnim Jenett (Würzburg).

Ort rescue fly stocks were obtained from Chi-Hon Lee (Bethesda); pUAST-HisCl-a1 was a generous gift from Benjamin White (Bethesda). The *ort* alleles (Gengs et al., 2002) used for rescue experiments were: *ort*^{1} (recombined with 21D-GAL4 and NP6298) and *ort*^{US2515} (combined with a second chromosome insertion of UAS-*ort*). Heteroallelic combinations were used to generate the mutant background. Positive controls were the respective driver or effector strain in a heterozygous mutant background (i.e. crossed to Canton S). Negative controls were driver or effector in a homozygous mutant background.

Immunohistochemistry

Immunohistochemical methods and protocols were developed in cooperation with I. Sinakevitch (Marseille) and N. Strausfeld (Tucson).

Agarose sections. Female flies were fixed in 4% paraformaldehyde in phosphate buffered saline (PBS, pH 7.0; Sigma, Taufkirchen, Germany) overnight at 4°C. Next, they were embedded in hot (T~65°C) 8% agarose and 70-90 µm horizontal head sections were cut with a vibratome (Leica, Nussloch, Germany). The agarose sections were washed 5x20 minutes in PBST (PBS containing 0.5% Triton X-100; Sigma, Steinheim, Germany) and then blocked for 1 hour with normal goat serum (Dianova, Hamburg, Germany) in PBST. Sections were then incubated overnight at 4°C with the primary antibody. This was either a polyclonal rat anti-n-Syb antibody (Wu et al., 1999; obtained from H. Bellen, Houston) diluted 1:500 in PBST and/or mouse monoclonal anti-CSP (ab 49; obtained from E. Buchner, Würzburg), diluted 1:100 in PBST, or polyclonal rabbit anti-GFP antiserum (1:1000, Molecular Probes, Eugene, Oregon, USA). After washing 5x20 minutes in PBST, incubation with PBST-diluted secondary antibody followed at 4°C overnight. This was either Alexa 488 anti-rat (1:200; Mobitec, Göttingen, Germany) and/or CY3 anti-mouse (1:1000; Dianova, Hamburg, Germany), goat anti-rabbit IgG Alexa Fluor 488 conjugated (Fab') fragment of IgG (1:100, Molecular Probes) or goat anti-rabbit Cy5-conjugated (Fab') fragment of IgG (1:100, Molecular Probes). Finally, sections were washed 1x20 minutes in PBST and 5x20 minutes in PBS before embedding in Entellan (Merck, Darmstadt, Germany). Three-dimensional image stacks were captured with a 40x or a 63x oil objective at 0.8 µm steps with a Leica confocal microscope and further processed using the software Amira (Mercury Computer Systems, Berlin).

Plastic sections. Fly brains were fixed in 4% paraformaldehyde using a special microwave (Ted Pella, Pelco 3450, Redding, CA, USA). Brains were microwaved for three 2-minute bursts each separated by 2 minutes hold and were left in the same fixative overnight at 4^{o}C. Next, brains were washed in PBST. Then, they were blocked with swine serum (Dako, Carpinteria, California, USA) for 1h at room temperature. The primary antibody (anti-GFP, see above) was added. The microwave treatment was repeated. The samples were placed on a shaker and then left at room temperature overnight. Next, they were washed in PBST. The secondary antibody was added (Cy5, see above). A third microwave treatment followed and the samples were left overnight at room temperature on a shaker. Next, the brains were washed in PBST three times for

20 min, then with PBS six times for 20 min. Brains were permeabilized by dehydration in an increasing series of ethanol (10 min in 70% EtOH, 10 min in 90% EtOH) and eventually washed two times for 10 min in pure EtOH. Next, they were placed first for 15 min in pure acetone, then for one hour in a 1:1 mixture of acetone and Spurr's plastic embedding medium (Spurr, 1969) and finally two times for 1h in pure Spurr's medium. After this, brains were embedded in pure Spurr's medium and were polymerized at 60^{o}C for 12 hours. Serial 15 μm horizontal sections were cut with a sliding microtome. Eventually, sections were mounted with Fluoromount (Serva, Heidelberg, Germany) and viewed with a confocal epifluorescence microscope (LSM 5 Pascal, Carl Zeiss, Thornwood, NY).

Induction protocol and staging of pupae

For temperature shift experiments, vials containing experimental or control pupae raised at 18°C were placed in an incubator set at 31.5°C. 24 hours later, they were shifted back to 18°C. Under these conditions, the average duration of pupal development from puparium formation until eclosion of adult flies was 191h. To allow precise staging according to external criteria (as described by Bainbridge and Bownes, 1981) before and after exposure to the restrictive temperature at the desired time point, experiments were performed with synchronized batches of pupae which had been collected as white prepupae. The respective developmental stages were timed more exactly by measuring the number of hours which had passed after puparium formation [time zero; i.e. 0% PP (pupal period)], and expressed as a % value after dividing by 191h (x100).

Electroretinogram (ERG)

Three to five days old female flies were briefly anesthetized by cooling and attached to a holder with nail polish which was also used to immobilize head and legs. ERGs were obtained by placing an indifferent (reference) glass microelectrode in the thorax and a recording glass microelectrode just beneath the cornea of the stimulated eye. Both were filled with *Drosophila* Ringer's solution. Recordings were performed at room temperature except in the case of *shibire* (and *shibire* control) experiments. For the latter, flies were attached to a metal tube, through which water of either 25°C (permissive temperature) or 31.5°C (restrictive temperature) was circulated.

Behavioral Assays

Optomotor responses in flight. The torque compensator (Fig. 3A) and preparation of flies has been described (Götz, 1964; Heisenberg and Wolf, 1984). Briefly, more than 12h before the experiment, flies were anesthetized by cooling to 4-7°C. Small hooks made of copper wire were attached between head and thorax with a UV sensitive glue that was hardened by illumination with a UV lamp (Megadent/Megalux CS). Flies were kept isolated in small plastic vials with few grains of sucrose and access to water.

In standard optomotor experiments, a striped drum pattern of defined pattern wavelength, contrast and background intensity (I=19 cd/m², see also Visual Stimuli) was rotated at constant speed around the animal for three minutes. The first minute of the recording was discarded. The rotatory direction was changed every 30 seconds. The optomotor response [mdyncm] was calculated by a software program developed by Reinhard Wolf (Würzburg) from the remaining 2x30s responses to clock- and counterclockwise rotation. For each fly, an averaged trace of these 2min recordings was obtained and an integral value of the torque in the direction of the moving pattern was calculated.

For stimulating only with front-to-back or back-to-front motion, a stationary concentric 315° cylinder out of white plastic was placed into the striped drum. The remaining 45° window was positioned at 15°-60° to the frontal right or left of the fly. Each fly was first tested for 30s with both rotatory directions on one eye and then on the other. Torque responses to front-to-back and back-to-front motion were calculated separately. Before the screen was moved to a new position between two consecutive recordings, the illumination of the arena was switched off in order to avoid responses of the fly to the moving screen.

Visually induced landing response. Flies were prepared the same way as for flight experiments. They were exposed to a spiral pattern (kindly provided by Roland Strauss, Mainz) generating the illusion of an image expansion when rotating in one direction. This visual flow field elicited the landing response (Fischbach, 1981), i.e. the fly lowered the second and third pairs of legs and stretched its forelegs above the head. Leg extension was visually recorded under a microscope. Each fly was tested ten times.

Head roll and yaw optomotor responses. Flies were briefly anesthetized by cooling and a small pin was glued to their thorax with nail polish. To prevent leg movements, the latter were either glued together or to the body by using nail polish. Flies were allowed to recover for at least 10 minutes. Visually induced head yaw and roll responses were measured as described by Heimbeck et al. (2001). The steady state angle of head yaw or roll in response to a moving vertical stripe pattern (λ=24°, w/λ=3Hz, I=240 cd/m²) was recorded for clockwise and counterclockwise rotation. Each fly was tested four times.

To separate the response to black to white ("on") and white to black ("off") edges, a pattern consisting of gray gradients from black to white and sharp white to black edges (pattern wavelength λ = 60°; contrast frequency: 1.5 Hz; see also Keller, 2002) was used. After clockwise stimulation the pattern was changed to one with an opposite orientation of the gradient and the direction of the drum rotation was also reversed. By this means, clockwise and counterclockwise stimulation consisted only of the same edge orientation. Head optomotor responses were measured as described above.

Optomotor response of walking flies. A grating of vertical stripes (λ=45°; w/λ=1Hz; I=1.3 cd/m²) rotated around a tethered fly that walked on an air-supported styrofoam ball. Its rotations were optoelectronically recorded and served as a quantitative measure of the optomotor turning response (Buchner, 1976). A response value of zero corresponds to purely forward walking, whereas a positive (negative) value indicates rotations with (against) the moving pattern.

Orientation behavior towards stationary objects. Object fixation behavior of walking flies was measured as described earlier (Heimbeck et al., 2001). At least one day prior to the experiment, flies were immobilized by cooling to 4°C and their wings were shortened to about one third of normal length. More than three hours before the experiment, flies were starved, but had access to water. Individual flies were placed in the centre of a circular arena (I=3200 cd/m²) that contained two opposing vertical black stripes (of different angular width, height: 64°) and was divided into 12 sectors. It was recorded in which of these sectors the flies crossed the line of a measuring circle (Fig. 29A; diameter: 10cm). Each fly performed 12 runs and the runs towards one of the stripes were counted.

Visual stimuli

Patterns. Square-wave patterns of desired spatial wavelength were designed with Adobe Photoshop and the respective contrast was adjusted. Patterns were printed on transparencies (Avery, Holzkirchen, Germany) with a HP4600 printer.

Illumination. The background light intensity of the arena of the respective paradigms was measured with a photometer (Minolta Luminance Meter 1°, Minolta, Ahrensberg, Germany). The intensity was reduced by using "Neutralglas" filters (NG, Schott, Germany). In order to observe the animals in these experiments, they were illuminated by infrared LEDs and recorded by an IR-sensitive camera.

Induction of the *shi*^{ts1} effector

Prior to testing, flies were attached via their hook (flight experiments, see Behavioral Assays) or pin (head optomotor experiments) to a metal clamp, or individually placed with clipped wings in a plastic vial (orientation experiments) that were fixed in a holder and placed above the water in an illuminated water bath (air temperature T=36-37°). Flies were kept under these conditions for 15min (optomotor experiments) or 15-20min (orientation experiments). During experiments, the arena was heated to the restrictive temperature.

Statistical Methods

For comparison between genotypes, a one-way ANOVA was performed, followed by the Student-Newman-Keuls Multiple Comparisons Test. Single genotypes were tested against chance level with a one sample t-test. The significance level between experimental flies and controls or chance level indicated in the figures refers to the highest p-value obtained for the comparisons. Data are represented as means +/- S.E.M.

5. References

Anderson, J. C., and Laughlin, S. B. (2000). Photoreceptor performance and the coordination of achromatic and chromatic inputs in the fly visual system. Vision Res *40*, 13-31.

Arnett, D. W. (1972). Spatial and temporal integration properties of units in the first optic ganglion of dipterans. J Neurophysiol *35*, 429-444.

Arnosti, D. N. (2003). Analysis and function of transcriptional regulatory elements: insights from *Drosophila*. Annu Rev Entomol *48*, 579-602.

Bainbridge, S. P., and Bownes, M. (1981). Staging the metamorphosis of *Drosophila melanogaster*. J Embryol Exp Morphol *66*, 57-80.

Baines, R. A., Uhler, J. P., Thompson, A., Sweeney, S. T., and Bate, M. (2001). Altered electrical properties in *Drosophila* neurons developing without synaptic transmission. J Neurosci *21*, 1523-1531.

Bausenwein, B., Dittrich, A. P., and Fischbach, K. F. (1992). The optic lobe of *Drosophila melanogaster*. II. Sorting of retinotopic pathways in the medulla. Cell Tissue Res *267*, 17-28.

Bausenwein, B., Wolf, R., and Heisenberg, M. (1986). Genetic dissection of optomotor behaviour in *Drosophila melanogaster*. Studies on wild-type and the mutant *optomotor-blind*^{H31}. J Neurogenet *3*, 87-109.

Bellen, H. J. (1999). Ten years of enhancer detection: lessons from the fly. Plant Cell *11*, 2271-2281.

Bellen, H., D'Evelyn, D., Harvey, M., and Elledge, S. (1992). Isolation of temperature-sensitive diphtheria toxins in yeast and their effects on *Drosophila* cells. Development *114*, 787-796.

Benzer, S. (1967). Behavioral mutants of *Drosophila* isolated by countercurrent distribution. Proc Natl Acad Sci USA *58*:1112-1119.

Blondeau, J., and Heisenberg, M. (1982). The 3-dimensional optomotor torque system of *Drosophila melanogaster*. Studies on wild-type and the mutant *optomotor-blind*^{H31}. J Comp Physiol *145*, 321-329.

Borst, A., and Egelhaaf, M. (1989). Principles of visual motion detection. Trends Neurosci *12*, 297-306.

Borst, A., and Egelhaaf, M. (1990). Direction selectivity of blowfly motion-sensitive neurons is computed in a two-stage process. Proc Natl Acad Sci USA *87*, 9363-9367.

Borst, A., and Haag, J. (2002). Neural networks in the cockpit of the fly. J Comp Physiol A *188*, 419-437.

Borycz, J., Borycz, J. A., Loubani, M., and Meinertzhagen, I. A. (2002). *tan* and *ebony* genes regulate a novel pathway for transmitter metabolism at fly photoreceptor terminals. J Neurosci *22*, 10549-10557.

Boschek, C. B. (1971). On the fine structure of the peripheral retina and lamina ganglionaris of the fly, *Musca domestica*. Z Zellforsch Mikrosk Anat *118*, 369-409.

Braitenberg, V. (1967). Patterns of projections in the visual system of the fly. I. Retina lamina projections. Exp Brain Res *3*, 271-298.

Braitenberg, V. (1970). Ordnung und Orientierung der Elemente im Sehsystem der Fliege. Kybernetik *7*, 235-242.

Braitenberg, V., and Debbage, P. (1974). A regular net of reciprocal synapses in the visual system of the fly, *Musca domestica*. J Comp Physiol *90*, 25-31.

Braitenberg, V., and Hauser-Holschuh, H. (1972). Patterns of projection in the visual system of the fly. II. Quantitative aspects of second order neurons in relation to models of movement perception. Exp Brain Res *16*, 184-209.

Brand, A., and Perrimon, N. (1993). Targeted gene expression as a means of altering cell fates and generating dominant phenotypes. Development *118*, 401-415.

Buchner, E. (1976). Elementary movement detectors in an insect visual system. Biol Cybern *24*, 85-101.

Buchner, E. (1991). Genes expressed in the adult brain of *Drosophila* and effects of their mutations on behavior: a survey of transmitter- and second messenger-related genes. J Neurogenet *7*, 153-192.

Buchner, E., Buchner, S., and Bülthoff, I. (1984). Deoxyglucose mapping of nervous activity induced in the *Drosophila* brain by visual movement. J Comp Physiol A *155*, 471-483.

Burg, M. G., Sarthy, P. V., Koliantz, G., and Pak, W. L. (1993). Genetic and molecular identification of a *Drosophila histidine decarboxylase* gene required in photoreceptor transmitter synthesis. EMBO J *12*, 911-919.

Burkhardt, W., and Braitenberg, V. (1976) Some peculiar synaptic complexes in the first visual ganglion of the fly, *Musca domestica.* Cell Tissue Res *173*, 287-308.

Campos-Ortega, J. A., and Strausfeld, N. J. (1973). Synaptic connections of intrinsic cells and basket arborizations in the external plexiform layer of the fly's eye. Brain Res *59*, 119-136.

Cerutti, H. (2003). RNA interference: traveling in the cell and gaining functions? Trends Genet *19*, 39-46.

Chang, M., Bramhall, J., Graves, S., Bonavida, B., and Wisnieski, B. (1989). Internucleosomal DNA cleavage precedes diphtheria toxin-induced cytolysis. Evidence

that cell lysis is not a simple consequence of translation inhibition. J Biol Chem *264*, 15261-15267.

Clifford, C. W., and Ibbotson, M. R. (2002). Fundamental mechanisms of visual motion detection: models, cells and functions. Prog Neurobiol *68*, 409-437.

Coombe, P. E. (1986). The large monopolar cells L1 and L2 are responsible for ERG transients in *Drosophila*. J Comp Physiol A *159*, 655-665.

Coombe, P. E., and Heisenberg, M. (1986). The structural brain mutant *Vacuolar medulla* of *Drosophila melanogaster* with specific behavioural defects and cell degeneration in the adult. J Neurogenet *3*, 135-158.

Coombe, P. E., Srinivasan, M. V., and Guy, R. G. (1989). Are the large monopolar cells of the insect lamina on the optomotor pathway? J Comp Physiol A *166*, 23-35.

de Belle, J. S., and Heisenberg, M. (1996). Expression of *Drosophila* mushroom body mutations in alternative genetic backgrounds: a case study of the *mushroom body miniature* gene (*mbm*). Proc Natl Acad Sci USA *93*, 9875-9880.

Deitcher, D. L., Ueda, A., Stewart, B. A., Burgess, R.W., Kidokoro, Y., and Schwarz, T.L. (1998). Distinct requirements for evoked and spontaneous release of neurotransmitter are revealed by mutations in the *Drosophila* gene *neuronal-synaptobrevin*. J Neurosci *18*, 2028-2039.

Delgado, R., Maureira, C., Oliva, C., Kidokoro, Y., and Labarca, P. (2000). Size of vesicle pools, rates of mobilization, and recycling at neuromuscular synapses of a *Drosophila* mutant, *shibire*. Neuron *28*, 941-953.

Di, A., Nelson, D.J., Bindokas, V., Brown, M.E., Libunao, F., and Palfrey, H.C. (2003) Dynamin regulates focal exocytosis in phagocytosing macrophages. Mol Biol Cell *14*, 2016–2028.

Diegelmann, S., Fiala, A., Leibold, C., Spall, T., and Buchner, E. (2002). Transgenic flies expressing the fluorescence calcium sensor Cameleon 2.1 under UAS control. Genesis *34*, 95-98.

Dietzl, G., Chen, D., Schnorrer, F., Su, K.-C., Barinova, Y., Fellner, M., Gasser, B., Kinsey, K., Oppel, S., Scheiblauer, S., Couto, A., Marra, V., Keleman, K., and Dickson, B. (2007). A genome-wide transgenic RNAi library for conditional gene inactivation in *Drosophila*. Nature *448*, 151-156.

Douglass, J. K., and Strausfeld, N. J. (1995). Visual motion detection circuits in flies: peripheral motion computation by identified small-field retinotopic neurons. J Neurosci *15*, 5596-5611.

Douglass, J. K., and Strausfeld, N. J. (2003). Anatomical organization of retinotopic motion-sensitive pathways in the optic lobes of flies. Microsc Res Tech *62*, 132-150.

Douglass, J. K., and Strausfeld, N. J. (2005). Sign-conserving amacrine neurons in the fly's external plexiform layer. Vis Neurosci *22*, 345-358.

Duffy, J. B. (2002). GAL4 system in *Drosophila*: a fly geneticist's Swiss army knife. Genesis *34*, 1-15.

Egelhaaf, M., and Borst, A. (1992). Are there separate ON and OFF channels in fly motion vision? Visual Neurosci *8*, 151-164.

Fernandez-Chacon, R., and Südhof, T. C. (1999). Genetics of synaptic vesicle function: toward the complete functional anatomy of an organelle. Annu Rev Physiol *61*, 753-776.

Fischbach, K. F. (1981). Habituation and Sensitization of the Landing Response of *Drosophila melanogaster*. Naturwissenschaften *68*, 332.

Fischbach, K. F. (1983) Neurogenetik am Beispiel des visuellen Systems von *Drosophila melanogaster*. Habilitation, University of Würzburg.

Fischbach, K. F., and Dittrich, A. P. M. (1989). The optic lobe of *Drosophila melanogaster*. I. A Golgi analysis of wild-type structure. Cell Tissue Res *258*, 441-475.

Franceschini, N. (1975). Sampling of the visual environment by the compound eye of the fly. Fundamentals and applications. In Photoreceptor optics, A. W. Snyder, and R. Menzel, eds. (Berlin, Springer), pp. 97-125.

Franceschini, N., Riehle, A., and Le Nestour, A. (1989). Directionally selective motion detection by insect neurons. In: Facets of Vision, Stavenga, D.G., and Hardie, R. C., eds. (Berlin, Springer), pp. 360-390.

Freeman, M. (1996). Reiterative use of the EGF receptor triggers differentiation of all cell types in the *Drosophila* eye. Cell *87*, 651-660.

Gengs, C., Leung, H. T., Skingsley, D. R., Iovchev, M. I., Yin, Z., Semenov, E. P., Burg, M. G., Hardie, R. C., and Pak, W. L. (2002). The target of *Drosophila* photoreceptor synaptic transmission is a histamine-gated chloride channel encoded by *ort* (*hclA*). J Biol Chem *277*, 42113-42120.

Gilbert, C., Penisten, D. K., and DeVoe, R. D. (1991). Discrimination of visual motion from flicker by identified neurons in the medulla of the fleshfly *Sarcophaga bullata*. J Comp Physiol A *168*, 653-673.

Gisselmann, G., Pusch, H., Hovemann, B. T., and Hatt, H. (2002). Two cDNAs coding for histamine-gated ion channels in *D. melanogaster*. Nat Neurosci *5*, 11-12.

Gorska-Andrzejak, J., Keller, A., Raabe, T., Kilianek, L., and Pyza, E. (2005). Structural daily rhythms in GFP-labelled neurons in the visual system of *Drosophila melanogaster*. Photochem Photobiol Sci *4*, 721-726.

Götz, K. G. (1964). Optomotorische Untersuchung des visuellen Systems einiger Augenmutanten der Fruchtfliege *Drosophila*. Kybernetik *2*, 77-92.

Götz, K. G. (1965). Die optischen Übertragungseigenschaften der Komplexaugen von Drosophila. Kybernetik *5*, 215-221.

Götz, K. G. (1968). Flight control in *Drosophila* by visual perception of motion. Kybernetik *4*, 199-208.

Götz, K. G. (1983). Genetic defects of visual orientation in *Drosophila*. Stuttgart, Gustav Fischer Verlag.

Götz, K. G., and Wenking, H. (1973). Visual control of locomotion in the walking fruitfly *Drosophila*. J Comp Physiol *85*, 235-266.

Han, D., Stein, D., and Stevens, L. (2000) Investigating the function of follicular subpopulations during *Drosophila* oogenesis through hormone-dependent enhancer-targeted cell ablation. Development *127*, 573-583.

Hardie, R. C. (1989). A histamine-activated chloride channel involved in neurotransmission at a photoreceptor synapse. Nature *339*, 704-706.

Hardie, R. C., and Raghu, P. (2001). Visual transduction in *Drosophila*. Nature *413*, 186-193.

Hardie, R. C., and Weckström, M. (1990). Three classes of potassium channels in large monopolar cells of the blowfly *Calliphora vicina*. J Comp Physiol A *167*, 723-736.

Hassenstein, B., and Reichardt, W. (1956). Systemtheoretische Analyse der Zeit-, Reihenfolgen- und Vorzeichenauswertung bei der Bewegungsperzeption des Rüsselkäfers *Chlorophanus*. Z Naturforsch *11b*, 513-524.

Hayashi, S., Ito, K., Sado, Y., Taniguchi, M., Akimoto, A., Takeuchi, H., Aigaki, T., Matsuzaki, F., Nakagoshi, H., Tanimura, T., *et al.* (2002). GETDB, a database compiling expression patterns and molecular locations of a collection of Gal4 enhancer traps. Genesis *34*, 58-61.

Heimbeck, G., Bugnon, V., Gendre, N., Keller, A., and Stocker, R. F. (2001). A central neural circuit for experience-independent olfactory and courtship behaviour in *Drosophila melanogaster*. Proc Natl Acad Sci USA *98*, 15336-15341.

Heisenberg, M. (1971). Separation of receptor and lamina potentials in the electroretinogram of normal and mutant *Drosophila*. J Exp Biol *55*, 85-100.

Heisenberg, M. (1972). Comparative behavioural studies on two visual mutants of *Drosophila*. J Comp Physiol *80*, 119-136.

Heisenberg, M. (1997). Genetic approaches to neuroethology. Bioessays *19*, 1065-1073.

Heisenberg, M., and Buchner, E. (1977). The role of retinula cell types in visual behaviour of *Drosophila melanogaster*. J Comp Physiol *117*, 127-162.

Heisenberg, M., and Götz, K.G. (1975). The use of mutations for the partial degradation of vision in *Drosophila melanogaster*. J Comp Physiol *98*, 217-241.

Heisenberg, M., and Wolf, R. (1984). Vision in *Drosophila*. Genetics of Microbehaviour, (Heidelberg, New York, Tokyo; Springer).

Heisenberg, M., Wonneberger, R., and Wolf, R. (1978). *Optomotor-blind*^{H31} – a *Drosophila* mutant of the lobula plate giant neurons. J Comp Physiol *124*, 287-296.

Hengstenberg, R. (1993). Multisensory control in insect oculomotor systems. In Reviews of oculomotor research. Visual motion and its role in the stabilization of gaze, F. A. Miles, and J. Wallman, eds. (Amsterdam, Elsevier), pp. 285-300.

Hengstenberg, R., and Götz, K. G. (1967). Der Einfluß des Schirmpigmentgehalts auf die Helligkeits- und Kontrastwahrnehmung bei *Drosophila*-Augenmutanten. Kybernetik *3*, 276-285.

Hiesinger, P. R., Zhai, R. G., Zhou, Y., Koh, T. W., Mehta, S. Q., Schulze, K. L., Cao, Y., Verstreken, P., Clandinin, T. R., Fischbach, K. F.*, et al.* (2006). Activity-independent prespecification of synaptic partners in the visual map of *Drosophila*. Curr Biol *16*, 1835-1843.

Hong, S. T., Bang, S., Paik, D., Kang, J., Hwang, S., Jeon, K., Chun, B., Hyun, S., Lee, Y., and Kim, J. (2006). Histamine and its receptors modulate temperature-preference behaviors in *Drosophila*. J Neurosci *26*, 7245-7256.

Ito, K., Okada, R., Tanaka, N. K., and Awasaki, T. (2003). Cautionary observations on preparing and interpreting brain images using molecular biology-based staining techniques. Microsc Res Tech *62*, 170-186.

Järvilehto, M., and Zettler, F. (1973). Electrophysiological-histological studies on some functional properties of visual cells and second order neurons of an insect retina. Z Zellforsch Mikrosk Anat *136*, 291-306.

Jansonius, N. M., and van Hateren, J. H. (1991). Fast temporal adaptation of on-off units in the first optic chiasm of the blowfly. J Comp Physiol A *168*, 631-637.

Johns, D. C., Marx, R., Mains, R.E., O'Rourke, B., Marban, E. (1999). Inducible Genetic Suppression of Neuronal Excitability. J Neurosci *19*, 1691-1697.

Kaiser, W. (1975). The relationship between visual movement detection and colour vision in insects. In The compound eye and vision of insects, G. A. Horridge, ed. (Oxford, Clarendon Press), pp. 359-377.

Kawasaki, F., Hazen, M., and Ordway, R. W. (2000). Fast synaptic fatigue in *shibire* mutants reveals a rapid requirement for dynamin in synaptic vesicle membrane trafficking. Nat Neurosci *3*, 859-860.

Keller, A. (2002) Genetic intervention in sensory systems of a fly. Dissertation, University of Würzburg.

Keller, A., Sweeney, S. T., Zars, T., O'Kane, C. J., and Heisenberg, M. (2002). Targeted expression of tetanus neurotoxin interferes with behavioural responses to sensory input in *Drosophila*. J Neurobiol *50*, 221-233.

Kern, R., van Hateren, J. H., and Egelhaaf, M. (2006). Representation of behaviourally relevant information by blowfly motion-sensitive visual interneurons requires precise compensatory head movements. J Exp Biol *209*, 1251-1260.

Kirschfeld, K. (1967). Die Projektion der optischen Umwelt auf das Raster der Rhabdomere im Komplexauge von *Musca*. Exp Brain Res *3*, 248-270.

Kitamoto, T. (2001). Conditional modification of behaviour in *Drosophila* by targeted expression of a temperature-sensitive shibire allele in defined neurons. J Neurobiol *47*, 81-92.

Kitamoto, T. (2002). Conditional disruption of synaptic transmission induces male-male courtship behaviour in *Drosophila*. Proc Natl Acad Sci USA *99*, 13232-13237.

Koenig, J. H., and Ikeda, K. (1989). Disappearance and reformation of synaptic vesicle membrane upon transmitter release observed under reversible blockage of membrane retrieval. J Neurosci *9*, 3844-3860.

Koenig, J., and Merriam, J. R. (1977). Autosomal ERG mutants. D. I. S. *52*, 50-51.

Kosaka, T., and Ikeda, K. (1983). Possible temperature-dependent blockage of synaptic vesicle recycling induced by a single gene mutation in *Drosophila*. J Neurobiol *14*, 207-225.

Kuffler, S. W. (1953). Discharge patterns and functional organization of mammalian retina. *J Neurophysiol 16*, 37–68.

Kumar, J. P., and Ready, D. F. (1995). Rhodopsin plays an essential structural role in *Drosophila* photoreceptor development. Development *121*, 4359-4370.

Land M. F. (1973). Head Movement of Flies during Visually Guided Flight. Nature *243*, 299-300.

Land, M. F. (1997). Visual acuity in insects. Ann Rev Entomol *42*, 147-177.

Laughlin, S. B. (1981a). The roles of parallel channels in early visual processing by the arthropod compound eye. In Photoreception and Vision in Invertebrates, M. A. Ali, ed. (New York and London, Plenum Press), pp. 457-481.

Laughlin, S. B. (1981b). A simple coding procedure enhances a neuron's information capacity. Z Naturforsch *36c*, 910-912.

Laughlin, S. B., and Osorio, D. (1989). Mechanisms for neural signal enhancement in the blowfly compound eye. J Exp Biol *144*, 113-146.

Lee, T., and Luo, L. (2001). Mosaic analysis with a repressible cell marker (MARCM) for Drosophila neural development. Trends Neurosci *24*, 251-254.

Livingstone, M., and Hubel, D. (1988). Segregation of form, color, movement, and depth: anatomy, physiology, and perception. Science *240*, 740-749.

Martin, J. R., Keller, A., and Sweeney, S. T. (2002). Targeted Expression of Tetanus Toxin: A New Tool to Study the Neurobiology of Behavior. Adv Genet *47*, 1-48.

McCann, G. D., MacGinitie, G. F. (1965). Optomotor response studies of insect vision. Proc R Soc Lond B Biol Sci *163*, 369-401.

McGuire, S. E., Le, P. T., and Davis, R. L. (2001). The role of *Drosophila* mushroom body signaling in olfactory memory. Science *293*, 1330-1333.

McGuire, S. E., Le, P. T., Osborn, A. J., Matsumoto, K., and Davis, R.L. (2003). Spatiotemporal rescue of memory dysfunction in *Drosophila*. Science *302*, 1765-1768.

McGuire, S. E., Roman, G., and Davis, R. L. (2004). Gene expression systems in *Drosophila*: a synthesis of time and space. Trends Genet *20*, 384-391.

Meinertzhagen, I. A., and O'Neil, S. D. (1991). Synaptic organization of columnar elements in the lamina of the wild type in *Drosophila melanogaster*. J Comp Neurol *305*, 232-263.

Meinertzhagen, I. A., and Sorra, K. E. (2001). Synaptic organization in the fly's optic lamina: few cells, many synapses and divergent microcircuits. Prog Brain Res *131*, 53-69.

Melzig, J., Burg, M., Gruhn, M., Pak, W. L., and Buchner, E. (1998). Selective histamine uptake rescues photo- and mechanoreceptor function of histidine decarboxylase-deficient *Drosophila* mutant. J Neurosci *18*, 7160-7166.

Menne, D., and Spatz, H.-C. (1977). Colour vision in *Drosophila melanogaster*. J Comp Physiol A *114*, 301-312.

Mimura, K. (1974). Analysis of visual information in lamina neurones of the fly. J Comp Physiol *88*, 335-372.

Mollereau, B., Wernet, M. F., Beaufils, P., Killian, D., Pichaud, F., Kuhnlein, R., and Desplan, C. (2000). A green fluorescent protein enhancer trap screen in *Drosophila* photoreceptor cells. Mech Dev *93*, 151-160.

Nässel, D. R. (1999). Histamine in the brain of insects: a review. Microsc Res Tech *44*, 121-136.

Osorio, D., Srinivasan, M. V., and Pinter, R. B. (1990). What causes edge fixation in walking flies? J Exp Biol *149*, 281-292.

Pak, W. (1975). Mutations affecting the vision of *Drosophila melanogaster*. In Handbook of Genetics, Vol. 3, King, R. C., ed., (Plenum, New York).

Pappenheimer, A. M. (1977). Diphtheria Toxin. Annual Review of Biochemistry *46*, 69-94.

Pauls, D. (2006) Genetische Intervention im visuellen System von *Drosophila melanogaster*. Diploma thesis, University of Würzburg.

Pflugfelder, G. O. (1998). Genetic lesions in *Drosophila* behavioural mutants. Behav Brain Res *95*, 3-15.

Pflugfelder, G. O., and Heisenberg, M. (1995). *Optomotor-blind* of *Drosophila melanogaster*: a neurogenetic approach to optic lobe development and optomotor behaviour. Comp Biochem Physiol *110*, 185-202.

Phelps, C. B., and Brand, A. H. (1998). Ectopic gene expression in *Drosophila* using GAL4 system. Methods *14*, 367-379.

Pick, B. (1974). Visual flicker induces orientation behaviour in the fly *Musca*. Z Naturforsch *29c*, 310-312.

Pick, B., and Buchner, E. (1979). Visual movement detection under light- and dark-adaptation in the fly, *Musca domestica*. J Comp Physiol *134*, 45-54.

Pollack, I., and Hofbauer, A. (1991). Histamine-like immunoreactivity in the visual system and brain of *Drosophila melanogaster*. Cell Tissue Res *266*, 391-398.

Reichardt, W. (1970). The insect eye as a model for analysis of uptake transduction and processing of optical data in the nervous system. In The neurosciences. Second study program, F. O. Schmitt, ed., New York, Rockefeller University Press, pp. 494-511.

Reichardt, W., and Poggio, T. (1976) Visual control of orientation behaviour in the fly. Part I. A quantitative analysis. Q Rev Biophys *9*, 311-375.

Richardt, A., Rybak, J., Stortkuhl, K. F., Meinertzhagen, I. A., and Hovemann, B. T. (2002). Ebony protein in the *Drosophila* nervous system: optic neuropile expression in glial cells. J Comp Neurol *452*, 93-102.

Roeder, T. (2003). Metabotropic histamine receptors-nothing for invertebrates? Eur J Pharmacol *466*, 85-90.

Roman, G. (2004). The genetics of *Drosophila* transgenics. Bioessays *26*, 1243-1253.

Schiavo, G., Benfenati, F., Poulain, B., Rossetto, O., DeLaureto, P. P., DasGupta B. R., Montecucco, C. (1992). Tetanus and botulinum-B neurotoxins block neurotransmitter release by proteolytic cleavage of synaptobrevin. Nature *359*, 832-835.

Schnell, B. (2006) Genetic intervention in the periphery of the visual system of *Drosophila melanogaster*. Diploma thesis, University of Würzburg.

Scholes, J. (1969). The electrical responses of the retinal receptors and the lamina in the visual system of the fly *Musca*. Kybernetik *6*, 149-162.

Schuling, F. H., Masterbroek, H., Bult, R., Lenting, B. (1989). Properties of elementary movement detectors in the fly *Calliphora erythrocephala*. J Comp Physiol A *165*, 179-192.

Shaw, S. R. (1984). Early visual processing in insects. J Exp Biol *112*, 225-251.

Spradling, A. C., and Rubin, G. M. (1982). Transposition of cloned P elements into Drosophila germ line chromosomes. Science *218*, 341-347.

Spradling, A. C., Stern, D. M., Kiss, I., Roote, J., Laverty, T., and Rubin, G. M. (1995). Gene disruptions using P transposable elements: an integral component of the *Drosophila* genome project. Proc Natl Acad Sci USA *92*, 10824-10830.

Spurr, A. R. (1969). A low-viscosity epoxy resin embedding medium for electron microscopy. J Ultrastruct Res *26*, 31-43.

Srinivasan, M. V., and Dvorak, D. R. (1980). Spatial processing of visual information in the movement detecting pathway of the fly *Lucilia sericata*. J Comp Physiol A *140*, 1-24.

Srinivasan, M. V., Poteser, M., and Kral, K. (1999). Motion detection in insect orientation and navigation. Vision Res *39*, 2749-2766.

Stebbins, M. J., Urlinger, S., Byrne, G., Bello, B., Hillen, W., and Yin, J. C. (2001). Tetracycline-inducible systems for *Drosophila*. Proc Natl Acad Sci USA *98*, 10775-10780.

Stockinger, P., Kvitsiani, D., Rotkopf, S., Tirian, L., and Dickson, B. J. (2005). Neural circuitry that governs *Drosophila* male courtship behavior. Cell *121*, 795-807.

Strausfeld, N. J. (1971). The Organization of the Insect Visual System (Light Microscopy) I. Projections and Arrangements of Neurons in the Lamina ganglionaris of Diptera. Z Zellforsch *121*, 377-441.

Strausfeld, N. J., and Braitenberg, V. (1970). The compound eye of the fly (*Musca domestica*): Connections between the cartridges of the lamina ganglionaris. Z vergl Physiologie *70*, 95-104.

Strausfeld, N.J., and Campos-Ortega, J. A. (1977) Vision in insects: pathways possibly underlying neural adaptation and lateral inhibition. Science *195*, 894-897.

Strausfeld, N. J., and Lee, J. K. (1991). Neuronal basis for parallel visual processing in the fly. Vis Neurosci *7*, 13-33.

Sweeney, S. T., Broadie, K., Keane, J., Niemann, H., and O'Kane, C.J. (1995). Targeted expression of tetanus toxin light chain in *Drosophila* specifically eliminates synaptic transmission and causes behavioral defects. Neuron *14*, 341-351.

Tix, S., Minden, J. S., and Technau, G. M. (1989). Pre-existing neuronal pathways in the developing optic lobes of *Drosophila*. Development *105*, 739-746.

True, J. R., Yeh, S. D., Hovemann, B. T., Kemme, T., Meinertzhagen, I. A., Edwards, T. N., Liou, S. R., Han, Q., and Li, J. (2005). *Drosophila tan* encodes a novel hydrolase required in pigmentation and vision. PLoS Genet *1*, e63.

White, B., Osterwalder, T., and Keshishian, H. (2001). Molecular genetic approaches to the targeted suppression of neuronal activity. Curr Biol *11*, 1041-1053.

Witte, I., Kreienkamp, H. J., Gewecke, M., and Roeder, T. (2002). Putative histamine-gated chloride channel subunits of the insect visual system and thoracic ganglion. J Neurochem *83*, 504-514.

Wolf, R., and Heisenberg, M. (1997). Visual space from visual motion: Turn integration in tethered flying *Drosophila*. Learn Mem *4*, 318-327.

Wu, M. N., Fergestad, T., Lloyd, T. E., He, Y., Broadie, K., and Bellen, H. J. (1999). Syntaxin 1A interacts with multiple exocytic proteins to regulate neurotransmitter release *in vivo*. Neuron *23*, 593-605.

Yang, H., and Kunes, S. (2004). Nonvesicular release of acetylcholine is required for axon targeting in the *Drosophila* visual system. Proc Natl Acad Sci USA *101*, 15213-15218.

Yang, Z., Li, H., Chai, Z., Fullerton, M.J., Cao, Y., Toh, B.H., Funder, J.W., and Liu, J.P. (2001). Dynamin II regulates hormone secretion in neuroendocrine cells. J Biol Chem *276*:4251–4260.

Zheng, L., de Polavieja, G. G., Wolfram, V., Asyali, M. H., Hardie, R. C., and Juusola, M. (2006). Feedback network controls photoreceptor output at the layer of first visual synapses in *Drosophila*. J Gen Physiol *127*, 495-510.

Zinsmaier, K. E., Eberle, K. K., Buchner, E., Walter, N., Benzer, S. (1994). Paralysis and early death in cysteine string protein mutants of *Drosophila*. Science *263*, 977-980.

6. List of abbreviations

amc: amacrine cell

$Cam^{2.1}$: $Cameleon^{2.1}$

CS: wildtype Canton S

CSP: cysteine string protein

δ: landmark width

Δφ: divergence angle between neighboring ommatidia

DTI: diphtheria toxin variant I

EMD: elementary motion detector

ERG: electroretinogram

GAL4: yeast transcription factor

GAL80: silencer of GAL4

GFP: green fluorescent protein

GMR: glass multimer reporter

h: hours

hiscl: *histamine gated chloride channel*

IMPTNTQ: impotent TNT insertion Q

I: light intensity

KIR: human inwardly rectifying potassium channel

L1-5: lamina monopolar cells 1-5

λ : pattern wavelength

M1-10: medulla layer 1-10

m: pattern contrast

n-Syb: neuronal Synaptobrevin

ort: outer rhabdomeres transientless

PP: pupal period

R1-8: photoreceptors 1-8

rh1: *rhodopsin 1*

T: temperature

TARGET: temporal and regional gene expression targeting

TNT: tetanus neurotoxin

UAS: upstream activation sequence

VSU: visual sampling unit

w/λ : contrast frequency

7. Summary

Vertebrate and invertebrate visual systems exhibit similarities in early stages of visual processing. For instance, in the human brain, the modalities of color, form and motion are separately processed in parallel neuronal pathways. This basic property is also found in the fly *Drosophila melanogaster* which has a similar division in color-sensitive and (color blind) motion-sensitive pathways that are determined by two distinct subsets of photoreceptors (the R1-6 and the R7/8 system, respectively).

Flies have a highly organized visual system that is characterized by its repetitive, retinotopic organization of four neuropils: the lamina, the medulla, the lobula and the lobula plate. Each of these consists of columns which contain the same set of neurons.
In the lamina, axon bundles of six photoreceptors R1-6 that are directed towards the same point in space form columnar structures called cartridges. These are the visual sampling units and are associated with four types of first-order interneuron that receive common input from R1-6: L1, L2, L3 and the amacrine cells (amc, together with their postsynaptic partner T1). They constitute parallel pathways that have been studied in detail at the anatomical level. Little is known, however, about their functional role in processing behaviorally relevant information, e.g. for gaze stabilization, visual course control or the fixation of objects.

The availability of a variety of neurogenetic tools for structure-function analysis in *Drosophila* allowed first steps into the genetic dissection of the neuronal circuitry mediating motion and position detection. In this respect, the choice of the effector turned out to be crucial. Surprisingly, it was found that the clostridial tetanus neurotoxin failed to block mature *Drosophila* photoreceptor synapses, but caused irreversible damage when expressed during their development. Therefore, the dominant-negative *shibire* allele shi^{ts1} which turned out to be better suited was used for blocking lamina interneurons and thereby analyzing the necessity of the respective pathways. To determine whether the latter were also sufficient for the same behavioral task, the inverse strategy was developed, based on the fact that lamina interneurons express histamine receptors encoded by the *ort* gene. The specific rescue of *ort* function in defined channels in an otherwise mutant background allowed studying their sufficiency in a given task.

Combining these neurogenetic methods with the optomotor response and object induced orientation behavior as behavioral measures, the aim of the present thesis was to answer the following questions: (a) Which pathways feed into elementary motion

detectors and which ones are necessary and/or sufficient for the detection of directional motion? (b) Do pathways exist which specifically mediate responses to unidirectional motion? (c) Which pathways are necessary and/or sufficient for object induced orientation behavior?

Some basic properties of the visual circuitry were revealed: The two central cartridge pathways, represented by the large monopolar cells L1 and L2, are key players in motion detection. Under a broad range of stimulatory conditions, the two subsystems are redundant and are able to process motion independently of each other. To detect an impairment when only one of the pathways is intact, one has to drive the system to its operational limits. At low signal to noise ratios, i.e. at low pattern contrast or low background illumination, the L2 pathway has a higher sensitivity. At intermediate pattern contrast, both pathways are specialized in mediating responses to unidirectional motion of opposite stimulus direction. In contrast, neither the L3, nor the amc/T1 pathway is necessary or sufficient for motion detection. While the former may provide position information for orientation, the latter has a modulatory role at intermediate pattern contrast.

Orientation behavior turned out to be even more robust than motion vision and may utilize a less sophisticated mechanism, as it does not require a nonlinear comparison of signals from neighboring visual sampling units. The position of objects is processed in several redundant pathways, involving both receptor subsystems. The fixation of objects does not generally require motion vision. However, motion detection improves the fixation of landmarks, especially when these are narrow or have a reduced contrast.

Zusammenfassung

Die visuellen Systeme von Vertebraten und Invertebraten weisen Ähnlichkeiten in den ersten Schritten visueller Informationsverarbeitung auf. Im menschlichen Gehirn werden zum Beispiel die Modalitäten Farbe, Form und Bewegung separat in parallelen neuronalen Pfaden verarbeitet. Dieses grundlegende Merkmal findet sich auch bei der Fliege *Drosophila melanogaster*, welche eine ähnliche Trennung in farbsensitive und (farbenblinde) bewegungssensitive Pfade aufweist, die durch zwei verschiedene Gruppen von Photorezeptoren (dem R1-6 und dem R7/8 System) determiniert werden.

Fliegen haben ein hoch organisiertes visuelles System, welches durch die repetitive, retinotope Organisation von vier Neuropilen charakterisiert ist: Dies sind die Lamina, die Medulla, die Lobula und die Lobulaplatte. Jedes einzelne besteht aus Kolumnen, die denselben Satz von Nervenzellen enthalten. In der Lamina formen Axonbündel von sechs Photorezeptoren R1-6, die auf denselben Bildpunkt blicken, Säulen, die als Cartridges bezeichnet werden. Diese sind die funktionellen visuellen „sampling units“ und sind mit vier Typen von Interneuronen erster Ordnung assoziiert, die von R1-6 den gleichen Input erhalten: L1, L2, L3 und die Amakrinzellen (amc, mit ihrem postsynaptischen Partner T1). Diese stellen parallele Pfade dar, die auf anatomischer Ebene im Detail untersucht wurden; jedoch ist wenig über ihre funktionelle Rolle bei der Verarbeitung für das Verhalten relevanter Information bekannt, z.B. hinsichtlich der Blickstabilisierung, der visuellen Kurskontrolle oder der Fixation von Objekten.

Die Verfügbarkeit einer Vielfalt von neurogenetischen Werkzeugen für die Struktur-Funktionsanalyse bei *Drosophila* ermöglicht es, erste Schritte in Richtung einer genetischen Zerlegung des visuellen Netzwerks zu unternehmen, das Bewegungs- und Positionssehen vermittelt. In diesem Zusammenhang erwies sich die Wahl des Effektors als entscheidend. Überraschenderweise wurde festgestellt, dass das clostridiale Tetanus-Neurotoxin die Photorezeptorsynapsen adulter *Drosophila* Fliegen nicht blockiert, hingegen irreversible Schäden bei Expression während deren Entwicklung verursacht. Aus diesem Grund wurde das dominant-negative *shibire* Allel *shi*^{ts1}, welches sich als geeigneter erwies, zur Blockierung der Lamina Interneurone verwendet, um die Notwendigkeit der jeweiligen Pfade zu analysieren. Um festzustellen, ob letztere auch hinreichend für das gleiche Verhalten waren, wurde für die umgekehrte Strategie die Tatsache ausgenutzt, daß die Lamina Interneurone Histaminrezeptoren exprimieren, die vom *ort* Gen kodiert werden. Die spezifische

Rettung der *ort* Funktion in definierten Pfaden im mutanten Hintergrund ermöglichte festzustellen, ob sie für eine bestimmte Funktion hinreichend waren.

Diese neurogenetischen Methoden wurden mit der optomotorischen Reaktion und dem objektinduzierten Orientierungsverhalten als Verhaltensmaß kombiniert, um folgende Fragen innerhalb dieser Doktorarbeit zu beantworten: (a) Welche Pfade stellen einen Eingang in elementare Bewegungsdetektoren dar und sind notwendig und/oder hinreichend für die Detektion gerichteter Bewegung? (b) Gibt es Pfade, die spezifisch Reaktionen auf unidirektionale Bewegung vermitteln? (c) Welche Pfade sind notwendig und/oder hinreichend für das objektinduzierte Orientierungsverhalten?

Einige grundlegende Eigenschaften des visuellen Netzwerks konnten dabei aufgedeckt werden: Die zwei zentralen Cartridge Pfade, die von den großen Monopolarzellen L1 und L2 repräsentiert werden, haben eine Schlüsselfunktion bei der Bewegungsdetektion. Über ein breites Spektrum von Reizbedingungen hinweg sind die beiden Subsysteme redundant und können Bewegung unabhängig voneinander verarbeiten. Um eine Beeinträchtigung des Systems festzustellen, wenn nur einer der beiden Pfade intakt ist, muß dieses an die Grenzen seiner Leistungsfähigkeit gebracht werden. Bei niedrigem Signal/Rauschverhältnis, d.h. bei geringem Musterkontrast oder geringer Hintergrundbeleuchtung, hat der L2 Pfad eine höhere Sensitivität. Bei mittlerem Musterkontrast sind beide Pfade auf die Verarbeitung unidirektionaler Bewegung in entgegengesetzten Reizrichtungen spezialisiert. Im Gegensatz dazu sind weder der L3, noch der amc/T1 Pfad notwendig oder hinreichend für die Detektion von Bewegungen. Während der erstere Positionsinformation für Orientierungsverhalten zu verarbeiten scheint, nimmt der letztere eine modulatorische Rolle bei mittlerem Kontrast ein.

Es stellte sich heraus, daß das Orientierungsverhalten noch robuster als das Bewegungssehen ist und möglicherweise auf einem weniger komplizierten Mechanismus beruht, da dieser keinen nichtlinearen Vergleich der Signale benachbarter visueller „sampling units“ benötigt. Die Fixation von Objekten setzt nicht grundsätzlich das Bewegungssehen voraus, allerdings verbessert die Detektion von Bewegung die Fixation von Landmarken, im besonderen, wenn diese schmal sind oder einen geringen Kontrast aufweisen.

8. Curriculum Vitae

Personal information

Name: Jens Rister

Citizenship: German

Date of birth: 15.05.1976

Place of birth: Ansbach, Germany

Education

1982-1986: Grundschule Feuchtwangen, Germany.

1986-1995: Gymnasium Feuchtwangen, Germany.

Social Service

1995-1996: Mobiler Sozialer Hilfsdienst, Diakoniestation Feuchtwangen.

Undergraduate and graduate studies

1996-2001: Study of Biology and Chemistry for teaching profession, University of Würzburg, Germany

2001: Staatsexamen (1.4)

2002-2007: PhD student in the lab of Prof. Martin Heisenberg, Department of Genetics and Neurobiology, University of Würzburg, Germany.

Teaching experience

2002, 2004: Supervisor of the course: "Exercises in genetics".

2002-2006: Supervisor of undergraduate practical courses in genetics and neurobiology.

Scholarships

2002-2005: Member of the International Research Training Groups Graduiertenkolleg GK 200 and 1156 (SFB 554).

Conference talks

2005: Rister, J., Sinakevitch, I., Strausfeld, N., and Heisenberg, M. Neurogenetic analysis of the functional role of the T1 basket cell, a prominent interneuron in the fly's visual system. 30th Göttingen Neurobiology Conference, Symposium 16, "New vistas on insect vision".

2007: Rister, J. (2007). The role of the first-order interneuron L2 in the peripheral visual system of *Drosophila*. Janelia Farm Conference 2007, "Visual Processing: From Anatomy to Behavior".

Lab visits

2003: Lab of Prof. Strausfeld, ARLDN Laboratories, Tucson, Arizona (USA).

2006: Lab of Prof. Liu, Institute of Biophysics, Chinese Academy of Sciences, Beijing (CN).

Publications

See list of publications.

9. List of publications and conference contributions

Publications

1) **Rister, J.**, Pauls, D., Schnell, B., Ting, C.-Y., Lee, C.-H., Sinakevitch, I., Morante, J., Strausfeld, N. J., Ito, K. and Heisenberg, M. (2007). Dissection of the peripheral motion channel in the visual system of *Drosophila melanogaster*. Neuron, in press.

2) **Rister, J.**, and Heisenberg, M. (2006). Distinct functions of neuronal synaptobrevin in developing and mature fly photoreceptors. J Neurobiol *66*, 1271-1284.

3) Thum, A. S., Knapek, S., **Rister, J.**, Dierichs-Schmitt, E., Heisenberg, M., and Tanimoto, H. (2006). Differential potencies of effector genes in adult *Drosophila*. J Comp Neurol *498*, 194-203.

4) Godenschwege, T. A., et al. (2004). Flies lacking all synapsins are unexpectedly healthy but are impaired in complex behaviour. Eur J Neurosci *20*, 611-622.

Conference contributions

1) **Rister, J.** (2007). The role of the first-order interneuron L2 in the peripheral visual system of *Drosophila*. Janelia Farm Conference 2007, "Visual Processing: From Anatomy to Behavior".

2) **Rister, J.**, Sinakevitch, J., Ito, K., Heisenberg, M. and Strausfeld, N. J. (2005). Neurogenetic analysis of the functional role of the T1 basket cell, a prominent interneuron of the fly's visual system. Proceedings of the 30th Göttingen Neurobiology Conference 2005, edited by N. Elsner and H. Zimmermann, p. 206

10. Acknowledgements

„Es ist schwierig, eine schwarze Katze in einem dunklen Raum zu fangen. Vor allem, wenn gar keine Katze darin ist.“ – Chinesische Weisheit

Das visuelle System der Fliege erwies sich als zäher Gegner und war zu allem Überfluss auch noch resistent gegen das Nervengift Tetanus Neurotoxin. Aus diesem Grund waren die ersten Ergebnisse meiner Arbeit gelegentlich auch eher ein Gift für die Nerven aller Beteiligten. Dennoch hat sich der Aufwand absolut gelohnt. Daher möchte ich mich an dieser Stelle bei vielen Leuten für ihre Unterstützung bedanken:

Ein besonderer Dank geht an meinen Doktorvater Prof. Heisenberg für die hervorragende Betreuung, sowie die spannenden und immer produktiven Diskussionen. Sehr gefreut hat mich, dass er über die vielen Jahre hinweg stets auf mich gesetzt und mich jederzeit unterstützt hat.

Außerdem stehe ich tief in der Schuld von Bettina Schnell und Dennis Pauls, die so tapfer waren, in der heißesten Phase meiner Doktorarbeit eine Diplomarbeit unter meiner „angenehm straffen Führung“ zu machen. Die Zusammenarbeit mit den beiden hat mir große Freude bereitet und war ein voller Erfolg.

Allen Doktorandenkollegen, die mir damals den Einstieg am Lehrstuhl sehr leicht gemacht haben, gilt ebenfalls mein Dank: Franco (bis heute dabei - ma che ooooooh!), Pavel, Markus, Isa und Simon. Auch den „crazy chicks“ Suse und Anne, sowie Tilman und Stephan (…ich hab noch überhaupt…ääh…NIX!) und vielen anderen Kollegen, die ich hier nicht alle aufzählen kann, danke ich ebenso für jede Menge Spaß.

Meinen chinesischen Freunden Liu Gang, Pan Yufeng, Jiang Huoqing und Liu Li möchte ich für die sensationelle Gastfreundschaft danken. Peking war einmalig und die Atmosphäre im Labor war phantastisch. Einige von Euch werde ich hoffentlich in den Staaten wieder sehen!

Den Werkstätten (v.a. Hans und Konrad) und den TAs, allen voran Conny, Susanne 1 + 2, Dieter und Barbara danke ich für ihre Hilfe, wenn ich mal wieder etwas ganz dringend brauchte, um mit meinem Projekt voranzukommen. Ebenso gilt meinen zahlreichen Kooperationspartnern ein großer Dank für die Bereitstellung wichtiger Informationen und Materialien.

Meinen „besten Kumbls“ danke ich für die Ablenkung vom Unistreß, im besonderen Gussler für die abwechslungsreichen und spannenden Kinoabende. Zu guter letzt möchte ich im besonderen meinen Eltern danken, die mich während meines Studiums und meiner Doktorarbeit jederzeit unterstützt haben.